UTS UNIVERSITY OF TECHNOLOGY SYDNEY

Computationally efficient adaptive algorithms for active control systems

by Somanath Pradhan

Thesis submitted in fulfilment of the requirements for the degree of

Doctor of Philosophy

under the supervision of A/Prof. Jinchen Ji
and
Dr. Guoqiang Zhang

University of Technology Sydney
Faculty of Engineering and Information Technology

January 2021

Certificate of Original Authorship

I, Somanath Pradhan declare that this thesis is submitted in fulfilment of the requirements for the award of Doctor of Philosophy, in the Faculty of Engineering and Information Technology at the University of Technology Sydney.

This thesis is wholly my own work unless otherwise referenced or acknowledged. In addition, I certify that all information sources and literature used are indicated in the thesis.

This document has not been submitted for qualifications at any other academic institution.

This research is supported by the Australian Government Research Training Program.

Production Note:
Signature removed prior to publication.

Somanath Pradhan

Date: 29-01-2021

Acknowledgement

First and foremost, I would like to express my sincere gratitude to my principal supervisor A/Prof. Jinchen Ji for his guidance, encouragement and support during my PhD candidature. I am grateful to Prof. Xiaojun Qiu, who was my previous principal supervisor, for providing me with knowledge, guidance and experience not only in research but also in many other aspects of life. I would like to express my appreciation to my co-supervisor Dr. Guoqiang Zhang for his insightful ideas for my research work and valuable suggestions.

I would like to thank my former academic mentor A/Prof. Nithin V. George from Indian Institute of Technology Gandhinagar for encouraging me to pursue a research career and supporting me since I entered the field of signal processing research five years ago.

I express my sincere thanks to my teammates Tong Xiao, Jiaxin Zhong, Dr. Sipei Zhao, Dr. Qiaoxi Zhu and Dr. Shuping Wang for their valuable assistance and suggestions during the research work. Thanks to all the academic staff members of the School of Mechanical and Mechatronic Engineering for always being friendly and helpful.

Further, I would like to thank my personal mentors Shakti Prasad Tripathy, Bibhu Prasad Tripathy, Dr. Nityananda Pattanaik and Tanmaya Kumar Sahoo for being continuous support for me. I am grateful to my high school teacher, Gurumaa, Ms. Sabitarani Mishra for teaching me lessons for life. I dedicate my PhD to her.

Finally, I would like to express my deepest gratitude to my parents (Mr. Tareswar Pradhan and Ms. Golap Pradhan), my grandmother Malika Pradhan, my sister Snehalata Parida and brother-in-law Sudarshan Parida for their unconditional love, support and encouragement during my research work.

List of Publications

Much of this work has either been published or submitted for publication as journal papers and conference proceeding. The list is as follows:

In International Journals

1. **Pradhan, S**. & Qiu, X. 2020, 'A 5-stage active control method with online secondary path modelling using decorrelated control signal', *Applied Acoustics*, vol. 164, p. 107252. https://doi.org/10.1016/j.apacoust.2020.107252
2. **Pradhan, S.**, Qiu, X. & Ji, J. 2019, 'A four-stage method for active control with online feedback path modelling using control signal', *Applied Sciences*, vol. 9, no. 15, p. 2973. https://doi.org/10.3390/app9152973
3. **Pradhan, S.**, Zhang, G. & Qiu, X. 2020, 'A time domain decentralized algorithm for two channel active noise control', *The Journal of the Acoustical Society of America*, vol. 147, no. 6, pp. 3808-13. https://doi.org/10.1121/10.0001401
4. **Pradhan, S.**, Qiu, X. & Ji, J. 2020, 'A time-frequency domain flexible structure of delayless partitioned block adaptive filters for active control', submitted to *Applied Acoustics* [under revision].

In conference proceeding

1. **Pradhan**, **S.**, Qiu, X. & Ji, J. 2021, 'Affine combination of the filtered-x LMS/F algorithms for active control', Vibration Engineering for a Sustainable Future, Springer, pp. 313-9.

The following papers are also the outcomes during PhD candidature, but not included in this thesis:

In International Journals

1. Bhattacharjee, S. S., **Pradhan, S.** & George, N. V. 2020, 'Design of a class of zero attraction based sparse adaptive feedback cancellers for assistive listening devices', *Applied Acoustics,* vol. 173, p. 107683. https://doi.org/10.1016/j.apacoust.2020.107683

2. Bhattacharjee, S. S., **Pradhan**, **S.**, George, N. V. & Nordholm, S. 2020, 'Multi microphone assisted variable step size delayless multiband-structured subband feedback cancellation for two microphone hearing aids', submitted to *Signal Processing* [under review].

In Conference Proceedings

1. **Pradhan, S.**, Qiu, X. & Ji, J. 2020, 'A variable step size improved multiband-structured subband adaptive feedback cancellation scheme for hearing aids', 2020 Asia-Pacific Signal and Information Processing Association Annual Summit and Conference (APSIPA ASC), IEEE, pp. 681-5.

Statement of Contribution of Authors

The chapters of this thesis contain materials from 4 papers published or submitted for publication in the top-tier journals and 1 conference proceeding, where I was the first author.

Pradhan, S. & Qiu, X. 2020, 'A 5-stage active control method with online secondary path modelling using decorrelated control signal', *Applied Acoustics*, vol. 164, p. 107252. https://doi.org/10.1016/j.apacoust.2020.107252

Contributor	Statement of Contribution	Thesis Chapters
Somanath Pradhan	Literature review, Conceptualization, Methodology, Validation, Investigation, Manuscript Writing- Original Draft. Overall contribution: 80%	Chapter 2 and 3
Xiaojun Qiu	Conceptualization, Manuscript Writing- Review & Editing, Supervision. Overall contribution: 20%	

Pradhan, S., Qiu, X. & Ji, J. 2019, 'A Four-Stage Method for Active Control with Online Feedback Path Modelling Using Control Signal', *Applied Sciences*, vol. 9, no. 15, p. 2973. https://doi.org/10.3390/app9152973

Contributor	Statement of Contribution	Thesis Chapters
Somanath Pradhan	Literature review, Conceptualization, Methodology, Validation, Investigation, Manuscript Writing- Original Draft. Overall contribution: 80%	Chapter 2 and 3
Xiaojun Qiu	Conceptualization, Manuscript Writing- Review & Editing, Supervision. Overall contribution: 10%	
Jinchen Ji	Manuscript Writing- Review & Editing Overall contribution: 10%	

Pradhan, S., Zhang, G. & Qiu, X. 2020, 'A time domain decentralized algorithm for two channel active noise control', *The Journal of the Acoustical Society of America*, vol. 147, no. 6, pp. 3808-13. https://doi.org/10.1121/10.0001401

Contributor	Statement of Contribution	Thesis Chapters
Somanath Pradhan	Literature review, Conceptualization, Methodology, Validation, Investigation, Manuscript Writing- Original Draft. Overall contribution: 80%	Chapter 2 and 6
Guoqiang Zhang	Conceptualization, Manuscript Writing- Review & Editing, Supervision. Overall contribution: 10%	
Xiaojun Qiu	Manuscript Writing- Review & Editing, Supervision. Overall contribution: 10%	

Pradhan, S., Qiu, X. & Ji, J. 2020, 'A time-frequency domain flexible structure of delayless partitioned block adaptive filters for active control', submitted to *Applied Acoustics* [under revision].

Contributor	Statement of Contribution	Thesis Chapters
Somanath Pradhan	Literature review, Conceptualization, Methodology, Validation, Investigation, Manuscript Writing- Original Draft. Overall contribution: 80%	Chapter 2 and 5
Xiaojun Qiu	Conceptualization, Manuscript Writing- Review & Editing, Supervision. Overall contribution: 10%	
Jinchen Ji	Manuscript Writing- Review & Editing. Overall contribution: 10%	

Pradhan, **S.**, Qiu, X. & Ji, J. 2019, 'Affine combination of the filtered-x LMS/F algorithms for active control', Vibration Engineering for a Sustainable Future, Springer, pp. 313-9.

Contributor	Statement of Contribution	Thesis Chapters
Somanath Pradhan	Literature review, Conceptualization, Methodology, Validation, Investigation, Manuscript Writing- Original Draft. Overall contribution: 80%	Chapter 2 and 4
Xiaojun Qiu	Conceptualization, Manuscript Writing- Review & Editing, Supervision. Overall contribution: 10%	
Jinchen Ji	Manuscript Writing- Review & Editing. Overall contribution: 10%	

Contents

Certificate of Original Authorship i

Acknowledgement ii

List of Publications iii

Statement of Contribution of Authors v

Contents viii

List of Figures xi

List of Tables xiv

Abbreviations xv

Abstract xvii

1 Introduction 1

1.1 Motivation and objectives 1

1.2 Contributions 6

1.3 Thesis outline 7

2 Literature review 10

2.1 Single channel feedforward ANC system 10

2.2 Online secondary path modelling 14

2.3 Online feedback path modelling 17

2.4 Convergence behaviour and noise reduction performance 21

2.5 Low-complexity algorithms for active control at high sampling rate 23

2.6 Decentralized algorithms for active control 26

2.7 Summary 28

3 Online modelling of acoustic paths in active control systems using control signal 31

3.1 Introduction 31

3.2 Online secondary path modelling 32

3.2.1 Proposed method 32

3.2.2 Numerical experiments 39

3.2.2.1 The five stage method 41

3.2.2.1.1 Case 1: Autoregressive signal 41

3.2.2.1.2 Case 2: Frequent acoustic path change 43
3.2.2.2 The decorrelation filter 46
3.2.2.2.1 Case 1: Autoregressive signal 46
3.2.2.2.2 Case 2: Broadband signal 47
3.2.2.2.3 Case 3: Mixture of white noise and multitone 49
3.2.2.3 The five-stage method with decorrelation filter 51
3.2.2.3.1 Case 1: Coloured signal 51
3.2.2.3.2 Case 2: Mixture of white noise and multitone 53
3.2.2.3.3 Case 3: Effect of measurement noise 54
3.2.3 Computational complexity 56
3.3 Online feedback path modelling 58
3.3.1 Proposed method 58
3.3.2 Numerical experiments 66
3.3.3 Computational complexity 72
3.4 Summary 73
4 Affine combination of adaptive filters for active control 75
4.1 Introduction 75
4.2 The proposed affine combination algorithm 75
4.3 Numerical experiments 79
4.3.1 Case 1: White noise 79
4.3.2 Case 2: Multitone noise 81
4.3.3 Case 3: Effect of imperfect secondary path model 83
4.4 Summary 84
5 A time-frequency domain flexible structure for active control 85
5.1 Introduction 85
5.2 The proposed structure 85
5.3 Numerical experiments 89
5.3.1 Case 1: White noise 89
5.3.2 Case 2: Traffic noise 93
5.4 Computational complexity 96

5.5 Summary 98

6 Decentralized algorithm for broadband active control 99

6.1 Introduction 99

6.2 The proposed algorithm 99

6.2.1 Framework description 99

6.2.2 Eigenvalue shaping in frequency domain 100

6.2.3 Scaling of the diagonal matrices 102

6.2.4 Auxiliary FIR filter design 103

6.2.5 The time domain control algorithm 104

6.3 Numerical experiments 106

6.3.1 Case 1: White noise 108

6.3.2 Case 2: Traffic noise 110

6.4 Computational complexity 112

6.5 Summary 113

7 Conclusions and future work 114

7.1 Conclusions 114

7.2 Future works 116

References 118

List of Figures

Figure 1.1	A basic single channel feedforward ANC system.	2
Figure 2.1	Schematic block diagram of a single channel ANC system.	11
Figure 2.2	Schematic block diagram of ANC system with acoustic feedback.	18
Figure 3.1	Block diagram of the proposed method for active control operation.	33
Figure 3.2	Flowchart of the proposed method.	34
Figure 3.3	Frequency response of (a) the primary path and (b) the secondary path.	40
Figure 3.4	Case 1: Learning curve for the 5-stage method obtained from an AR(1) input signal.	43
Figure 3.5	Case 2: Learning curve for the 5-stage method obtained from an AR(1) input signal with a frequent acoustic path change.	44
Figure 3.6	Relative modelling error for the AR(1) signal.	47
Figure 3.7	(a) Relative modelling error for the full frequency range, (b) Relative modelling error for the frequency band of [100 500] Hz	49
Figure 3.8	Relative modelling error for the mixture of white noise and multitone signal.	50
Figure 3.9	Learning curve for the 5-stage method obtained from a coloured input signal.	52
Figure 3.10	Learning curve for the 5-stage method obtained from a mixture of white noise and multitone input signals.	54
Figure 3.11	Learning curves for the proposed method obtained from a colored input signal and different level of measurement noise. (a) SNR = 30 dB, (b) SNR = 20 dB, (c) SNR = 10 dB and (d) SNR = 0 dB.	55
Figure 3.12	Schematic diagram of the proposed method for active control with online feedback path modelling using the control signal.	59

Figure 3.13	Flowchart of the proposed feedback path modelling method.	60
Figure 3.14	Effect of different value of β on mapping of r(n) to the linear range of tanh function.	62
Figure 3.15	Frequency response of (a) the primary path and the secondary path and (b) feedback path.	67
Figure 3.16	Feedback path modelling error in the second stage.	68
Figure 3.17	(a) Feedback path modelling error, (b) learning curve for the whole duration of control operation.	70
Figure 4.1	Schematic block diagram of the proposed affine combination algorithm.	77
Figure 4.2	Case 1: (a) ANR for white noise, (b) variation of combining parameter.	80
Figure 4.3	Case 2: (a) ANR for multi-tone noise, (b) variation of combining parameter.	82
Figure 4.4	Case 3: (a) ANR and (b) variation of mixing parameter with an imperfect secondary path model.	84
Figure 5.1	Block diagram of the proposed structure for a single channel feedforward ANC system.	86
Figure 5.2	(a) Acoustic path measurement setup in a duct, (b) impulse responses of the primary and secondary paths.	90
Figure 5.3	(a) Normalized MSE curves for white noise using different algorithms and (b) the power spectral density with and without noise control.	92
Figure 5.4	(a) Position of source and sensor in the measurement and (b) Impulse responses of the primary and secondary paths measured in a normal room.	94

Figure 5.5 (a) Normalized MSE curves for traffic noise using different algorithms and (b) the power spectral density with and without noise control. 96

Figure 6.1 Schematic diagram of the proposed time domain two channel decentralized algorithm. 105

Figure 6.2 Arrangement of the sources and the sensors in a normal room for multiple channel acoustic path measurement. 107

Figure 6.3 Normalized MSE curves for zero-mean white Gaussian noise using different algorithms when they (a) converge and (b) diverge. 109

Figure 6.4 (a) Normalized MSE curves for traffic noise using different algorithms and (b) the power spectral density with and without noise control. 111

List of Tables

Table 3.1	The five stages of the proposed method.	38
Table 3.2	Residual noise levels of different methods for different measurement noise levels.	56
Table 3.3	Computational complexity of different methods.	57
Table 3.4	Computational complexity of different methods.	73
Table 5.1	The average number of real multiplications required for different algorithms.	97
Table 5.2	The average number of real multiplications required with respect to the number of partitions used for control signal generation.	98
Table 6.1	Procedure of the proposed decentralized algorithm.	105
Table 6.2	Computational complexity per sample of different algorithms.	112

Abbreviations

WHO	world health organization
NIOSH	national institute for occupational safety and health
ANC	active noise control
ADC	analog-to-digital converter
DAC	digital-to-analog converter
FIR	finite impulse response
IIR	infinite impulse response
LMS	least mean square
FxLMS	filtered-x least mean square
NLMS	normalized least mean square
FBPM	feedback path modelling
FBPN	feedback path neutralization
FBPMN	path modelling and neutralization
CS	convergence speed
NR	noise reduction
FxAP	filtered-x affine projection
FAP	fast affine projection
VSS	variable step size
FxLMF	filtered-x least mean fourth
FxGMN	filtered-x generalized mixed norm
FFT	fast Fourier transformation
IFFT	inverse fast Fourier transformation
FBFxLMS	frequency domain block FxLMS
MDF	multidelay adaptive filter
PBFDAF	partitioned block frequency domain adaptive filter
FPBFxLMS	frequency domain partitioned block FxLMS
DANC	decentralized active noise control

FxLMS/F	filtered-x least mean square and fourth
A-FxLMS/F	affine combination of the FxLMS/F
S/P	serial-to-parallel converter
P/S	parallel-to-serial converter
TFPBFxLMS	time-frequency domain delayless partitioned block FxLMS
GA	genetic algorithm
MSE	mean square error
EF	extended filtering
SNR	signal to noise ratio
AR	autoregressive
ANR	averaged noise reduction

Abstract

As the side effect of urbanization, acoustic noise from various sources is the most common health threat in our day-to-day life. Passive noise control methods are constrained by several factors such as frequency content of noise, absorbing material type, thickness and geometry. Alternatively, active noise control method has emerged as a promising solution to control low-frequency noise cost-effectively. In an active noise control system, the acoustic path from the control source to the error microphone affects the control performance. If the reference microphone is placed in close proximity of the control source, an unwanted acoustic feedback signal from the control source will be captured by the reference microphone, which may lead to system instability. Furthermore, the adaptive control algorithms have a high computational complexity, which limits its application with high sampling frequency and the scalability of a control system for generating a larger quiet zone. Various algorithms have been proposed in literature for modelling acoustic paths, low-complexity implementation of single and multiple channel control systems. However, they are still constrained by factors such as computational complexity, noise reduction performance, causality issue and stability issue.

The objectives of this PhD research are to develop low-complexity algorithms for (1) online modelling of acoustic paths without affecting noise reduction performance, (2) achieving improved control performance at transient and steady state, (3) high sampling frequency operation and broadband noise control and (4) multiple channel decentralized algorithm for broadband noise control.

In the first aspect of this thesis, the online modelling of secondary path and feedback path are explored and two active control methods are proposed. One method is for online modelling of secondary path, and the other is for online modelling of feedback path.

Unlike the existing methods in literature, the proposed methods do not require auxiliary noise injection, rather uses the control signal and decorrelation filters to model the acoustic paths. The simulation results demonstrate the improved control performance and low computational complexity of the proposed method compared to the existing methods in literature.

In the second aspect of this thesis, an affine combination of adaptive filters are investigated for active control operation. Unlike the convex combination, the combining parameter in this linear combination is not constrained to lie in a specific interval and plays a vital role in deciding the overall control performance. An adaptation rule is developed for updating the combining parameter. The simulation results demonstrate that the proposed algorithm provides faster convergence and improved steady-state control performance.

In the third aspect of this thesis, a time-frequency domain flexible structure is proposed for active control operation, which has no signal path delay and is well suited for low-cost DSP implementation. The proposed structure divides the long filters into many equal partitions and carry out the control filter update in frequency domain while generating the control signal in both time and frequency domains. The simulation results using the measured acoustic paths in a duct and in a normal room demonstrate that the proposed structure maintains similar performance as that of the time domain algorithm but with much less computational complexity.

In the last aspect of this thesis, a multiple channel decentralized control algorithm is proposed to achieve the similar noise reduction performance as the centralized one. Auxiliary filters are introduced to filter the reference signal for control filter update and a unique design method is proposed to shape the frequency response of the auxiliary

filters. The simulation results using the measured acoustic paths demonstrate the efficacy of the proposed algorithm for broadband noise control.

In summary, online acoustic path modelling methods are proposed using the control signal; an affine combination of adaptive filters are proposed for improved control performance; a time-frequency domain flexible structure is proposed for active control operation for high sampling frequency operation; a decentralized algorithm is proposed to achieve similar noise reduction performance as the centralized one for broadband control.

Keywords: Active control system, online secondary path modelling, online feedback path modelling, computational complexity, decentralized control.

1 Introduction

As the side effect of urbanization, acoustic noise from various sources is the most common health threat in our day-to-day life, which includes discomfort, annoyance, hearing loss, cardiovascular diseases, cognitive impairment, sleep disturbance, and tinnitus (Kujawa & Liberman 2009; Münzel et al. 2014). The World Health Organization (WHO 2018) recently published a report that covers all aspects of negative effect of environmental noise and provided recommendation for protection of human health. According to National institute for occupational safety and health (NIOSH), the maximum allowable exposure time to a sound (say 85 dBA) in hours per day reduces significantly to half with an increase in sound pressure level by 3 dBA (Prince et al. 1997). Exposure to loud noise can lead to serious health threat. Therefore, there is a need for controlling acoustic noise for a quality life. The noise might be controlled at the source location or along the propagation path or at the receiving end.

1.1 Motivation and objectives

The methods to control acoustic noise are broadly classified into three categories such as passive, active and semi-active control. The passive control method is generally used to control acoustic noise at the source location by means of absorbing materials, however, the noise control performance depends on frequency content, absorbing material type, thickness and geometry. The passive control method earns its reputation for controlling high frequency noise and becomes less effective for low frequency noise. Alternatively, active noise control (ANC) method, which works on principle of destructive interference of acoustic waves have been emerged to control low frequency noise and cost-effective. The semi-active control method integrates both the passive and active control methods for an effective control of both high and low frequency noise. The unwanted noise is

called primary noise. The system uses control sources, also known as secondary sources, to generate anti-noise noise signal, which is of same magnitude and opposite phase to that of the unwanted noise (Elliott 2000; Hansen et al. 2012; Kuo & Morgan 1996). Several applications of ANC includes duct noise reduction (Kajikawa, Gan & Kuo 2012), noise cancelling headphones (Kuo et al. 2018; Kuo, Mitra & Gan 2006), vehicle interior noise control (Jung, Elliott & Cheer 2019; Lee et al. 2018), noise control in machines (Reddy, Panahi & Briggs 2010) and active headrest systems (Buck, Jukkert & Sachau 2018; Pawelczyk 2004). Although the ANC technology is tested successfully for several applications, most of them are prototype, and requires further development for availability to the end user at low cost.

In practice, the unwanted noise is time varying in nature, thus it is required to have an adaptive controller to generate the necessary anti-noise for effective noise control. A reference microphone is used for sensing the unwanted noise and the signal captured by the reference microphone is processed by the controller to generate an anti-noise signal that drives the control source. An error microphone is used to obtain residual noise. The controller equipped with an adaptive algorithm uses both the microphone signals to generate the necessary anti-noise. Depending on with and without the reference sensor, the ANC system is classified as feedforward or feedback system, respectively. This thesis is focused on feedforward ANC system.

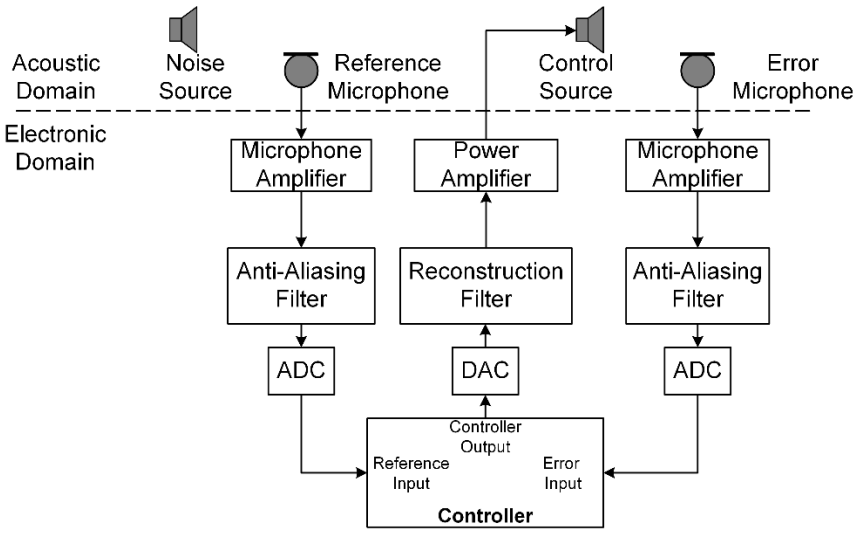

Figure 1.1 A basic single channel feedforward ANC system.

Figure 1.1 illustrates the basic single channel ANC system, where the primary noise is generated by the noise source, a reference sensor is placed upstream to capture the primary noise through a preamplifier, an anti-aliasing filter and an analog-to-digital converter (ADC). The sensed signal is processed by the controller and the generated anti-noise drives the control source through a digital-to-analog converter (DAC), a reconstruction filter, and a power amplifier. An error sensor is placed downstream to monitor the residual noise through a preamplifier, an anti-aliasing filter and an ADC. The controller is used in such way that the noise level is reduced near the error sensor. The acoustic path from the control source to the error sensor is called the secondary path or cancellation path. The controller used in an ANC system is an adaptive finite impulse response (FIR) filter, and its coefficients are updated using a suitable learning rule.

The filtered-x least mean square (FxLMS) algorithm is commonly employed in ANC system for control filter update. In the FxLMS algorithm, a model of the secondary path is used to filter the reference signal, which is further used to update the control filter coefficients. An imperfect model of secondary path affects the control performance (Saito & Sone 1996); hence offline modelling is adopted before control operation (Elliott 2000).

However, the acoustic path from control source to the error sensor is time varying in nature due to the environment such as variable operating temperature, change in flow rate, change in sound speed, surrounding changes and component aging. Therefore, an online modelling of secondary path is required. White noise can be used for online modelling the secondary paths; however, the injected white noise affects the noise reduction performance.

In certain applications, where the reference microphone is placed in close proximity of the control source, an unwanted acoustic feedback signal from the control source will be captured by the reference microphone. This acoustic feedback will lead to instability of the ANC system (Kuo & Morgan 1996). Directional sensors can be used to avoid such acoustic feedback; however the application is limited due to the poor directivity in low frequency range (Eghtesadi & Leventhall 1981). Non-acoustic sensors can be used to avoid the interference of feedback signal (Nelson & Elliott 1991). However, the available techniques are applicable for tonal noise only. The common method for solving the feedback problem is the FIR-based feedback neutralization, where a fixed neutralization filter is used to subtract the feedback signal from the reference signal. In certain applications, the feedback path is time varying in nature due to environment such as variable operating temperature, change in flow rate, change in sound speed, surrounding changes and component aging. Therefore, an online modelling of feedback path is utmost important. White noise can be used for online modelling the feedback paths; however, the injected white noise affects the noise reduction performance (Kuo 1999).

The FxLMS algorithm used for control filter update has a good balance among the convergence speed, noise reduction performance and computational complexity. On the other hand, its complexity increases significantly with the length of the secondary path model and the control filter. In some applications, the order of these filters can be very

high at the required sampling frequencies, which imposes a significant amount of computational burden for the implementations (Kuo & Morgan 1996; Song & Zhao 2019). The frequency domain FxLMS algorithms has been implemented by using block operation such as the frequency domain block FxLMS (Das, Panda & Kuo 2007) and partitioned block FxLMS (Rout, Das & Panda 2015) to reduce the computational burden. However, these algorithm cannot eliminate the associated block delay in the forward path, which is not desired for broadband control to maintain the causality requirement (Zhang & Qiu 2014). Unfortunately, the large size fast Fourier transform based frequency domain implementation of the FxLMS algorithm results in additional quantization error.

In a single channel ANC system, the noise is reduced around the error sensor. In order to control noise in a multidimensional space, i.e., for global noise control multiple channel ANC systems have been used (Elliott, Stothers & Nelson 1987; Kuo & Morgan 1996), where one or more reference sensor is used to capture the noise, multiple control sources are used to generate necessary anti-noise, multiple error sensors are deployed to monitor the residual noise around the zone of interest (Ferrer et al. 2008; Gonzalez et al. 2003). When the number of channel increases, the computational complexity of the adaptive algorithm increases dramatically. In addition, the cost of wiring, the communication overhead between the error sensors and the controller and the offline modelling of secondary paths limits its application. Decentralized ANC systems have been used in lieu of the centralized multiple ANC system to address above issues. However, the stability of the system cannot be guaranteed if the magnitude of the control signals are not limited, which in turn affects the noise reduction performance (Elliott & Boucher 1994).

Therefore, developing adaptive algorithms for online modelling of acoustic paths without affecting noise reduction, broadband noise control and multiple channel decentralized ANC system without stability issue are crucial. This motivated the research

of this PhD thesis to develop low-complexity adaptive algorithms for active control systems. Following an extensive literature survey and a study on the crucial issues in the area of active noise control, the objectives of this thesis are defined and listed below:

1. To develop a low-complexity algorithm for online modelling of the secondary path and the feedback path in ANC system without affecting noise reduction performance.
2. To develop an algorithm using linear combination of adaptive filters for improved control performance.
3. To develop a time-frequency domain flexible structure based on frequency domain adaptive filtering technique that is suitable for low-cost DSP implementation and controlling broadband noise with high sampling frequency.
4. To develop multiple channel decentralized algorithm for broadband noise control that can achieve similar noise reduction as that of the centralized counterpart.

1.2 Contributions

The main contributions of this thesis includes:

- proposing an active control method with online secondary path modelling using the control signal;
- proposing an active control method with online feedback path modelling using the control signal;
- proposing an affine combination of adaptive filters for faster convergence in transient state and lower residual noise at steady state;
- developing a time-frequency domain flexible structure based on frequency domain adaptive filtering technique for controlling broadband noise at high sampling rate and maintaining the causality requirement; and

- developing time domain decentralized algorithm for broadband noise control without sacrificing noise reduction performance.

1.3 Thesis outline

The thesis is organized into seven chapters including the introduction chapter.

Chapter 1: Introduction

This chapter gives a brief introduction to the area of active control and presents the motivation and objectives of this thesis. The contributions are also listed. An outline of the thesis is presented.

Chapter 2: Literature review

This chapter gives an extensive and critical literature review in the field of active noise controls, which includes online secondary path modelling, online feedback path modelling, improving convergence speed and noise reduction performance, low-complexity frequency domain implementation of the control algorithms and multiple channel ANC system for global noise control.

Chapter 3: Online modelling of acoustic paths in active control systems using control signal

This chapter describes the methodology adopted for online modelling of the acoustic paths without using auxiliary noise. With an objective to improve the control performance in a scenario of time-varying secondary path, a practical method with online secondary path modelling is proposed without using auxiliary white noise. The proposed method consists of five stages such as the primary path estimation, controller initialization, secondary path estimation, primary and secondary path change detection and active control operation. Adaptive decorrelation filters have been deployed to accelerate the secondary path modelling process. Furthermore, a four-stage method is proposed to carry

out online feedback path modelling with the control signal, which consists of controller initialization, feedback path modelling using decorrelation filters, active control operation, and feedback path change detection for maintaining the control operation. Adaptive decorrelation filters are used to increase the feedback path modelling performance. Numerical experiments reveal the effectiveness of the proposed methods.

Chapter 4: Affine combination of adaptive filters for active control

The commonly used FxLMS algorithm has a trade-off between the convergence speed and noise reduction performance, and an imperfect secondary path model and long control filter has significant effect on the convergence behaviour. In this chapter, an affine combination of adaptive filters is proposed to achieve both faster convergence and better noise reduction performance. Unlike the convex combination approach, the mixing parameter in the proposed approach is not forced to lie in any restricted interval and does not need any exponential function evaluation, thereby reduces the computational burden. The improved control performance has been illustrated through numerical experiments.

Chapter 5: A time-frequency domain flexible structure for active control

Frequency domain FxLMS algorithms can reduce the computational complexity of the time domain implementation with long filters, but it suffer from large block delay, additional quantization error and implementation difficulties in existing DSP hardware. In this chapter, an attempt has been made to design a time-frequency domain flexible structure to remove the signal path delay for low-cost DSP implementation while maintaining low computational complexity. Numerical experiments using measured acoustic paths demonstrate the usefulness of the proposed structure for broadband control.

Chapter 6: Decentralized algorithm for broadband active control

A single channel ANC system cannot control noise in a multidimensional space. Multichannel ANC systems have been used for generating a larger zone of quiet at the cost of high computational load, cost of wiring and communication overhead between sensors. A decentralized algorithm is developed in this chapter for active control of broadband noise which can achieve similar noise reduction performance as that of the centralized counterpart with much less computational complexity. Numerical experiments using measured acoustic paths reveal the effectiveness of the proposed algorithm for broadband control.

Chapter 7: Conclusions and future work

The concluding remarks are drawn in this chapter. This chapter also discusses areas in which work may be carried out in the future.

2 Literature review

This chapter provides a brief overview of the background knowledge concerning the ANC systems. Firstly, the operation of a single channel feedforward ANC system using the FxLMS algorithm is described. Secondly, several online modelling of secondary path approaches are reviewed. Thirdly, the effect of acoustic feedback and existing solutions for online modelling of acoustic feedback paths are discussed. Fourthly, some existing approaches are reviewed for faster convergence and lower residual noise for ANC systems. This is followed by a review of several low-complexity algorithms for controlling broadband noise at high sampling frequency. Finally, a review of the decentralized multiple channel active control system is presented. At the end of this chapter, the research questions are identified.

2.1 Single channel feedforward ANC system

The ANC systems, based on system identification, are widely used as they are able to control both narrowband and broadband noises. Furthermore, they have potential benefits in size, weight, volume and cost. Since the acoustic characteristics and environment are time varying in nature, the ANC system must generate anti-noise adaptively. Adaptive filters such as adaptive FIR and adaptive IIR filter are used to accomplish this task. The most common form of adaptive filter is the transversal filter, which uses least mean square (LMS) algorithm (Haykin 2005).

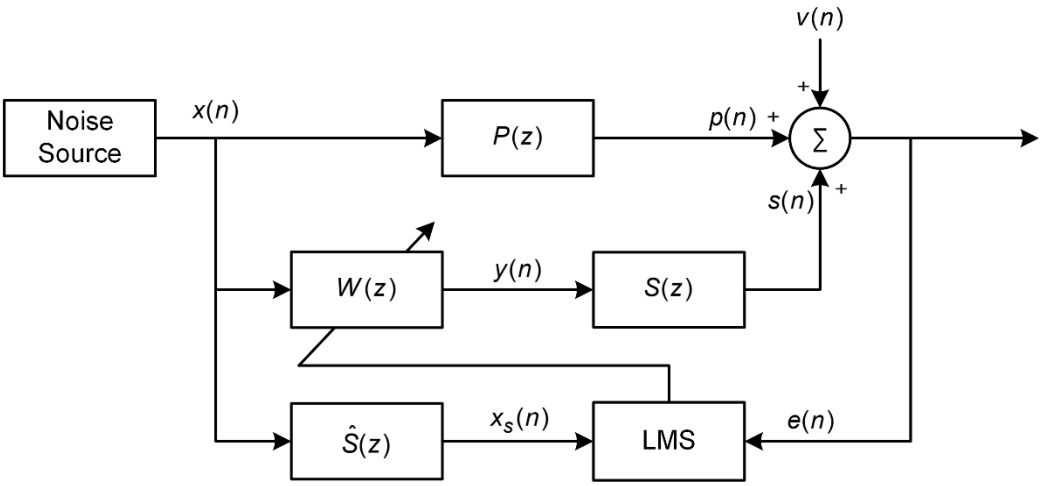

Figure 2.1 Schematic block diagram of a single channel ANC system.

The schematic block diagram of a single channel feedforward ANC system is depicted in Figure 2.1. The acoustic path (transfer function) $P(z)$ represents primary path transfer function between the noise source and the error microphone, which includes a DAC, reconstruction filter and the power amplifier before noise source and microphone amplifier, anti-aliasing filter and ADC after error microphone (see Figure 1.1). The acoustic path $S(z)$ represents secondary path transfer function between the control source and the error microphone, which includes a DAC, reconstruction filter and the power amplifier before control source and microphone amplifier, anti-aliasing filter and ADC after error microphone. $p(n)$ is the unwanted noise reaching the error microphone, $v(n)$ is the measurement noise associated with the system, $s(n)$ is the anti-noise reaching the error microphone, $y(n)$ is the controller output signal. The presence of the physical path between the controller and the error sensor leads to instability when adapted using the LMS algorithm. To alleviate this problem, the FxLMS algorithm was developed, which uses $x(n)$ filtered through a model of the secondary path $\hat{S}(z)$ as the reference signal for the conventional LMS algorithm (Bjarnason 1995; Morgan 1980).

From Figure 2.1, the residual error signal can be represented as (neglecting $v(n)$)

$$e(n) = p(n) + s(n) \tag{2.1}$$

where $s(n) = \boldsymbol{s}^{\mathrm{T}}(n)\boldsymbol{y}(n)$, $\boldsymbol{s}(n) = \left[s_0(n), s_1(n), \dots, s_{L_s-1}(n)\right]^{\mathrm{T}}$, $\boldsymbol{y}(n) = [y(n), y(n-1), \dots, y(n-L_{\mathrm{s}}+1)]^T$, $y(n) = \boldsymbol{w}^{\mathrm{T}}(n)\boldsymbol{x}(n)$, $\boldsymbol{w}(n) = \left[w_0(n), w_1(n), \dots, w_{L_w-1}(n)\right]^{\mathrm{T}}$, $\boldsymbol{x}(n) = [x(n), x(n-1), \dots, x(n-L_{\mathrm{w}}+1)]^{\mathrm{T}}$, L_{w} is length of control filter and L_{s} is the length of secondary path. The cost function of the mean square is assumed as

$$\zeta(n) = E[e^2(n)], \tag{2.2}$$

and the adaptive filter minimizes the instantaneous squared error $\zeta(\mathrm{n}) = e^2(n)$. Using the steepest descent algorithm, the weight vector is updated in the negative gradient direction with step size μ

$$\boldsymbol{w}(n) = \boldsymbol{w}(n) - \frac{\mu}{2}\nabla\hat{\zeta}(n) \tag{2.3}$$

where $\nabla\hat{\zeta}(n)$ is the instantaneous estimate of the mean square error (MSE) gradient at time *n*, which is expressed as

$$\nabla\hat{\zeta}(n) = \nabla e^2(n) = 2[\nabla e(n)]e(n). \tag{2.4}$$

From Eq. (2.1), we have $\nabla e(n) = \boldsymbol{x}_{\mathrm{s}}(n)$, where $\boldsymbol{x}_s(n) = [x_s(n), x_s(n-1), \dots, x_s(n-L_{\mathrm{w}}+1)]^T$ with $x_{\mathrm{s}}(n)$ is the signal $x(n)$ filtered through $S(z)$. The gradient estimate becomes

$$\nabla\hat{\zeta}(n) = 2\boldsymbol{x}_{\mathrm{s}}(n)e(n). \tag{2.5}$$

Substituting Eq. (2.4) in (2.3), we have

$$\boldsymbol{w}(n) = \boldsymbol{w}(n) - \mu\boldsymbol{x}_{\mathrm{s}}(n)e(n). \tag{2.6}$$

In practice, $S(z)$ is unknown and must be estimated by a filter $\hat{S}(z)$. Hence, the filtered reference signal $x_{\mathrm{s}}(n)$ is generated by passing $x(n)$ through the model of secondary path $\hat{S}(z)$. The expression in Eq. (2.6) is called FxLMS based update rule. The FxLMS algorithm is forbearing to the error between the physical secondary path and its model,

which is generally obtained offline before control operation. A variation of the FxLMS algorithm such as the Leaky FxLMS is proposed to enhance the control performance of the FxLMS algorithm (Tobias & Seara 2005; Wu, Qiu & Guo 2018).

For the purpose of analysis, neglecting the measurement noise $v(n)$, the z-transform of the error signal is represented as

$$E(z) = [P(z) + S(z)W(z)]X(z). \tag{2.7}$$

After convergence of the adaptive filter $W(z)$, the residual error is zero (i.e., $E(z) = 0$). This requires to realize the optimal transfer function of the control filter as

$$W(z) = \frac{-P(z)}{S(z)} \tag{2.8}$$

From Eq. (2.8), it is clear that adaptive filter $W(z)$ has to simultaneously model $P(z)$ and inversely model $S(z)$. If $S(z)$ is a minimum phase filter, $W(z)$ can inversely model it. However, an inverse model of a non-minimum phase $S(z)$ is not stable. Hence it is expected that a near perfect control is possible in case of a minimum phase secondary path, and perfect control cannot be achieved for non-minimum phase secondary path. The optimal control filter can be expressed using the Weiner solution as (Elliott 2000)

$$\boldsymbol{w}_{opt} = \boldsymbol{R}_{x_s x_s}^{-1} \boldsymbol{r}_{x_s p} \tag{2.9}$$

where $\boldsymbol{R}_{x_s x_s} = E[\boldsymbol{x}_s(n)\boldsymbol{x}_s^{\mathrm{T}}(n)]$ is the autocorrelation matrix of the filtered reference signal, $\boldsymbol{r}_{x_s p} = E[\boldsymbol{x}_s(n)p(n)]$ is the cross-correlation vector between the filtered reference signal and unwanted disturbance signal $p(n)$.

The above discussed FxLMS algorithm has a trade-off between convergence speed and noise reduction performance. It is also assumed that a perfect estimate of the secondary path is available before control operation. It is also assumed that there is no acoustic feedback from the control source to the reference sensor. However, in several ANC applications, the reference signal is contaminated by the unwanted signal leading to

ANC system instability. The computational complexity of the algorithm also increases drastically with large control filter and secondary path model at high sampling frequency. The single channel ANC system is well-suited for controlling both narrowband and broadband disturbances, and the noise control is possible around the error sensor with a spatial limit being approximately $\lambda_{max}/10$, where λ_{max} is the wavelength of the highest undesired disturbance frequency (Lorente et al. 2014). Therefore, to achieve noise control over a larger area, multiple channel ANC system is required, which in turn increases the computational complexity, cost of wiring and communication overhead between sensors and control sources.

2.2 Online secondary path modelling

The FxLMS algorithm used in the active control system is tolerant to modelling error between $S(z)$ and $\hat{S}(z)$. Within the limit of slow adaptation, the algorithm can converge with approximately 90° of phase error (Elliott 2000; Saito & Sone 1996). Offline modelling can be used to estimate the secondary path for ANC applications. However, in certain applications, the secondary path is time varying due to the acoustic surrounding, so online secondary path estimation is needed (Hansen et al. 2012; Kuo & Morgan 1996).

White noise can be used to estimate the secondary path online (Eriksson & Allie 1989). In this method, the injected white noise is mixed with the residual error signal, thereby affecting the noise reduction performance. A modelling technique is reported for both online and offline modelling of secondary path in the presence of primary disturbance, where adaptive prediction error filters are used to eliminate the effect of interference in the modelling process (Kuo & Vijayan 1997). An online secondary path modelling method has been proposed using an adaptive filtering with averaging based filtered-x algorithm in control process, in which the interference in the secondary path modelling process is removed quickly thereby leading to faster convergence (Akhtar, Abe &

Kawamata 2005). However, it has poor tracking performance. A two adaptive filter-based method has been proposed in which the modified FxLMS algorithm is used in adapting the control filter and a new variable step size LMS algorithm is used for adapting the secondary path estimation filter (Akhtar, Abe & Kawamata 2006). An optimal variable step size algorithm is proposed for updating both the control and secondary path estimation filters along with a self-tuning power scheduling strategy for the auxiliary noise (Carini & Malatini 2008). A power scheduling algorithm is proposed to increase the convergence speed when sudden changes happen in the secondary path (Lopes & Gerald 2015). However, these algorithms involve complicated power scheduling strategy or proper selection of crucial tuning parameters, which in turn increases the computational burden. To make it easy for implementation, a three adaptive filter-based ANC system is reported with a simple power scheduling method and regularized step size for secondary path estimation (Yang et al. 2018). A stage switching algorithm is recently proposed, in which the secondary path modelling and control filter update are separated based only on the residual error signal. In addition, a scheduled step size normalized least mean square algorithm is adapted for robust operation (Kim, Hur & Park 2020).

The control signal can be used for online secondary path modelling as well but often with a biased estimation (Kuo & Morgan 1999). An overall online secondary path modelling is capable of reducing the bias by introducing an extra adaptive filter to model the primary path. The LMS algorithm is used to estimate both the primary and the secondary paths simultaneously, while the control filter is updated with the FxLMS algorithm. The convergence of this algorithm is highly reliant on the control signal characteristics. Unlike the white noise injection method, the estimated secondary path must be copied more frequently to the FxLMS algorithm for smooth operation of active

control system, which in turn requires faster and reasonable accurate modelling of the secondary path.

A modified FxLMS algorithm based on offline and online secondary path modelling is proposed to control transformer noise (Zhao et al. 2017). The secondary path estimated offline is used as the initial value for online modelling, which uses control signal for secondary path estimation. An estimate of the primary path obtained offline is also used to remove the disturbance in modelling the secondary path. However, the system fails if the primary path changes. The change in primary path hinders the convergence of the secondary path estimation and ANC operation. Recently, an online secondary path modelling was studied for a single channel ANC system from the view point of acoustic echo cancellation, where it was found that an effective secondary path modelling is possible as long as the control filter is sufficiently large. In addition, without any restriction on control filter length, the time varying nature of the control filter also facilitates the effective modelling (Hu et al. 2019). The proposed method was extended for online modelling of secondary paths in multiple channel ANC system (Hu, Xue & Lu 2019). However, the change in primary path degrades the secondary path modelling and ANC operation.

Several active control algorithms that do not require secondary path estimation have been proposed. A delayed-x least mean square algorithm was investigated for active control operation for narrow band noise by approximating the secondary path model as a delay, where the delay is estimated using an adaptive delay estimation method (Kim & Park 1998). A direction selection update algorithm can choose either a positive or a negative direction for adaptive control by monitoring the excess residual noise power (Zhou & DeBrunner 2007). To increase the converge speed of the algorithm when the phase angle of the secondary path is close to ±90°, a frequency domain delayless subband

architecture has been proposed, where four update directions are used to minimize the error signal (Wu, Chen & Qiu 2008). Nevertheless, the architecture possesses high computational complexity as the weight update is performed in frequency domain. To reduce the implementation complexity, a simplified subband structure is proposed, which is more flexible (Gao, Lu & Qiu 2016). However, the convergence of these algorithms is much slower than the conventional FxLMS algorithm.

In summary, most of the existing online secondary path modelling techniques were based on injection of auxiliary white noise and complicated power scheduling strategies, which in turn affects the noise reduction performance and adds computational burden to the algorithm. Furthermore, the online modelling of the secondary path using control signal were found to be ineffective when the primary path changes. Though several methods that does not require the secondary path modelling were proposed, they are limited by their convergence behaviour. Therefore, a method is desired for online modelling of secondary path without injection of auxiliary white noise when both the primary and secondary path changes.

2.3 Online feedback path modelling

The signal generated by the control source in an ANC system propagates towards the reference sensor and the error sensor. Therefore, the anti-noise not only cancels the primary disturbances, but also corrupts the reference signal. In scenarios, where the ANC system is very small, the close proximity between the reference microphone and control loudspeaker leads to a very strong acoustic feedback. This feedback degrades the noise reduction performance of the ANC system and sometimes the ANC system becomes unstable.

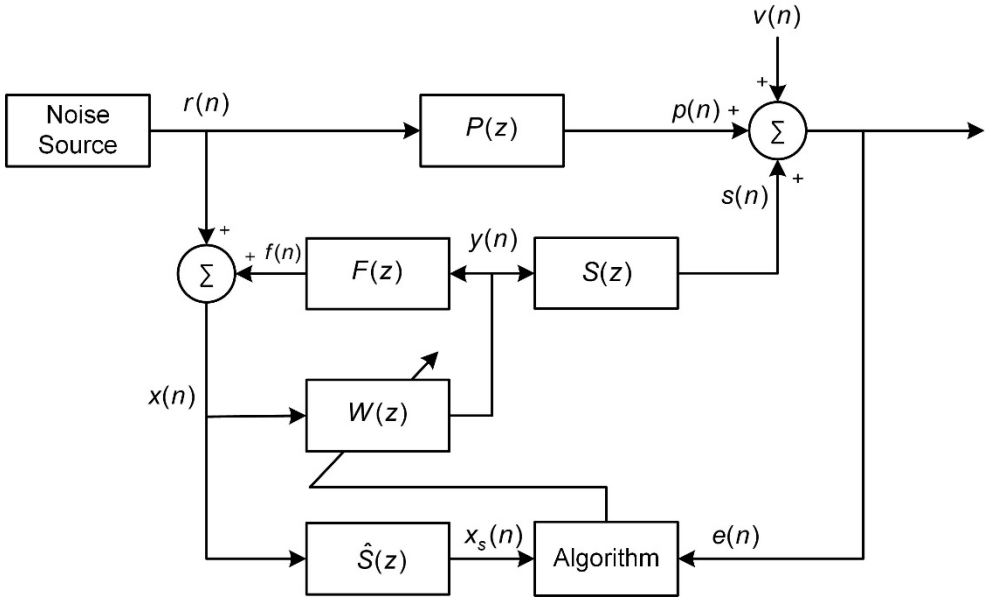

Figure 2.2 Schematic block diagram of ANC system with acoustic feedback.

Figure 2.2 illustrates the schematic block diagram of a single channel ANC system in the presence of acoustic feedback. The acoustic path $F(z)$ represents the feedback path transfer function between the control source and the reference microphone. The only difference between Figure 2.1 and Figure 2.2 is the presence of acoustic feedback. The z-transform of the error signal is represented as

$$\begin{aligned} E(z) &= P(z)R(z) + S(z)Y(z) \\ &= P(z)R(z) + S(z)\frac{W(z)R(z)}{1-W(z)F(z)}. \end{aligned} \tag{2.10}$$

After convergence of the adaptive filter $W(z)$, the residual error is zero (i.e., $E(z) = 0$). This requires the optimal transfer function of the control filter to converge to

$$W(z) = \frac{-P(z)}{S(z) - P(z)F(z)} \tag{2.11}$$

The above analysis indicates that the acoustic feedback will cause the system instability if the coefficients of the $W(z)$ are large enough so that $W(z)\,F(z) = 1$ at some frequency and the control filter cannot converge to the ideal optimal solution.

Several approaches have been proposed to overcome this issue. Directional microphones and loudspeakers can be used to avoid the acoustic feedback (Canevet 1978; Eghtesadi & Leventhall 1981). However, these techniques are expensive, the directivity is poor in the low frequency range and the performance is limited. The use of non-acoustic sensors to obtain the reference signal avoids the acoustic feedback, but the existing one is only applicable for narrowband and tonal noise control (Chaplin & Smith 1983; Ziegler Jr 1989).

Signal processing techniques have been used to overcome the feedback issues. The IIR based adaptive feedback neutralization methods have been proposed, but are constrained by the local minimum solution and stability issue (Crawford & Stewart 1997; Eriksson 1991). To address the stability issue of the IIR adaptive filtering, the lattice form IIR filter is introduced (Lu et al. 2003). However, the algorithm assumes that the acoustic feedback is very weak and the feedback loop gain is much less than unity at all frequencies. The most popular method for solving the feedback problem is the FIR based feedback neutralization, where a fixed neutralization filter is used to subtract the feedback signal from the reference signal (Kuo & Morgan 1996; Warnaka, Poole & Tichy 1984). Incorporating frequency weighted penalties, a robust controller was designed with a fixed feedback neutralization filter to control noise in a ventilation duct system (An et al. 2019). In some applications, the feedback path is time varying, so online feedback path modelling is needed to ensure the stability of the ANC system.

Auxiliary noise generated by a white noise generator can be injected into the system for online feedback path modelling, but the injected signal is mixed with the residual noise and deteriorates the noise reduction performance (Kuo 2002). A three adaptive filter based method (Akhtar, Abe & Kawamata 2007) has been proposed to control both the predictable and broadband noise with online feedback path modelling using auxiliary

noise, in which an adaptive control filter is used to update the control coefficients, a feedback path modelling filter is used to compensate the acoustic feedback, and the third filter is used to remove the disturbance during the modelling of the feedback path. Nevertheless, the above method uses separate filters for feedback path modelling (FBPM) and feedback path neutralization (FBPN), which in turn increases the computational burden.

A computationally efficient feedback path modelling and neutralization (FBPMN) method has been proposed for multichannel active noise control systems by combining the FBPM and FBPN filters into a single FBPMN filter (Akhtar et al. 2009). A variable step size technique has been used for updating the coefficients of the FBPMN filter, which improves the performance of the online feedback path modelling for both the single channel and multiple channel ANC system (Akhtar & Mitsuhashi 2011). A robust variable step size method for feedback path modelling and neutralization in a single channel narrowband system is proposed to achieve faster convergence (Haseeb et al. 2018). However, in all the above methods, the injected auxiliary noise affects the noise reduction performance.

A power scheduling strategy was imposed for the auxiliary noise used for modelling the feedback path to meet the conflicting requirement of faster convergence of feedback path modelling and lower steady-state residual error (Ahmed, Akhtar & Zhang 2013). A three adaptive filter based method (Ahmed & Akhtar 2016) has been proposed including a control filter, linear prediction filter and FBPMN filter for both single channel and multiple channel ANC system, which uses a tuning free gain scheduling strategy for injection of auxiliary noise. Recently, a feedback path neutralization filter is used to compensate feedback and a time varying gain is incorporated for generating the auxiliary noise (Tufail et al. 2019). Furthermore, a self-adapting variable step size normalized least

mean square algorithm is proposed for acoustic feedback path modelling, in which the gain of the auxiliary noise power is varied according to the modelling accuracy (Aslam, Shi & Lim 2021).

In summary, the online modelling of feedback path using auxiliary noise and gain scheduling strategy have been studied by several researchers; however, the proposed approaches either have limitation on noise reduction due to the former or computational complexity due to the later. Therefore, a method is desired for online modelling of feedback path without injection of auxiliary white noise for effective control operation.

2.4 Convergence behaviour and noise reduction performance

The FxLMS algorithm commonly employed in active noise control systems uses an adaptive filter for generating the control signal, and the performance of the systems is highly reliant on the transient and steady-state behaviour of the control filter (Ardekani & Abdulla 2010). Despite having a simple structure, the FxLMS algorithm with a fixed step size maintains a balance between convergence speed (CS) and noise reduction (NR). Furthermore, the imperfect secondary path model and long-tap control filter affect the convergence.

In order to circumvent the above issue, variable step size (VSS) techniques have been incorporated with the FxLMS algorithm with moderately increased computational load (Chang & Chu 2013; Huang et al. 2012). Filtered-x affine projection (FxAP) algorithms have been proposed to improve the convergence behaviour of the control filter (Carini & Sicuranza 2007). An optimal variable step-size filtered-x affine projection algorithm for active control has been proposed (Song & Park 2015). Furthermore, fast affine projection (FAP) based single channel and multiple channel ANC systems have been proposed (Bouchard 2003). However, the FxAP algorithms exhibit a trade-off between the

convergence speed and computational complexity as a result of increased projection order and matrix inversion operation.

Convex combination of adaptive filters have been proposed to achieve improved performance in transient and steady-state, in which the overall adaptive filter exploits the abilities of the component filters (Arenas-Garcia et al. 2015; Arenas-Garcia, Figueiras-Vidal & Sayed 2006). Furthermore, a convex combination of variable tap-length LMS algorithms for a low signal-to-noise environment is proposed (Zhang & Chambers 2006). Several researchers have integrated the convex combination into the ANC systems, in which multiple control signals are combined to produce the necessary cancelling signal. A convex combination of the FxLMS algorithms with different step sizes has been proposed for single channel and multiple channel feedforward ANC systems, which is shown to outperform the variable step size-FxLMS algorithm (Ferrer et al. 2012). Motivated by the limiting performance the FxLMS algorithm under low signal-to-noise environment, the filtered-x least mean fourth (FxLMF) and leaky-FxLMF algorithms are studied; moreover, the convex combination strategy of the FxLMF algorithms with different step sizes has been introduced for active control (Al Omour et al. 2016). A filtered-x generalized mixed norm (FxGMN) algorithm and its convex combination have been reported (Song & Zhao 2018). In order to exploit the advantages of both the least mean square and fourth based learning rule, recently, a FxLMS/F algorithm is introduced for ANC applications (Song & Zhao 2019); with an aim to boost the control performance of the FxLMS/F in both transient and steady state, a convex combination strategy is integrated. A convex-combined step size based modified normalized FxLMS algorithm has been proposed for active control of impulsive noise, where the step-size is automatically tuned by a combining parameter (Akhtar 2020). The combining parameter in all the above convex combination strategies are restricted to lie in the range (0,1) and

requires an exponential function evaluation, thereby increasing the computational burden of the algorithm.

In summary, several approaches have been proposed to achieve faster convergence and lower residual noise for effective control operation, which includes variable step size techniques, affine projection algorithms and convex combination of adaptive filters. Though the control performance of the convex combination approach is promising, its computational complexity is increased. Therefore, it is desired to reduce the computational load of the combination strategy for active control.

2.5 Low-complexity algorithms for active control at high sampling rate

In order for active noise control systems to be effective at higher frequencies and generate larger quite zones, high sampling frequency and multiple channel ANC system have to be adopted. The most commonly used algorithm in ANC is the filtered-x least mean square (FxLMS) algorithm, which has a good balance among the convergence speed, noise reduction performance and computational complexity. However, its complexity increases significantly with the length of the secondary path modelling filter and the control filter. In some applications, the order of these filters can be very high at the required sampling frequencies, which imposes a significant amount of computational burden for the implementations (Elliott 2000; Hansen et al. 2012; Kuo & Morgan 1996).

Many approaches have been proposed to reduce the computational burden of the ANC systems such as the decentralized ANC system (Elliott & Boucher 1994), distributed ANC system (Ferrer et al. 2015; Kukde, Manikandan & Panda 2019) and subband techniques (Park et al. 2001; Qiu et al. 2006; Thi & Morgan 1993). The frequency domain adaptive filtering techniques reduce the computational complexity by exploiting the advantages of the Fast Fourier Transformation (FFT) to implement the convolution and

correlation operations (Ferrara 1980; Shynk 1992). There are two ways to implement the FxLMS algorithm in frequency domain. One is carrying out both the control signal generation and control filter update in frequency domain, while the other generates control signal in time domain and does control filter update in frequency domain.

The frequency domain FxLMS algorithm can be implemented by using block operation (Shen & Spanias 1992; Shen & Spanias 1996). An efficient implementation of the frequency domain block FxLMS (FBFxLMS) has been proposed (Das, Panda & Kuo 2007), where all the filtering and weight update operations are carried out in frequency domain. The authors also proposed Fast Hartley Transform based ANC structure. Later, the work has been extended to the multiple channel active control systems (Das & Satapathy 2008). In order to reduce the computational burden of the time domain virtual FxLMS algorithm, a block frequency domain virtual ANC algorithm has been proposed (Das, Moreau & Cazzolato 2013). A combining strategy of the bin-normalized frequency domain block LMS algorithm (Farhang-Boroujeny & Chan 2000) and the modified frequency domain block LMS algorithm (Lu, Qiu & Zou 2014) has been proposed for ANC to exploit the advantages of the former and the later in both transient and steady states (Wang et al. 2019). A zero forcing block adaptive filtering technique is proposed for active noise control incorporating the filter adaptation on a block-by-block basis in the frequency domain and control signal generation in the time domain thereby reducing the complexity and minimizing the latency (Gaiotto et al. 2020).

For some applications, it is hard to use large block size in the FBFxLMS algorithm. For example, the algorithm introduces a delay of at least one block size for control signal generation, and the delay might violate the causality constraint for broadband control (Kong & Kuo 1999; Zhang & Qiu 2014). Furthermore, most of the available DSP processors are designed and optimized for small size FFT operation, typically 256 points,

and large size FFT implementation might introduce additional quantization errors due to the increased number of multiplications and scaling operations (Soo & Pang 1990).

The multidelay adaptive filter (MDF), which is also known as the partitioned block frequency domain adaptive filter (PBFDAF), has been studied extensively to address the issues raised due to the large block size. In MDF, a long filter is partitioned into small sub-filters so that the small size FFT can be implemented to reduce the block processing delay and memory requirement (Borrallo & Otero 1992; Soo & Pang 1990). The convergence of the PBFDAF algorithms has been analysed (Chan & Farhang-Boroujeny 2001; Moulines, Amrane & Grenier 1995). A generalized framework is recently studied for the transient analysis of both the constrained and unconstrained PBFDAF algorithms (Yang, Enzner & Yang 2019), where the expression for mean and mean square performance are derived. A frequency domain partitioned block FxLMS (FPBFxLMS) algorithm has been proposed to reduce the computational complexity and delay in the control signal generation (Rout, Das & Panda 2015). However, this algorithm cannot eliminate the associated delay in the forward path, and might affect the performance for broadband control.

In some ANC applications, some part of the primary disturbance might take a very short time to propagate from the noise source to the error microphone. In such a situation, the block size in the FPBFxLMS algorithm for control signal generation must be less than the delay to account for this part of the primary disturbance. Nevertheless, a small block size would reduce the efficacy of implementing the FFT. Hence, there is a desire to eliminate the associated block delay completely and yet exploit the advantages of the FFT operation. In the context of acoustic echo cancellation, some delayless PBFDAF algorithms have been studied using time-frequency structures (Bendel et al. 2001; Yang, Wu & Yang 2013; Zhou, Chen & Li 2007).

In summary, several transform domain algorithms such as block frequency domain and partitioned block frequency domain algorithms have been proposed to reduce the computational complexity of the time domain implementation of ANC systems. However, these algorithms have a trade-off between the block delay and computational complexity. Large delay might affect the causality requirement for broadband control and small delay reduces the efficacy of transform domain implementation. Therefore, an adaptive filtering technique is a desirable to eliminate the block delay completely and reduce the computational complexity simultaneously.

2.6 Decentralized algorithms for active control

The FxLMS algorithm is the most commonly used algorithm in ANC applications due to its robustness and low computational complexity. To achieve global noise control, a centralized multiple channel ANC system can be employed, which requires many secondary path models for generating the filtered reference signals and all the error signals to update the control filters (Kuo & Morgan 1999). When the number of channels increases, the computational complexity of the centralized algorithm increases significantly, and the complexity and cost of wiring and communication overhead between error sensors and the controller cause a big problem (George & Panda 2012; Shi et al. 2019).

Many approaches have been proposed to reduce computational complexity of multiple channel systems. A mixed-error approach has been proposed by combining all the error signals into one and used it for centralized control (Murao et al. 2017); however, the system possesses high communication load to feed all the error signals to the centralized controller. Alternatively, a distributed control approach has been proposed by considering each secondary source as a node in a ring network, in which the computational burden is distributed across all the nodes, but at the cost of high transmission bandwidth and delay

(Ferrer et al. 2015). Recently, a distributed control strategy is reported using multiple channel filtered-x affine projection algorithm with a ring topology and incremental communication, where strategies have been proposed to lessen the computational burden (Ferrer et al. 2020).

Due to their low computational complexity, reduced wiring cost, and flexibility of scaling up, decentralized multiple channel ANC systems are attractive in many applications, in which a number of smaller subsystems are employed to update the control filter independently with only the associated error signal. A study on a two channel frequency domain decentralized ANC (DANC) system shows that the system stability cannot be maintained if the control signals are not constrained in magnitude (Elliott & Boucher 1994). A practical stability condition for decentralized feedback ANC systems has been derived by taking into account the geometrical configuration of secondary sources and error sensors (Leboucher et al. 2002). It has been found that reducing the number of channels and the distance between secondary loudspeakers and error microphones can increase system stability but at the cost of smaller noise reduction (Tao et al. 2016). A decentralized scheme for active noise control from a game-theory standpoint was studied, in which the Nash equilibrium is formalized to examine the interaction between the controllers for ensuring system stability (Quintana & Patino 2018). A decentralized feedback control strategy using the H^{∞} method for each controller is applied for active control of sound inside the automobile cabin by considering the uncertainty caused by the movement of the occupants (Ghanati & Azadi 2020).

Recently, it is shown that a two channel DANC system can achieve the same noise reduction performance as the centralized one by shaping the eigenvalues of a 2×2 matrix for each frequency bin properly such that they lie on the right complex domain (Zhang et al. 2018). However, it only considers single frequency. An *et al*. proposed a time domain

multiple channel DANC system for controlling periodic disturbances recently, but their method has two limitations (An, Cao & Liu 2018). First, N nonlinear equations are required to be solved to shape the eigenvalues of an $N \times N$ matrix for each frequency, which remains an open problem without knowing whether a solution exists or not; second, when converting the solution from frequency to time domain, the design of the auxiliary filter to filter the reference signal (to be used in the FxLMS algorithm) is complicated. The sensitive shaping parameters and the filter delay introduced in their system affect the convergence speed of the control algorithm. By generalizing the eigenvalue shaping approach by An *et al.* (2018), a DANC system is proposed for overdetermined ANC system for controlling periodic disturbances (An, Cao & Liu 2021). However, the convergence behaviour exhibits some ripples. Though the convergence ripples can be restricted by a criterion function, the complete removal of ripple is not guaranteed.

In summary, the decentralized algorithms are effective in reducing the computational burden and cost of implementation compared to the centralized counterpart. However, the stability of the algorithms cannot be guaranteed and the noise reduction might be affected. Though certain decentralized algorithms can achieve similar noise reduction as that of centralized algorithm, they are effective for single frequency or periodic disturbances. Little research has been done for controlling broadband noise using decentralized algorithm. Therefore, it is desirable to develop a multiple channel decentralized algorithm for broadband noise control.

2.7 Summary

This chapter presents an extensive literature review on the online modelling of acoustic paths for active control operation, improving convergence and noise reduction performance, low-complexity algorithms at high sampling operation and decentralized multiple channel active control systems. In Section 2.1, the basic operation of a single

channel feedforward ANC system is presented. Several algorithms for online modelling of secondary path are summarized in Section 2.2, which includes auxiliary white noise injection and auxiliary noise power scheduling strategies. A few methods that does not require secondary path modelling are also briefed. In Section 2.3, several algorithms for online modelling of feedback path are summarized including the auxiliary white noise injection and power scheduling strategies. These sections provide the background knowledge for the two proposed methods for online modelling of acoustic paths using the control signal. One is for online modelling of secondary path, and the other is for online modelling of feedback path.

In Section 2.4, several algorithms for active control are summarized for faster convergence and better noise reduction performance, which includes variable step size approaches, affine projection algorithms and convex combination of adaptive filters. This motivates to develop low-complexity algorithm for faster convergence in transient state and lower residual noise at steady state.

In Section 2.5, computationally efficient transform domain control algorithms for high sampling frequency operation are summarized including the frequency domain block implementation and partitioned block frequency domain implementation. This section motivates to develop adaptive algorithm to remove block processing delay and achieve computational saving.

Finally, the decentralized algorithms for multiple channel active control operations are summarized in Section 2.6. Controlling broadband noise using decentralized algorithms is challenging, this motivates to develop multiple channel decentralized algorithm for broadband noise control.

To develop computationally efficient algorithms for active control operation, the following research questions are identified:

- How can the acoustic paths be modelled online using the available control signal?
- How can the computational complexity of the combination strategy of adaptive filters be reduced?
- How can the unwanted block delay in the transform domain active control be compensated and the computational complexity be reduced simultaneously?
- How can a similar noise reduction performance of the decentralized algorithm as that of the centralized one for broadband control be achieved?

3 Online modelling of acoustic paths in active control systems using control signal

3.1 Introduction

The time-varying acoustic paths in active control systems degrade the control performance. In this chapter, emphasis was given on online modelling of the acoustic paths. An active control method is proposed with online secondary path modelling[1]. The proposed method consists of five stages, i.e., primary path estimation, controller initialization, secondary path estimation, primary and secondary path changing detection, and active control operation, where the speed of the secondary path modelling is improved by incorporating decorrelation filters. The simulation results demonstrate the proposed method is capable of tracking the changes in both primary and secondary paths, remodelling the secondary path, and maintaining the noise reduction performance and stability of the system when both primary and secondary paths change.

The presence of control signal feedback to the reference microphone in feedforward active control systems deteriorates the control performance. A four-stage method is proposed in this chapter to carry out online feedback path modelling with the control signal[2]. It consists of controller initialization, feedback path modelling using decorrelation filters, active control operation, and feedback path change detection for maintaining control operation. In contrast to the existing auxiliary noise injection method, the proposed method uses five switches and three thresholds to control and maintain the system stability by avoiding the interference between control operation and feedback path

[1] A portion of this chapter has been published as: Pradhan, S. & Qiu, X. 2020, 'A 5-stage active control method with online secondary path modelling using decorrelated control signal', *Applied Acoustics*, vol. 164, p. 107252. https://doi.org/10.1016/j.apacoust.2020.107252.

[2] A portion of this chapter has been published as: Pradhan, S., Qiu, X. & Ji, J. 2019, 'A four-stage method for active control with online feedback path modelling using control signal', *Applied Sciences*, vol. 9, no. 15, p. 2973. https://doi.org/10.3390/app9152973.

modelling, and adaptive decorrelation filters are used to increase the feedback path modelling performance. Simulation results reveal that the proposed method is capable of tracking feedback path changes without injecting any auxiliary noise and maintaining the noise reduction performance and stability of the system.

3.2 Online secondary path modelling

3.2.1 Proposed method

Though the extended adaptive filtering methods (Kuo & Morgan 1999; Zhao et al. 2017) are capable of estimating the secondary path using the control signal, the performance is deteriorated as the primary noise characteristics changes. An intelligent ANC system should be able to detect the changes in both primary and secondary paths, and remodel those paths for effective operation. This section proposes a 5-stage active control method with online secondary path modelling using the decorrelated control signal. The contributions made in this work are: (1) a new systematic method for active control with online secondary path modelling using the control signal, which includes primary path estimation, controller initialization, secondary path estimation, primary and secondary path changing detection, and active control operation; and (2) increasing the modelling speed of the secondary path with the control signal by using decorrelation filters.

Figure 3.1 shows the block diagram of the proposed method, which consists of five stages, i.e., primary path estimation, controller initialization, secondary path estimation, primary and secondary path changing detection, and active control operation. In the block diagram, three switches, K_1, K_2 and K_3, are used for choosing the active control operation, the primary path modelling and the secondary path modelling, respectively. Figure 3.2 presents the flowchart of the proposed method, where the normal noise reduction, primary path modelling accuracy, and secondary path modelling accuracy are assumed to be T_{r0},

T_{p0}, and T_{s0}, respectively. The toggling of three switches associated with different stages and the corresponding operations of the active control system are briefed sequentially.

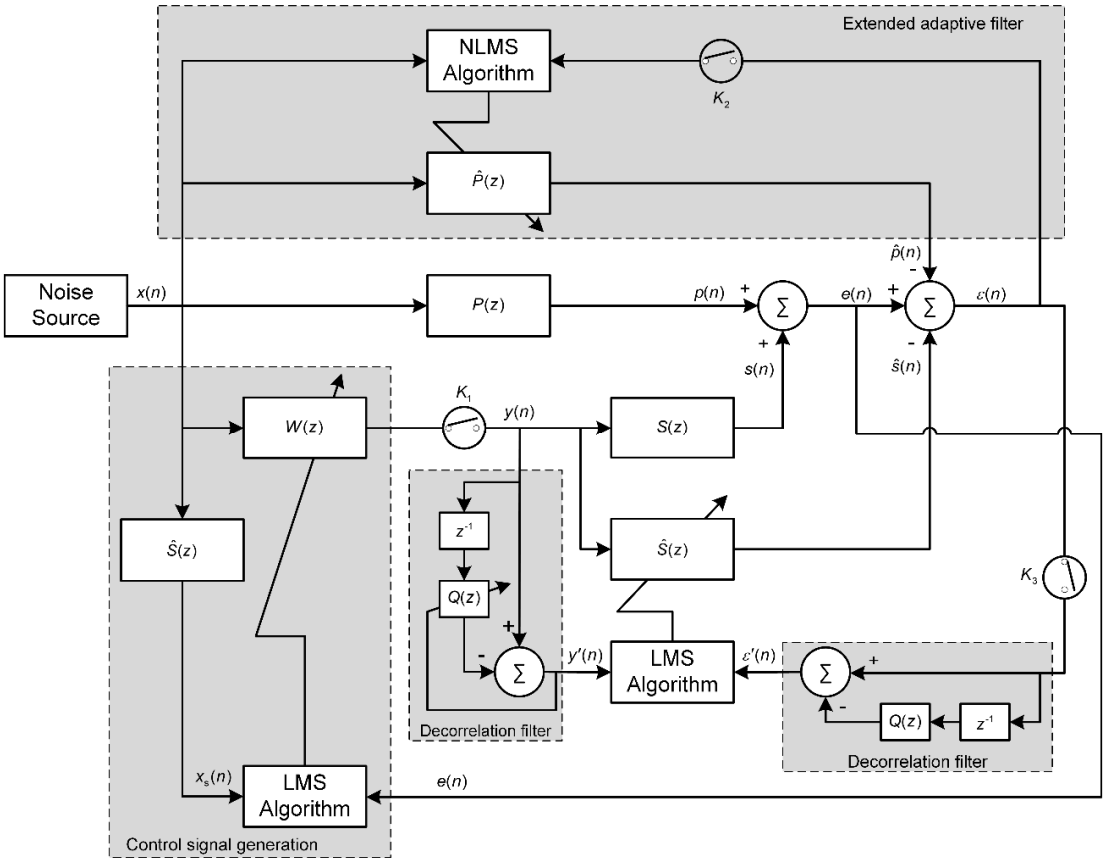

Figure 3.1 Block diagram of the proposed method for active control operation.

The first stage is for the primary path estimation. When the system starts, K_1 and K_3 are turned off, and K_2 is turned on. The cancelling signal $s(n)$ and estimated cancelling signal $\hat{s}(n)$ are absent, $p(n)$ and $\hat{p}(n)$ represent the undesired noise and its estimate. The primary path $P(z)$ between the reference microphone and error microphone is estimated using the NLMS algorithm. The adaptive filter estimating the primary path is updated by

$$\widehat{\boldsymbol{p}}(n+1) = \widehat{\boldsymbol{p}}(n) + \mu_{\mathrm{p}} \frac{\varepsilon_{\mathrm{p}}(n)\boldsymbol{x}_{\mathrm{p}}(n)}{\boldsymbol{x}_{\mathrm{p}}^{\mathrm{T}}(n)\boldsymbol{x}_{\mathrm{p}}(n)} \tag{3.1}$$

where $\boldsymbol{x}_{\mathrm{p}}(n) = [x(n), x(n-1), \ldots, x(n-L_{\mathrm{p}}+1)]^{\mathrm{T}}$ is the L_{p} sample reference signal vector, μ_{p} is the step size, and $\varepsilon_{\mathrm{p}}(n) = \varepsilon(n)$ is the error signal when K_1 and K_3 are turned off.

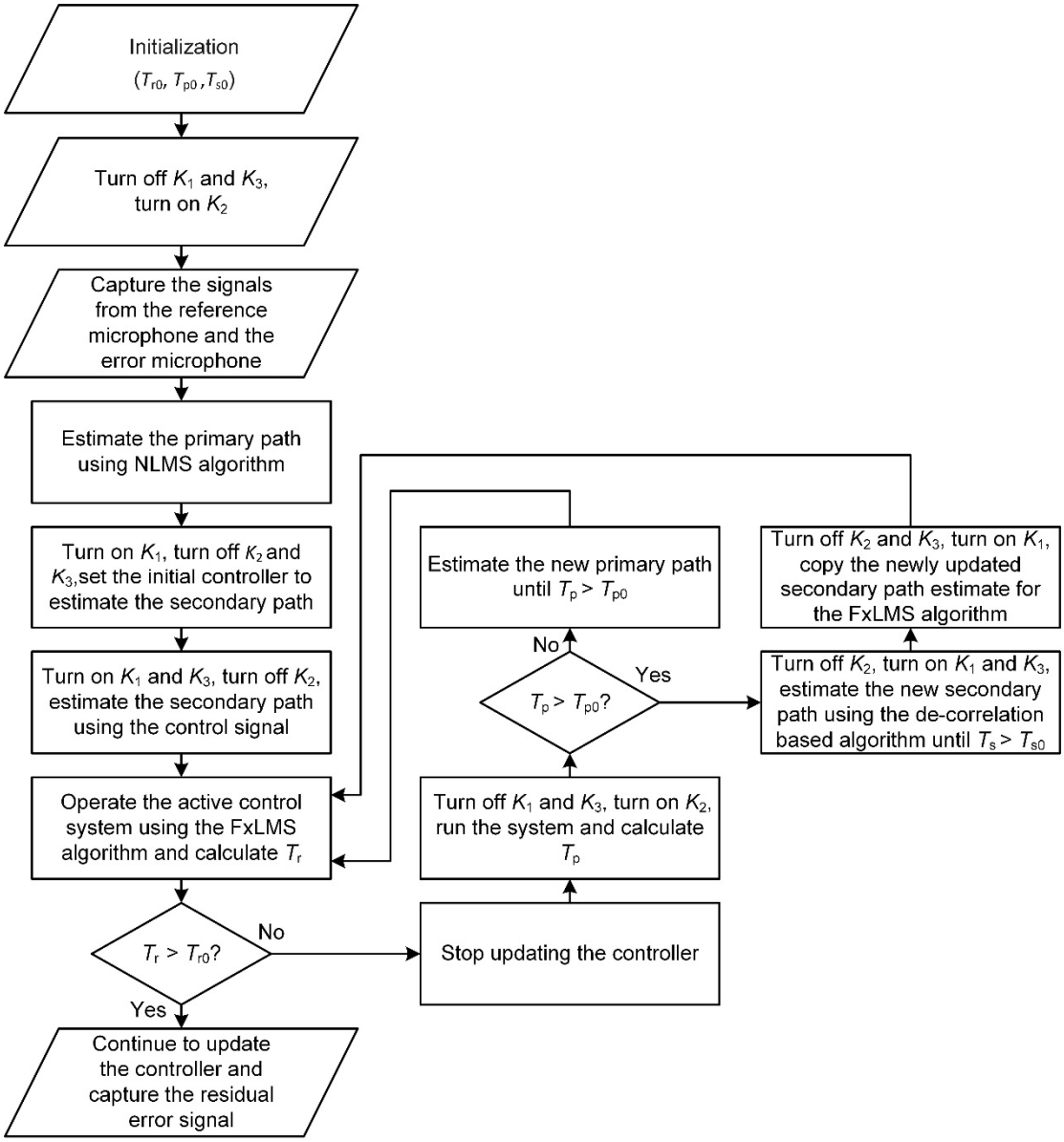

Figure 3.2 Flowchart of the proposed method.

In the second stage, K_1 is turned on and K_2 and K_3 are turned off for controller initialization. An initial controller with a single gain G is set for ANC operation, i.e., $W(z) = G$. The gain is tuned in such a way that the amplitude of the error signal $e(n)$ is higher than that of $p(n)$. In the process, the initial controller G is increased from a small pre-defined value (for example, G = 1% of the maximal gain can be applied on the system) by two times each step until $\sigma_e^2 > \sigma_p^2$, where σ_e^2 is the power of the error signal $e(n)$, which can be estimated by

$$\sigma_e^2(n) = \lambda\sigma_e^2(n-1) + (1-\lambda)e^2(n) \tag{3.2}$$

where λ is the forgetting factor ($0.9 < \lambda < 1$), σ_p^2 is the power of the primary disturbance, which can be estimated before controller initialization similarly with Eq. (3.2) by turning off the controller with K_1.

The third stage involves the estimation of the secondary path $S(z)$ using the control signal, for which K_1 and K_3 are turned on, and K_2 is turned off. The control signal $y(n) = Gx(n)$ is used as the excitation signal for estimating the secondary path. In this case, the primary signal $p(n)$ acts as an interference signal in the estimation process, so the filter $\hat{P}(z)$ (estimated in the first stage) is used to remove this interference. The final error signal $\varepsilon(n) = p(n) + s(n) - \hat{s}(n) - \hat{p}(n)$ is used in the update rule given by

$$\hat{\boldsymbol{s}}(n+1) = \hat{\boldsymbol{s}}(n) + \mu_s\varepsilon(n)\boldsymbol{y}(n) \tag{3.3}$$

where $\boldsymbol{y}(n) = [y(n), y(n-1), \ldots, y(n-L_s+1)]^T$ is the L_s sample control signal vector, μ_s is the step size. Hence, a bias free estimation of $S(z)$ is possible. If $y(n)$ is a coloured signal, the modelling may be improved by incorporating pre-whitening filters.

The fourth stage is for the complete active control operation. After obtaining the initial $\hat{P}(z)$ and $\hat{S}(z)$, the switches K_2 and K_3 are turned off, and K_1 is turned on. This means there is no update for $\hat{P}(z)$ and $\hat{S}(z)$, and the FxLMS algorithm is used for ANC operation. The control weights are updated as

$$\boldsymbol{w}(n+1) = \boldsymbol{w}(n) - \mu_w e(n)\boldsymbol{x}_s(n) \tag{3.4}$$

where $\boldsymbol{x}_s(n) = [x_s(n), x_s(n-1), \ldots, x_s(n-L_w+1)]^T$, $x_s(n)$ is the reference signal $x(n)$ filtered through the secondary path estimate $\hat{\boldsymbol{s}}(n)$ and μ_w is the step size.

The active control operation is prone to acoustic path change. To detect which path changes, three thresholds are defined.

$$T_{\mathrm{r}} = 10 \log_{10} \left[\frac{\sigma_{\mathrm{p}}^2}{\sigma_{\mathrm{e}}^2} \right] \tag{3.5}$$

$$T_{\mathrm{p}} = 10 \log_{10} \left[\frac{\sigma_{\mathrm{e}}^2}{\sigma_{\varepsilon}^2} \right] \tag{3.6}$$

$$T_{\mathrm{s}} = 10 \log_{10} \left[\frac{\sigma_{\mathrm{e}'}^2}{\sigma_{\varepsilon}^2} \right] \tag{3.7}$$

T_{r} is the threshold to detect sudden rise in the residual error signal $e(n)$, T_{p} and T_{s} are the thresholds to detect if the estimated acoustic paths are accurate, $\sigma_{e'}^2$ is the power of the error signal $e'(n) = e(n) - \hat{p}(n)$ during secondary path modelling.

Assume that the normal noise reduction is 10 dB for the system, i.e., T_{r0} =10, and if suddenly it becomes less than 10 dB, i.e., $T_{\mathrm{r}} < 10$ dB, there should be an acoustic path change, which may come from the primary path or the secondary path or $x(n)$, the update for $W(z)$ is ceased. To check whether the change is due to the primary path, K_1 and K_3 are turned off, K_2 is turned on, and the threshold T_{p} is checked. Assume that normal acoustic path modelling accuracy is 20 dB for the system, i.e., $T_{\mathrm{p0}} = 20$, and if it becomes less than 20 dB, i.e., $T_{\mathrm{p}} < 20$ dB, it is confirmed that the preciously estimated acoustic path is no more matching with the changed acoustic path.

For $T_{\mathrm{p}} < 20$, it is confirmed that there is a change in the primary path. Hence, $\hat{P}(z)$ is updated until the condition $T_{\mathrm{p}} > 20$ is met, and then the FxLMS algorithm is used for ANC operation. If the condition $T_{\mathrm{p}} > 20$ is valid, the change in $e(n)$ might be due to the change in secondary path. To update $\hat{S}(z)$, K_2 is turned off and K_1 and K_3 are turned on. The secondary path modelling is carried out until the condition $T_{\mathrm{s}} > T_{\mathrm{s0}}$ is met with the previously obtained $W(z)$. The normal secondary path modelling accuracy can be assumed to be 20 dB, i.e., $T_{\mathrm{s0}} = 20$.

Decorrelation filters are widely employed for adaptive filtering application such as feedback cancellation in hearing aids (Rotaru, Albu & Coanda 2012). However, they have

little application in active control operation. Two identical adaptive decorrelation filters $D(z)=1-z^{-1}Q(z)$ are introduced to accelerate the convergence behaviour of the secondary path modelling process, where $Q(z)$ is the z-transform of $\boldsymbol{q}(n) = [q_0(n), q_1(n), \dots, q_{M-1}(n)]^{\mathrm{T}}$ with M representing the tap-weight length of $Q(z)$ (Zhang et al. 2017; Zhang, Zhang & Han 2016). The signal $y(n)$ passes through the adaptive decorrelation filter to provide the signal $y'(n) = y(n) - \boldsymbol{q}^{\mathrm{T}}(n)\boldsymbol{y}_1(n)$, where $\boldsymbol{y}_1(n) = [y(n\text{-}1), y(n\text{–}2), \dots, y(n\text{–}M)]^{\mathrm{T}}$. Similarly, the error signal $\varepsilon(n)$ passes through the decorrelation filter to provide $\varepsilon'(n) = \varepsilon(n) - \boldsymbol{q}^{\mathrm{T}}(n)\boldsymbol{\varepsilon}_1(n)$, where $\boldsymbol{\varepsilon}_1(n)= [\varepsilon(n\text{-}1), \varepsilon(n\text{–}2), \dots, \varepsilon(n\text{–}M)]^{\mathrm{T}}$. The signals $y'(n)$ and $\varepsilon'(n)$ are used to update the filter $\hat{S}(z)$. The decorrelation filter can pre-whiten the updating signals $y(n)$ and the error signal $\varepsilon(n)$, which in turn accelerates the convergence of $\hat{S}(z)$. The adaptive decorrelation filters is updated using the NLMS algorithm as

$$\boldsymbol{q}(n+1) = \boldsymbol{q}(n) + \mu_{\mathrm{q}} \frac{y'(n)\boldsymbol{y}_1(n)}{\boldsymbol{y}_1^{\mathrm{T}}(n)\boldsymbol{y}_1(n)} \tag{3.8}$$

The tap-weights of the of $\hat{S}(z)$ are updates as

$$\hat{\boldsymbol{s}}(n+1) = \hat{\boldsymbol{s}}(n) + \mu_{\mathrm{s}}\varepsilon'(n)\boldsymbol{y}'(n) \tag{3.9}$$

where $\boldsymbol{y}'(n) = [y'(n), y'(n-1), \dots, y'(n-L_{\mathrm{s}}+1)]^{\mathrm{T}}$.

After obtaining $\hat{S}(z)$, K_2 and K_3 are turned off, K_1 is turned on, the new secondary path estimate is used in the FxLMS algorithm for active control operation by updating the control coefficients as in Eq. (3.4). The stages involved in the proposed method are summarized in Table 3.1.

Table 3.1 The five stages of the proposed method.

Stage 1: Primary path estimation

Turn off K_1 and K_3, turn on K_2

Estimate of the primary path $\hat{P}(z)$

$$\hat{\boldsymbol{p}}(n+1) = \hat{\boldsymbol{p}}(n) + \mu_{\mathrm{p}} \frac{\varepsilon_{\mathrm{p}}(n)\boldsymbol{x}_{\mathrm{p}}(n)}{\boldsymbol{x}_{\mathrm{p}}^{\mathrm{T}}(n)\boldsymbol{x}_{\mathrm{p}}(n)}$$

Stage 2: Controller initialization

Turn on K_1, turn off K_2 and K_3

Set the initial controller

Stage 3: Secondary path estimation

Turn on K_1 and K_3, turn off K_2

Estimate of the secondary path $\hat{S}(z)$ using control signal

$$\hat{\boldsymbol{s}}(n+1) = \hat{\boldsymbol{s}}(n) + \mu_{\mathrm{s}}\varepsilon(n)\boldsymbol{y}(n)$$

Stage 4: Primary and secondary path changing detection in active control operation

Operate the active control system

$$\boldsymbol{w}(n+1) = \boldsymbol{w}(n) - \mu_{\mathrm{w}}e(n)\boldsymbol{x}_{\mathrm{s}}(n)$$

if $T_{\mathrm{r}} < T_{\mathrm{r0}}$, A path change is detected.

To check primary path change, turn off K_1 and K_3, turn on K_2, run the system

if $T_{\mathrm{p}} < T_{\mathrm{p0}}$, update $\hat{P}(z)$.

else, turn on K_1 and K_3, turn off K_2, update $\hat{S}(z)$ using

$$\boldsymbol{q}(n+1) = \boldsymbol{q}(n) + \mu_{\mathrm{q}} \frac{\boldsymbol{y}'(n)\boldsymbol{y}_1(n)}{\boldsymbol{y}_1^{\mathrm{T}}(n)\boldsymbol{y}_1(n)}$$

$$\hat{\boldsymbol{s}}(n+1) = \hat{\boldsymbol{s}}(n) + \mu_{\mathrm{s}}\varepsilon'(n)\boldsymbol{y}'(n)$$

Stage 5: Active control operation

Turn off K_2 and K_3, turn on K_1

Operate the active control system with updated $\hat{S}(z)$

If rise in $e(n)$ is detected, follow the procedures of Stage 4

3.2.2 Numerical experiments

In this subsection, the results obtained from numerical experiments using available acoustic paths for active control operation, are presented. A detailed discussion on results are also included, and the results are compared by means of performance metrics with the state-of-the-art methods to validate the effectiveness of the proposed method. Furthermore, the advantages and pitfalls of the method are found.

In the simulations, the primary path $P(z)$ and secondary path $S(z)$ are FIR filters of length 48 and 16 respectively which are obtained from the data provided by Kuo and Morgan (1996), the frequency response of which are depicted in Figure 3.3. Part A represents the normal paths, Part B represents the path after a sudden change. The estimated secondary path and control filter are FIR filters of length $L_s = 16$ and $L_w = 48$, respectively. The adaptive decorrelation filter $Q(z)$ is an FIR filter of length $M = 5$. The sampling frequency used in the simulation is 2000 Hz. The mean square error (MSE) and the relative modelling error ΔS are used as the metrics for comparison, which are defined as

$$\text{MSE} = 10\log_{10}\{E[e^2(n)]\} \tag{3.10}$$

$$\Delta S\ (\text{dB}) = 10\log_{10}\left\{\frac{\|\boldsymbol{s}(n) - \hat{\boldsymbol{s}}(n)\|^2}{\|\boldsymbol{s}(n)\|^2}\right\}. \tag{3.11}$$

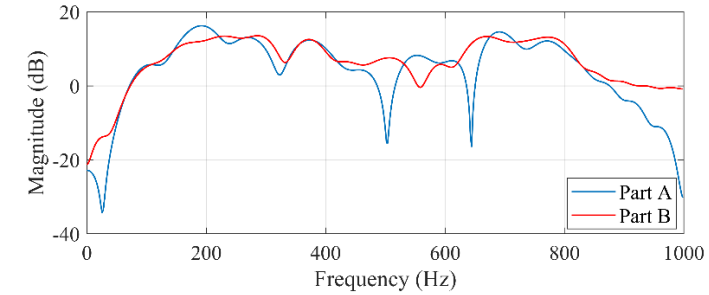

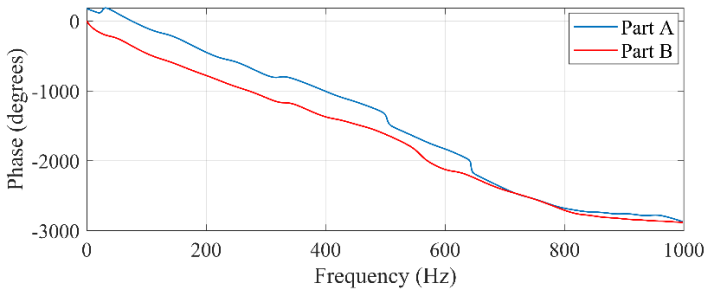

(a)

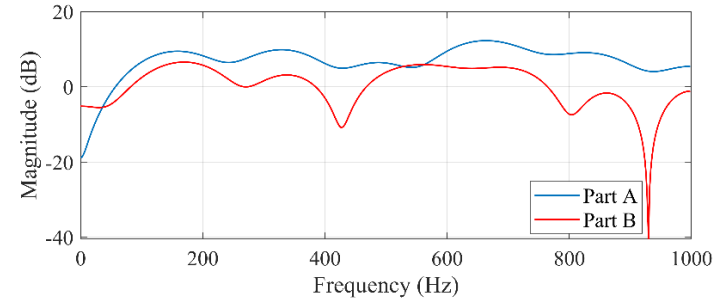

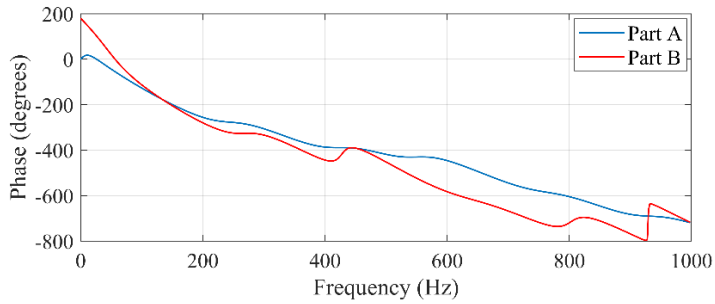

(b)

Figure 3.3 Frequency response of (a) the primary path and (b) the secondary path.

Simulations have been carried out to compare the performance of the proposed five-stage method with the extended filtering (EF) method (Zhao et al. 2017), which is hereafter referred to as EF-1, the conventional extended adaptive filter method (Kuo &

Morgan 1999), which is hereafter referred to as EF-2, Carini's method (Carini & Malatini 2008) and Yang's method (Yang et al. 2018). In EF-1, the extended filter is the estimate of the primary path, which is fixed for control operation, whereas the extended filter is adaptive one for EF-2. Both Carini's method and Yang's method use auxiliary noise with an initialized variance of 0.05 and power scheduling strategy for simultaneous update of the control filter and secondary path modelling filter. All the results obtained are averaged over ten independent trials.

3.2.2.1 The five stage method

In this subsection, simulation has been carried out for different situations to test the efficacy of the five-stage method for both the primary and the secondary path change.

3.2.2.1.1 Case 1: Autoregressive signal

In this case, the input signal $x(n)$ is generated from a first order autoregressive (AR) process

$$x(n) = 0.9x(n-1) + v(n) \tag{3.12}$$

where $v(n)$ is a white noise of zero mean and unit variance. A white Gaussian measurement noise with a signal to noise ratio (SNR) of 40 dB is considered. The simulation runs for 50 sec and suddenly both the primary and secondary paths are changed (Part B). The simulation parameters used for the proposed method are: μ_p = 0.5, μ_s = 0.004, μ_w = 0.0001, and for the EF methods are: μ_p = 0.008, μ_s = 0.02, μ_w = 0.0001. The simulation parameters used for Yang's method are: μ_w = 0.000005, α = 0.02 and μ_h=0.003, c = 1, λ = 0.999, and for Carini's method are: $\mu_{s_{min}}$= 0.001, delay D = 8, $\hat{\lambda}$ = 0.8, R = 1. The step sizes and other simulation parameters are chosen by trial and error to keep the system stability for normal acoustic paths and yet with the best possible control performance.

The learning curves are shown in Figure 3.4. The proposed method maintains the control after both the primary and the secondary path change, while the EF-1 and EF-2 algorithms diverge. The methods of Yang and Carini are able to maintain the control operation before and after the acoustic path change. However, the control performance is limited compared to the proposed method due to the fact that the control operation and secondary path modelling process interfere with each other, and the injected auxiliary noise in these two methods affect the residual noise level. Furthermore, it is to be noted that the initial residual error levels (Part A) of the two methods are higher than that of the other methods due the injection of auxiliary noise. For the proposed algorithm, after the detection of the path change at 50^{th} second, the controller update is ceased, K_1 and K_3 are turned off, K_2 is turned on, and the primary path is remodelled. Hence, the residual error becomes exactly same as the primary disturbance during that time, which is clear from the learning curve (50^{th}-60^{th} sec). During the secondary path modelling, K_1 and K_3 are turned on, K_2 is turned off, the controller preserves the previously updated coefficients (60^{th}-70^{th} sec). After the modelling of the acoustic paths are completed, K_2 and K_3 are turned off, K_1 is turned on, the controller is continued to update to reduce residual noise.

For Part A, the proposed method, EF-1 and EF-2 are able to reach same residual noise level of approximately –11.5 dB, where that from Yang's method and Carini's method is about –7.5 dB despite having the fact that the convergence behavior of Yang's method is the worst among the methods under study. After acoustic path change, the achieved residual noise levels for the proposed method, Yang's method and Carini's method are –11 dB, 2 dB and –0.07 dB, respectively. The improved performance of Carini's method (among Yang's method and Carini's method) might be attributed to the use of optimal variable step size for control filter update and secondary path modelling and appropriate auxiliary noise power scheduling.

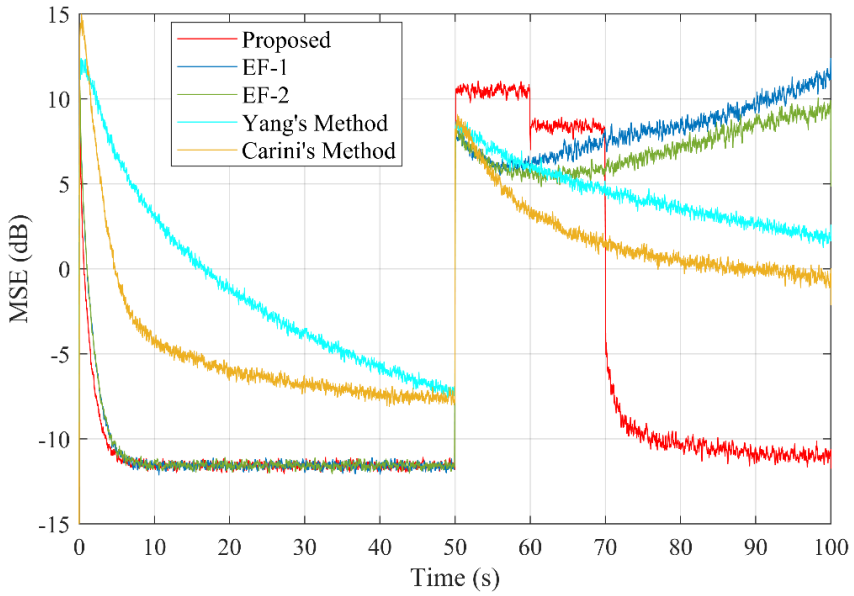

Figure 3.4 Case 1: Learning curve for the 5-stage method obtained from an AR(1) input signal.

The deterioration in performance for the EF methods after both the primary and the secondary path change is due to the fact that it is not capable of estimating the changed paths accurately. It is found that the phase error between the actual and estimated secondary path for the EF-1 and EF-2 methods is greater than ±90°, thereby making both the algorithms diverge. Furthermore, in the simultaneous update of secondary path estimation filter and the control filter, both the processes interfere with each other. An inaccurate secondary path estimation filter leads to increased interferences in control operation.

3.2.2.1.2 Case 2: Frequent acoustic path change

In this case, a more critical scenario is considered, where both the primary and secondary paths change frequently. The input signal is same as Case 1. The simulation runs for 25 seconds with normal acoustic paths (Part A), and then both the paths are changed (Part

B). The acoustic paths again changes to Part A and Part B at 50th and 75th second, respectively. The simulation parameters used for this case are: the proposed method (μ_p = 0.5, μ_s = 0.004, μ_w = 0.0001), the EF methods (μ_p = 0.0005, μ_s = 0.001, μ_w = 0.0001), Yang's method (μ_w = 0.000005, α = 0.02 and μ_h = 0.003, c = 1, λ = 0.999) and Carini's method ($\mu_{s_{min}}$ = 0.001, delay D = 8, $\hat{\lambda}$ = 0.8, R = 1). The step sizes are chosen by trial and error to have same initial convergence (the proposed method and EF methods), and stability of all the methods for the normal acoustic paths. The operation of the switches are same as Case 1. The learning curves are shown in Figure 3.5, which shows the superiority of the proposed method after sudden path change. The EF-1 and EF-2 algorithms diverge after the acoustic path change for the same reason as Case 1. Though Yang's method and Carini's method offer control operation after each path change, their control performance is limited due to the simultaneous update of control filter and secondary path modelling filter and the existence of auxiliary noise in the residual error signal.

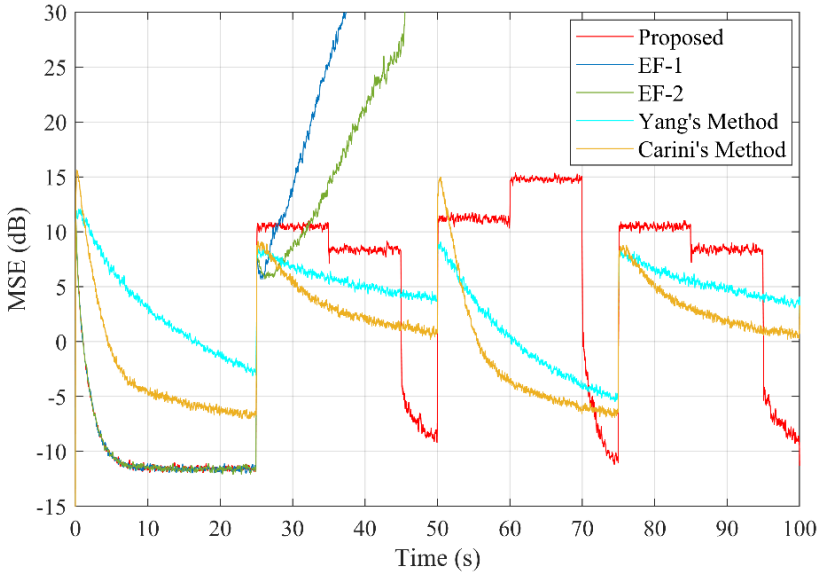

Figure 3.5 Case 2: Learning curve for the 5-stage method obtained from an AR(1) input signal with a frequent acoustic path change.

For normal acoustic path (Part A), the proposed method, EF-1 and EF-2 are able to reach the same residual noise level (that is around –11.5 dB), whereas Yang's method and Carini's method achieve –2.8 dB and –6.5 dB, respectively. The residual noise levels for the proposed method, Yang's method and Carini's method for the first acoustic path change are –9 dB, 4 dB and 1 dB, respectively, while such obtained values for the second path change are –10.8 dB, –5 dB and –6.5 dB, respectively. Also, the third acoustic path change offers –9.5 dB, 3.5 dB and 0.9 dB, respectively for the 3 methods.

One can observe from the results that the proposed method is able to achieve similar level of noise reduction only after remodelling the acoustic paths. The primary path modelling is carried out during 25^{th}-35^{th} second, 50^{th}-60^{th} second and 75^{th}-85^{th} second. Similarly, the secondary path modelling is carried out during 35^{th}-45^{th} second, 60^{th}-70^{th} second and 85^{th}-95^{th} second. The remodelling process took longer time compared to the controller update duration, which means the unwanted disturbance is present for a long time. Hence, it is expected that the time duration for remodelling the acoustic paths could be shorter compared to the time gap between two consecutive path changes. The convergence time might otherwise be reduced at the expense of modelling accuracy, which in turn would affect the control performance, i.e., the convergence of the control filter would be slower. However, it is not desirable in an active control system. Alternatively, shorter remodelling time may be achieved by accelerating the convergence behaviour of the adaptive filters used for modelling. The adaptive decorrelation filters are introduced in Section 3.2.2.2 to reduce the modelling time.

There might be some situations where only one acoustic path changes. If $T_r < T_{r0}$, the controller is ceased, K_1 and K_3 are turned off, K_2 is turned on. If $T_p < T_{p0}$, it confirms the need for remodelling of the primary path. However, the remodelling of primary path takes some time. After the remodelling is completed, the controller update is continued, which

means the convergence of the FxLMS algorithm in such a case depends on the primary path remodelling time. Similarly, if $T_r < T_{r0}$, and $T_p > T_{p0}$, it confirms the need for remodelling of the secondary path, for which K_1 and K_3 are turned on and K_2 is turned off. The controller update is continued after remodelling of the secondary path, which means the convergence of the FxLMS algorithm in such a case depends on the secondary path remodelling time.

In summary, the proposed 5-stage method is capable of maintaining the noise reduction performance even both the primary and the secondary path change. However, one weakness of this method is that it takes some time for remodelling the acoustic paths, which makes it ill-suited for the situation where the changes in the acoustic paths occur more frequently before one remodelling is completed.

3.2.2.2 The decorrelation filter

In this subsection, the advantages of using the adaptive decorrelation filter is illustrated through simulations. For applying the decorrelation filter for modelling the secondary path (Part B), the modelling signal used is the controller output signal from Part A. After the confirmation of secondary path change, K_1 and K_3 are turned on, K_2 is turned off, the controller preserves the previously updated coefficients (from Part A). Please note that this decorrelation filter is not effective for tonal and white excitation signal.

3.2.2.2.1 Case 1: Autoregressive signal

The input signal and other simulation parameters are same as the Case 1 of previous section. The step size used for updating the coefficients of the decorrelation filter is μ_q = 0.01. It is evident from Figure 3.6 that the decorrelation filter accelerates the convergence behaviour of the secondary path modelling filter. Unlike the conventional LMS adaptive

filter, the decorrelation adaptive filter takes approximately 2 second to achieve similar modelling accuracy. That means the use of adaptive decorrelation filter can reduce the overall modelling time. The improvement in the convergence behaviour of the decorrelation adaptive filter is due to its pre-whitening operation, which decreases the spectral dynamic range of the excitation signal used for modelling.

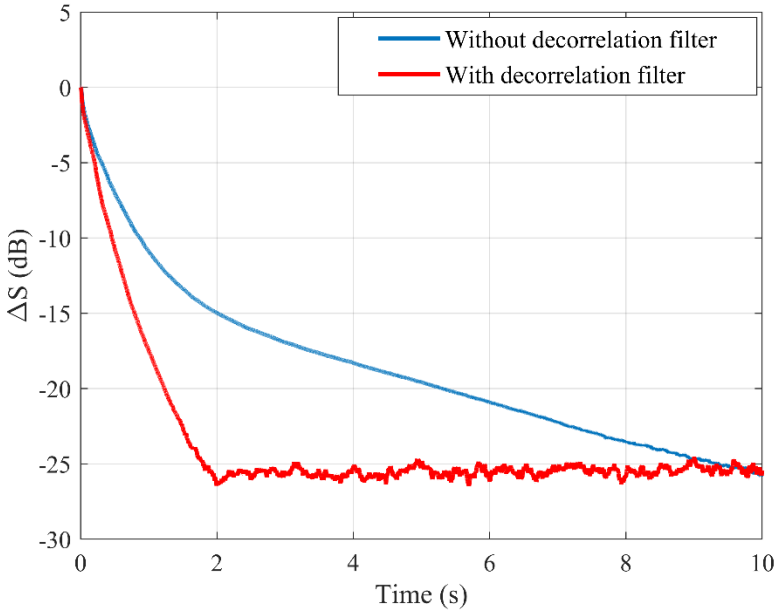

Figure 3.6 Relative modelling error for the AR(1) signal.

3.2.2.2.2 Case 2: Broadband signal

A broadband reference noise signal is considered in this case. A 21 order FIR filter with a pass band of [100 500] Hz is designed using *fir1* MATLAB command. A white noise of zero mean and unit variance is filtered through this bandpass filter to generate the reference signal $x(n)$. A white Gaussian measurement noise with an SNR of 40 dB is considered. The acoustic paths used in the simulation are shown in Figure 3.3. The control operation is carried out for Part A and the acoustic paths are changed suddenly (Part B). The decorrelation adaptive filter is used for remodelling the secondary path. The

simulation parameters used for the proposed method are: $\mu_p = 0.9$, $\mu_s = 0.01$, $\mu_w = 0.00005$ and $\mu_q = 0.01$.

The relative modelling error is shown in Figure 3.7(a), from which one can notice that the proposed decorrelation filter is improving the modelling accuracy by approximately 3 dB. The adaptive filter without the decorrelation filter takes 10 second to achieve approximately –4 dB modelling error, while the decorrelation adaptive filter reaches the same level at around 2 second. The reason for such improvement is explained in the previous case. In this case, the reference signal has bandwidth [100 500] Hz, and the secondary path can be modelled accurately only in that band. Figure 3.7(b) shows the modelling error in the frequency band of the reference signal, from which it is clear that the modelling is improved using the decorrelation filter. The modelling error in Figure 3.7(a) is higher compared to the previous case as it is obtained by considering the whole range of frequency response of the secondary path. However, the condition $T_s > T_{s0}$ is met.

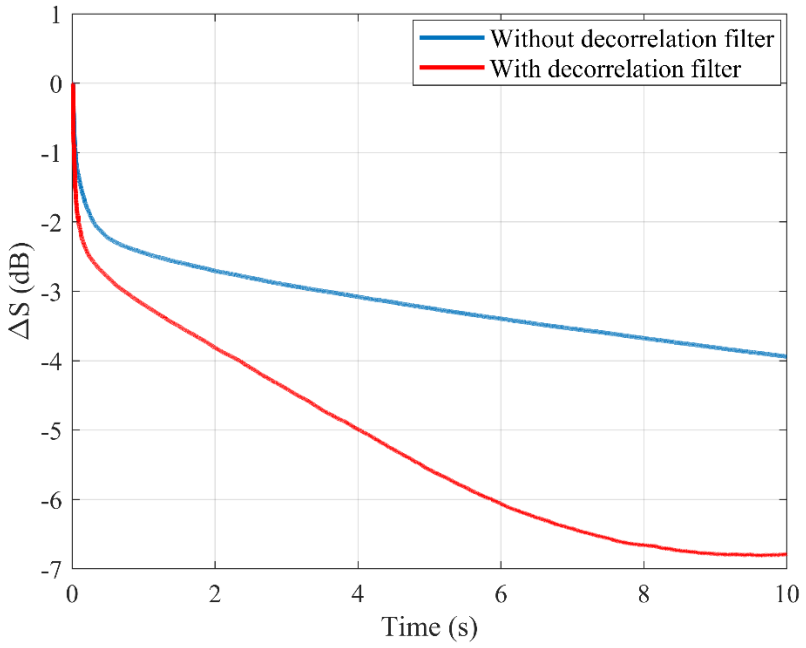

(a)

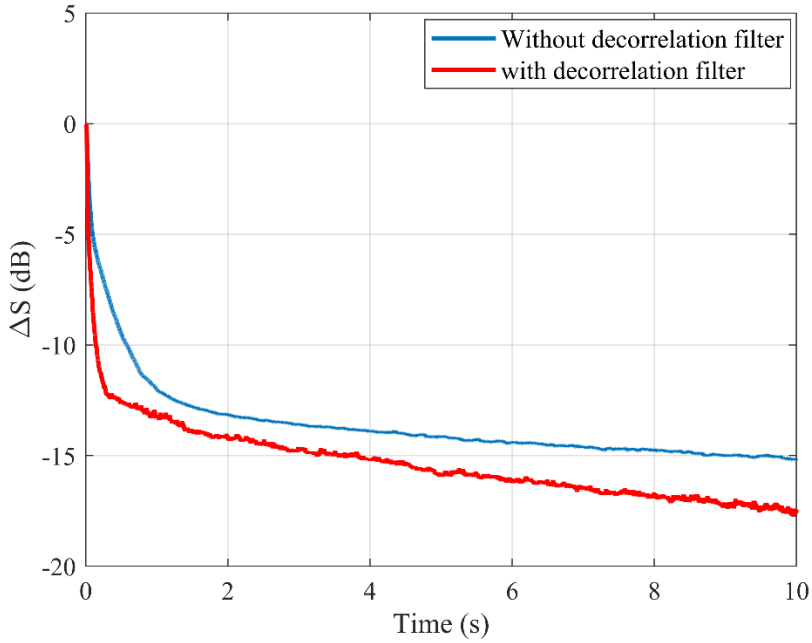

(b)

Figure 3.7 (a) Relative modelling error for the full frequency range, (b) Relative modelling error for the frequency band of [100 500] Hz.

3.2.2.2.3 Case 3: Mixture of white noise and multitone

In this case, the reference signal is a mixture of white noise with zero mean and unit variance and multitone signal comprising frequencies of 100, 200, 300, 400 and 500 Hz. The variance of the multitone signal is adjusted to 2. A white Gaussian measurement noise with an SNR of 40 dB is considered. The acoustic paths used in the simulation are shown in Figure 3.3. The control operation is carried out for Part A and the acoustic paths are changed suddenly (Part B). The decorrelation adaptive filter is used for remodelling the secondary path. The simulation parameters used for the proposed method are: μ_p = 0.9, μ_s = 0.003, μ_w = 0.0002 and μ_q = 0.004.

The relative modelling error is illustrated in Figure 3.8, from which it is clear that the decorrelation filter accelerates the convergence speed of the secondary path modelling filter. Although the reference signal constitutes white noise, the presence of the control

filter makes the output of controller as a correlated (coloured) signal, increasing the spectral dynamic range. The adaptive decorrelation filter, in such a case, improves the convergence speed. It is to be noted that if the controller output, the excitation signal for modelling the secondary path is white or tonal, the decorrelation filter is not more effective than that without using the decorrelation filter for modelling the secondary path.

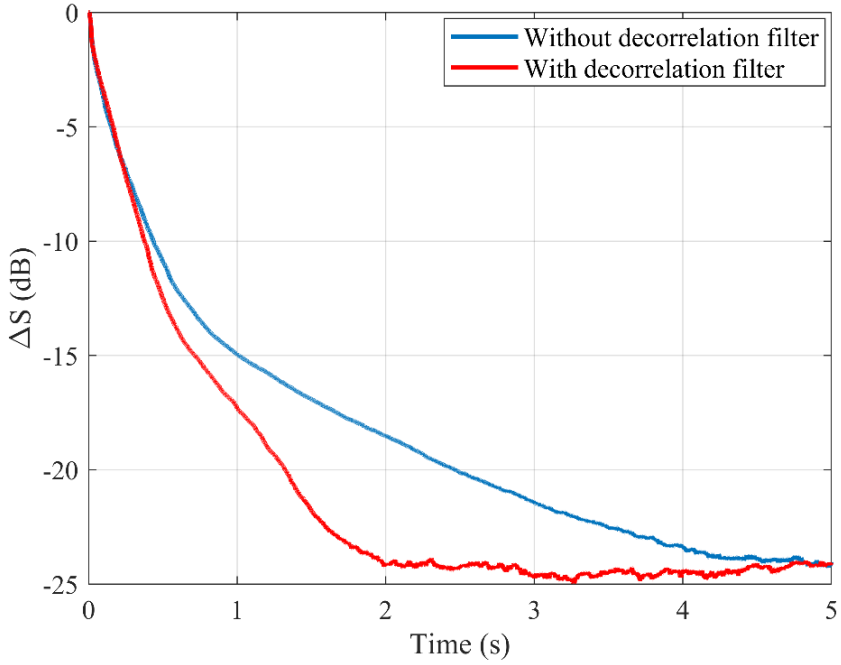

Figure 3.8 Relative modelling error for the mixture of white noise and multitone signal.

In summary, although the decorrelation filter is not effective to increase the convergence speed for tonal and white excitation signals, it can accelerate the convergence speed of the secondary path modelling for broadband and narrowband signals. Even though the reference signal might be white noise, the presence of the control filter, the frequency response of which is not flat in general, converts a white reference input signal to a coloured excitation signal for the secondary path modelling, which makes the decorrelation filter become effective. The effectiveness decreases with the reduction of bandwidth of the excitation signal. The order of the decorrelation filter also plays a

role in improving the convergence speed. In the simulations, a small order filter is considered. However, a higher order filter may be chosen for complicated coloured signals.

3.2.2.3 The five-stage method with decorrelation filter

In this subsection, the complete ANC operation is carried out, which includes the proposed five-stage method and the adaptive decorrelation filter. Three cases have been considered here.

3.2.2.3.1 Case 1: Coloured signal

The input signal considered in this case is a coloured signal, generated by passing a white noise with zero mean and unit variance through a filter $(1 + 0.5z^{-1} + 0.81z^{-2})/(1 - 0.59z^{-1} + 0.4z^{-2})$. A white Gaussian measurement noise with an SNR of 40 dB is considered. The acoustic paths considered are depicted in Figure 3.3. The simulation is carried out with normal acoustic paths (Part A), then there is a sudden change in both the acoustic paths at 40th second. The operation of the switches for remodelling of acoustic paths and control operation are same as previous cases. The simulation parameters used for this case are: the proposed method (μ_p = 0.5, μ_s = 0.004, μ_w = 0.0001, μ_q = 0.5), the EF methods (μ_p = 0.01, μ_s = 0.004, μ_w = 0.0001), Yang's method (μ_w = 0.000005, α = 0.02 and μ_h = 0.003, c = 1, λ = 0.999) and Carini's method ($\mu_{s_{min}}$ = 0.06, delay D = 8, $\hat{\lambda}$ = 0.9, R = 1).

In the proposed method, the primary path modelling is carried out during 40th-50th second. After the detection of secondary path change, K_2 is turned off, K_1 and K_3 are turned on. The secondary path modelling can be completed earlier using the decorrelation filter because the controller output signal is coloured. The adaptive decorrelation filter

reduces the spectral dynamic range of the control signal, thereby improves the convergence speed of the modelling filter. Unlike the LMS adaptive filters, the decorrelation adaptive filter takes approximately 2 second (50^{th}-52^{nd} second) data samples for the secondary path modelling. The learning curves of the system are shown in Figure 3.9, from which it is clear that the decorrelation filter reduces the remodelling time and helps to resume the control operation. The steady-state performance with and without the decorrelation filter are similar. It is also evident that both the primary and the secondary path change cause the EF-1 and EF-2 algorithms diverge, while the proposed algorithm is able to achieve similar level of noise reduction. Yang's method and Carini's method are also capable of maintaining control operation after acoustic path change, but the control performances are lesser than the proposed method due to the simultaneous update of control filter and secondary path modelling filter and the existence of injected auxiliary noise in the residual error signal.

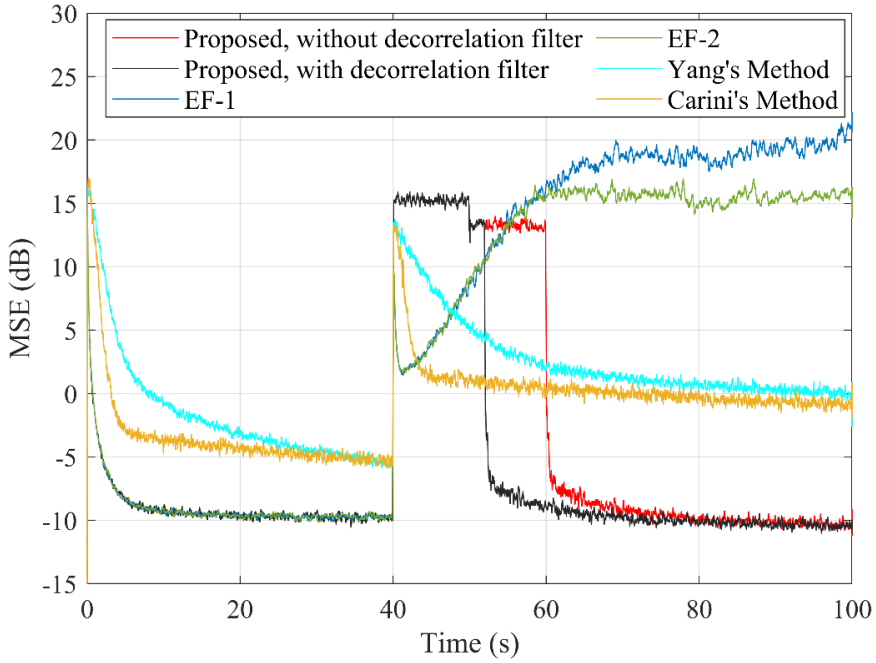

Figure 3.9 Learning curve for the 5-stage method obtained from a coloured input signal.

For Part A, the proposed method (with and without decorrelation filter), EF-1 and EF-2 reach the same residual noise level, i.e., around –9.5 dB, whereas Yang's method and Carini's method achieves similar residual noise level, i.e., around –5.5 dB. The residual noise levels for the proposed methods, Yang's method and Carini's method after the acoustic path change are –10.2 dB, –0.1 dB and –0.8 dB, respectively.

3.2.2.3.2 Case 2: Mixture of white noise and multitone

In this case, the input signal and other simulation parameters (for the proposed methods) are same as the Case 3 of Section 3.2.2.2. The simulation is carried out with normal acoustic paths (Part A), then there is a sudden change in both the acoustic paths at 25th second. The operation of the switches for remodelling of acoustic paths and control operation are same as previous cases. The simulation parameters used for the existing methods are: the EF methods (μ_p = 0.001, μ_s = 0.01, μ_w = 0.0002), Yang's method (μ_w = 0.00001, α=0.07 and μ_h=0.003, c=1, λ=0.999) and Carini's method ($\mu_{s_{min}}$= 0.02, delay D=8, $\hat{\lambda}$=0.9, R=1).

It can be observed from the relative modelling error depicted in Figure 3.8 that the decorrelation adaptive filter can remodel the secondary path earlier compared to the LMS counterpart. The primary path remodelling is carried out fast, within one second as the reference signal constitutes a white noise. The LMS adaptive filter remodels the secondary path during 26th-31st second, while the decorrelation adaptive filter can do it in 2 second. The learning curves of the system are shown in Figure 3.10, from which it is clear that the decorrelation filter reduces the remodelling time and the control operation is maintained. The EF-1 and EF-2 algorithms diverge after both the primary and the secondary path change.

For Part A, the proposed method (with and without decorrelation filter), EF-1 and EF-2 reach the same residual noise level, i.e., around –9.3 dB, whereas Yang's method and Carini's method achieves similar level of residual noise, i.e., around –8 dB. The residual noise levels for the proposed methods, Yang's method and Carini's method after the acoustic path change are –10.5 dB, 2.4 dB and –0.5 dB, respectively. It can also be noticed from part A that the initial residual noise levels for Yang's method and Carini's method are higher than that of the other methods, which are caused by the power scheduling of the injected auxiliary noise.

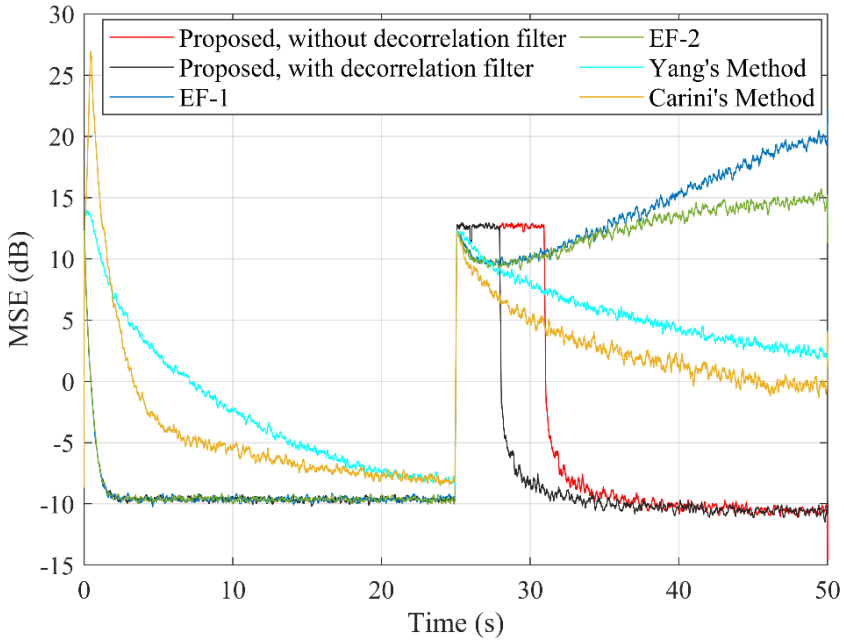

Figure 3.10 Learning curve for the five-stage method obtained from a mixture of white noise and multitone input signals.

3.2.2.3.3 Case 3: Effect of measurement noise

In this case, the effect of different level of measurement noise on the performance of the proposed method is demonstrated. The input signal, simulation condition and all other simulation parameters are same as Case 1 of Section 3.2.2.3. A white Gaussian measurement noise with 4 SNR values of 30 dB, 20 dB, 10 dB and 0 dB are considered.

The obtained learning curves are depicted in Figure 3.11. As shown in Figure 3.9, the EF-1 and EF-2 diverge after the acoustic path changes, so only Yang's method and Carini's method are compared with the proposed method with decorrelation filters. The residual noise levels for Part A and Part B are shown in Table 3.2, from which one can observe that the SNR values of 30 dB and 20 dB has little effect on the residual noise levels for the methods, but all the 3 methods are affected by the measurement noise with SNR values of 10 dB and 0 dB. Furthermore, the proposed method outperforms Yang's and Carini's methods and achieves lower level of residual noise for all SNR values.

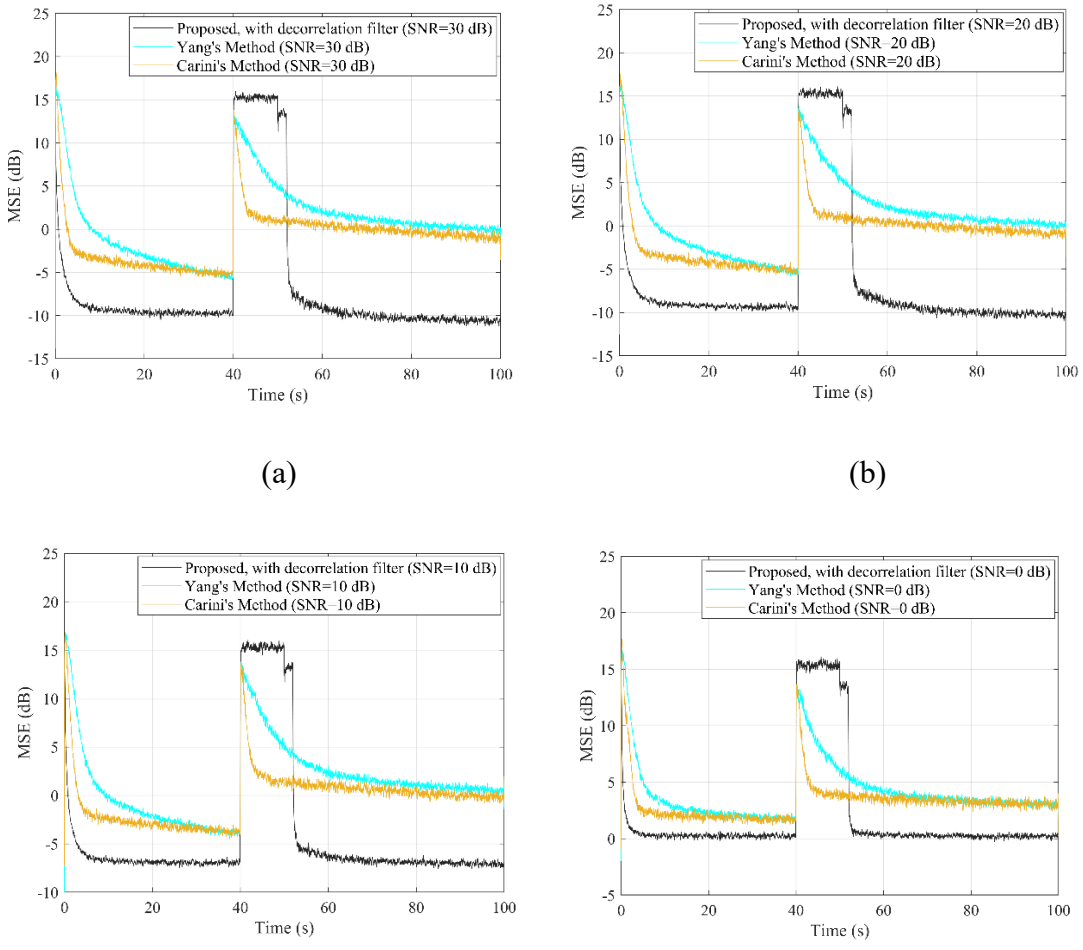

Figure 3.11 Learning curves for the proposed method obtained from a colored input signal and different level of measurement noise. (a) SNR = 30 dB, (b) SNR = 20 dB, (c) SNR = 10 dB and (d) SNR = 0 dB.

Table 3.2 Residual noise levels of different methods for different measurement noise levels.

	Residual noise level (dB)							
	SNR=30 dB		SNR = 20 dB		SNR = 10 dB		SNR = 0 dB	
Methods	Part A	Part B	Part A	Part B	Part A	Part B	Part A	Part B
Proposed	-9.5	-10.2	-9.2	-10.0	-6.7	-7.3	0.3	0.1
Yang's	-5.4	-0.1	-5.2	0.0	-3.8	0.6	1.9	3.0
Carini's	-5.0	-0.8	-5.0	-0.7	-3.8	0.0	1.8	3.0

3.2.3 Computational complexity

A detailed computational complexity of the proposed method is discussed in this section. For an active control system with a control filter of length L_{w}, a secondary path modelling filter of length L_{s}, a primary path modelling filter (extended filter) of length L_{p}, and decorrelation filters of length M, the proposed method requires L_{w} multiplications and $L_{\mathrm{w}}-1$ additions to obtain the control output; L_{s} multiplications and $L_{\mathrm{s}}-1$ additions to obtain the filtered reference signal; L_{s} multiplications and $L_{\mathrm{s}}-1$ additions to obtain the estimated cancelling signal; L_{p} multiplications and $L_{\mathrm{p}}-1$ additions to obtain the output of extended adaptive filter; $2M$ multiplications and $2(M-1)$ additions to obtain the decorrelation filter outputs; $L_{\mathrm{w}}+1$ multiplications and L_{w} additions to update the control filter; $2L_{\mathrm{p}}+1$ multiplications, $2L_{\mathrm{p}}-1$ additions and 1 division to update the extended adaptive filter $\hat{P}(z)$; $L_{\mathrm{s}}+1$ multiplications and L_{s} additions to update the secondary path modelling filter; $2M+1$ multiplications, $2M-1$ additions and 1 division for updating the decorrelation filter. For calculating the thresholds, 6 multiplications, 6 additions, 3 divisions and 3 logarithmic operations are required. So, the proposed method may requires a total of $2L_{\mathrm{w}}+3L_{\mathrm{s}}+3L_{\mathrm{p}}+4M+10$ multiplications, $2L_{\mathrm{w}}+3L_{\mathrm{s}}+3L_{\mathrm{p}}+4M-2$ additions, 5 divisions and 3 logarithmic operations. Hence, $4L_{\mathrm{w}}+6L_{\mathrm{s}}+6L_{\mathrm{p}}+$

$8M + 16$ computations are required per sample. However, it is to be noted that the secondary path modelling and control operations are decoupled by means of the threshold detection and the toggling of the switches, which may lead to a reduced computational complexity than the above mentioned values.

Table 3.3 Computational complexity of different methods

Methods	Total computations per sample	Example
Proposed Method	$4L_{\mathrm{w}} + 6L_{\mathrm{s}} + 6L_{\mathrm{p}} + 8M + 16$	632
EF-1	$4L_{\mathrm{w}} + 6L_{\mathrm{s}} + 2L_{\mathrm{p}} - 4$	380
EF-2	$4L_{\mathrm{w}} + 6L_{\mathrm{s}} + 6L_{\mathrm{p}}$	576
Yang's Method	$4L_{\mathrm{w}} + 6L_{\mathrm{s}} + 4L_{\mathrm{h}} + 24$	344
Carini's Method	$13L_{\mathrm{w}} + 12L_{\mathrm{s}} + 8D + 25$	905
Gao's Method	$L_{\mathrm{w}} + L + \Delta + \frac{N_{\mathrm{a}}(2L_{\mathrm{w}} + 1)}{N_{\mathrm{D}}} + \frac{3(K_{\mathrm{L}} + N_{\mathrm{t}}\log_2 N_{\mathrm{t}})}{N_{\mathrm{D}}} + N_{\mathrm{a}}(10 + 8L_{\mathrm{w}})$	1778

For comparison purposes, the computational complexity of some existing approaches is summarized in Table 3.3, which includes the extended filtering method (Zhao et al. 2017), conventional extended filtering method (Kuo & Morgan 1999), Yang's method (Yang et al. 2018), Carini's method (Carini & Malatini 2008) and Gao's method (Gao, Lu & Qiu 2016). To make a straightforward comparison, one example is provided, where L_{w}= 48, L_{s}= 16, L_{p}=48, M= 5, and for Gao's method, the length of the prototype filter K_{L}=128, the down sampling rate N_{D}=10, the number of total subband N_{t}=20, the number of actual used subband N_{a}=4, direct path delay Δ=17, length of Hilbert filter L=34. The details of the computational complexity of Gao's method can be found in (Gao, Lu & Qiu 2016). It can be observed from Table 3.3 that the computational complexity of the

proposed method is higher than that of the extended filtering methods and Yang's method. However, it is lesser compared to that of Carini's and Gao's methods.

3.3 Online feedback path modelling

3.3.1 Proposed method

To avoid using auxiliary sound for feedback path modelling, in this work, we propose to use the control signal for online feedback path modelling and neutralization. A systematic method is proposed, which includes controller initialization, feedback path estimation, active control operation, and feedback path changing detection for maintaining control operation. In the online feedback path modelling, de-correlation filters are used to increase the convergence rate and reduce the bias of the feedback path modelling. Unlike the existing methods, the proposed method has three advantages. First, it avoids the need of an extra auxiliary noise generator; second, it uses a single filter for feedback path modelling and neutralization to reduce the overall computational complexity, and third, it decouples the feedback path modelling and control process to improve the performances. Furthermore, a stability detector is set in the ANC system to ensure the system stability in the event of howling or a feedback path change. In the first stage of the proposed method, if a howling is detected, a nominal estimate of the feedback path is used in order to stabilize the system. Then feedback path is estimated followed by the control operation. If a feedback path change is detected depending upon the preset thresholds in the middle of control operation, the control filter update is ceased and feedback path is remodeled. The proposed method therefore helps in decoupling the control operation and feedback path modelling.

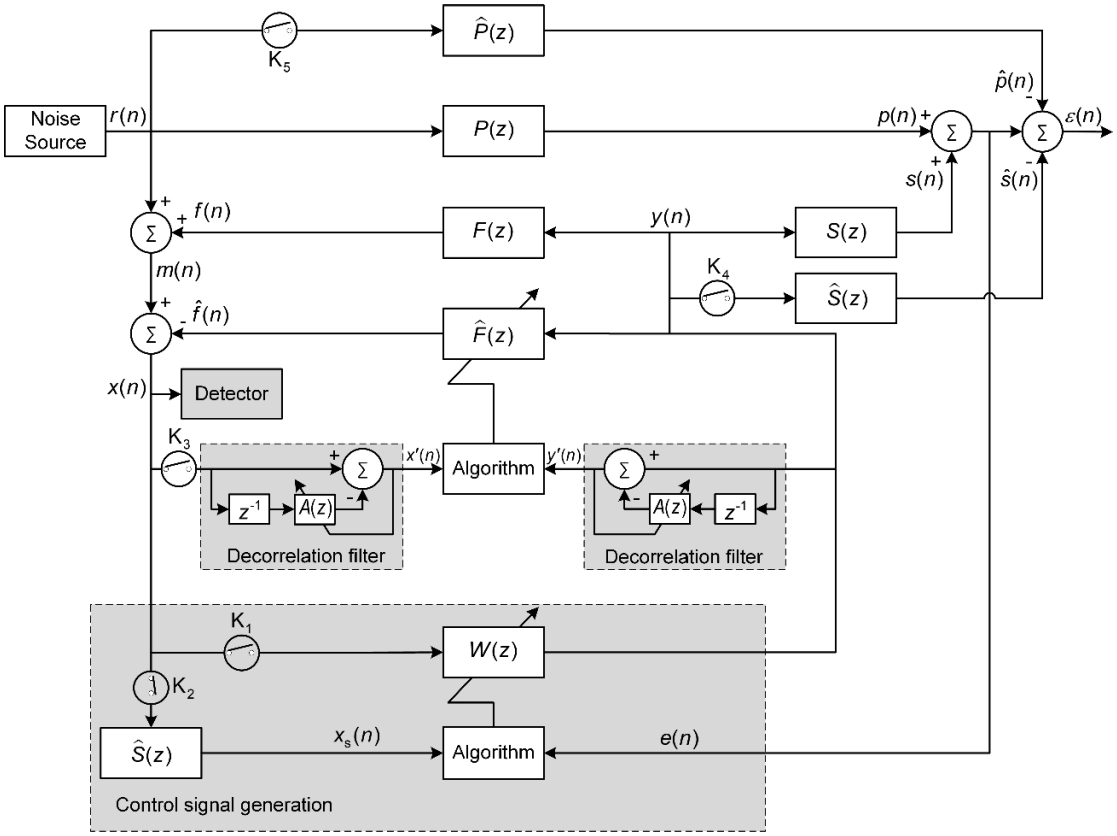

Figure 3.12 Schematic diagram of the proposed method for active control with online feedback path modelling using the control signal.

The proposed method shown in Figure 3.12 consists of four stages: controller initialization, feedback path estimation, active control operation, and feedback path changing detection for maintaining control operation. $P(z)$ is the primary path between the reference microphone and error microphone, $\hat{P}(z)$ is the estimate of the primary path, $F(z)$ is the acoustic feedback path from output of control filter $W(z)$ to the reference microphone, $\hat{F}(z)$ is the estimate of $F(z)$, $S(z)$ is the secondary path from output of control filter to the error microphone, and $\hat{S}(z)$ is the estimated secondary path. Five switches are used to manage the control flow: control signal generation (K_1), control filter update (K_2), feedback path estimation (K_3), detection of secondary path change (K_4, K_5).

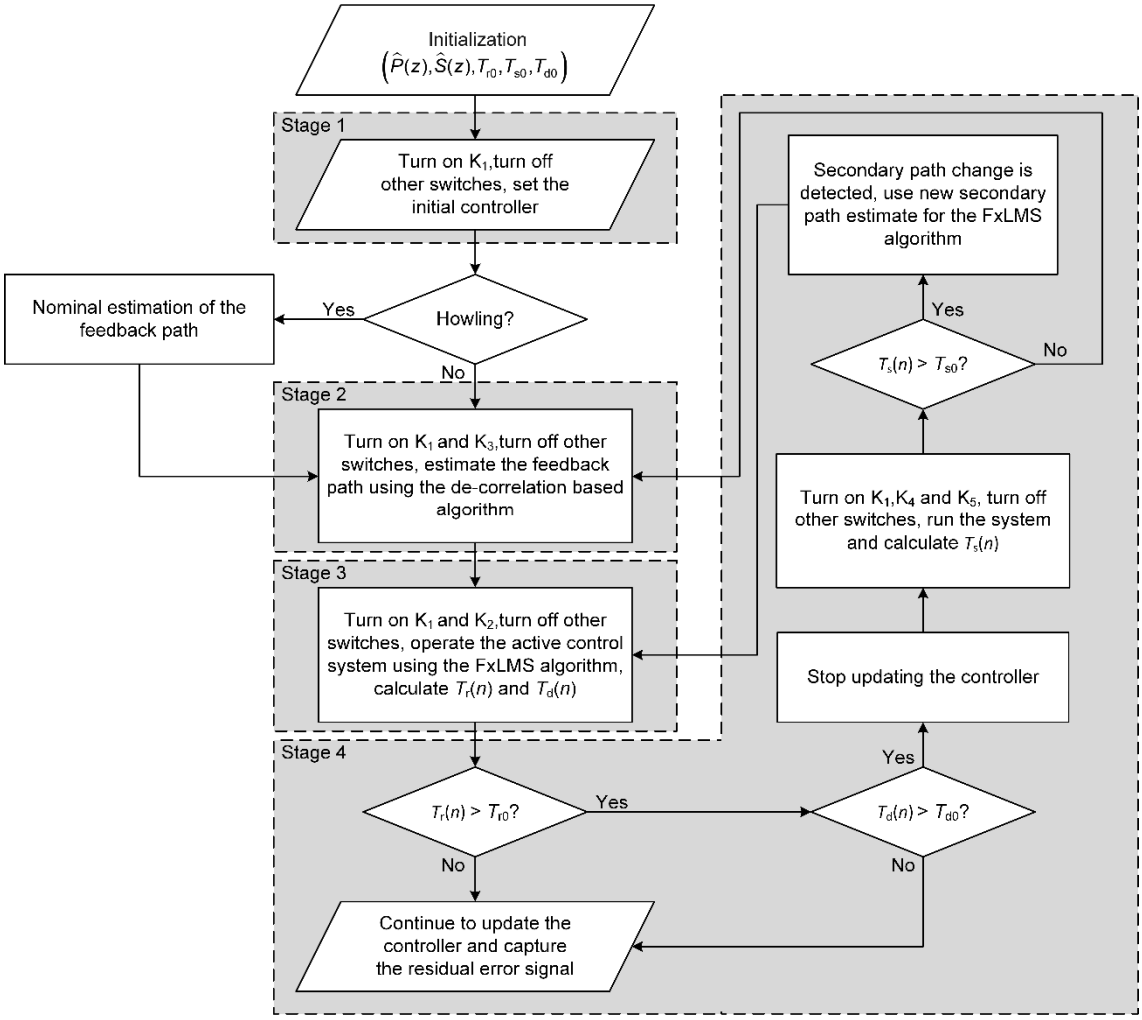

Figure 3.13 Flowchart of the proposed feedback path modelling method.

Figure 3.13 depicts the flowchart of the proposed method. In the initialization, the primary path estimate $\hat{P}(z)$ can be obtained by using the reference microphone signal and the error microphone signal with K_1 switched off, and the estimated secondary path $\hat{S}(z)$ is assumed to be identified as $S(z)$ to focus on feedback path modelling in the paper. To detect the path changes, three thresholds are defined

$$T_{\mathrm{r}}(n) = 10\log_{10}\left[\frac{\sigma_{\mathrm{e}}^2(n)}{\sigma_{\mathrm{p}}^2(n)}\right] \tag{3.13}$$

$$T_{\mathrm{s}}(n) = 10\log_{10}\left[\frac{\sigma_{\varepsilon}^2(n)}{\sigma_{\mathrm{p}}^2(n)}\right] \tag{3.14}$$

$$T_{\mathrm{d}}(n) = 10\log_{10}|\sigma_{\mathrm{x}}^2(n) - \sigma_{l}^2(n)|, \tag{3.15}$$

where $T_r(n)$ is the threshold to detect the residual noise level, $T_s(n)$ is the threshold to detect the accuracy of the estimated secondary path, $T_d(n)$ is the threshold to detect the feedback path change (stability). $\sigma_e^2(n)$ is the power of the measured error signal $e(n)$, which can be estimated by

$$\sigma_e^2(n) = \lambda\sigma_e^2(n-1) + (1-\lambda)e^2(n), \tag{3.16}$$

where $\lambda = 0.999$ is the forgetting factor with $\sigma_e^2(0) = 0$, and the range of λ is $0.9 < \lambda < 1$, in general (Benesty et al. 2006). $\sigma_p^2(n)$ is the power of the primary disturbance, which can be estimated similarly with Eq. (3.16) by turning off K_1. For $\sigma_\varepsilon^2(n)$ is the power of the modelling error signal $\varepsilon(n)$, and $\sigma_x^2(n)$ is the power of the signal $x(n)$. $\sigma_l^2(n)$ is the power of the signal $x_l(n) = \beta\tanh(x(n)/\beta)$, where β is a scaling parameter that determines the mapping of the signal $x(n)$ to the linear range of tanh function. The value of β is chosen by trial and error in such a way that the most likely range of the incoming reference signal $r(n)$ lies in the linear range of the tanh function, i.e., $r(n) \approx \beta\tanh(r(n)/\beta)$, which is depicted in Figure 3.14. The normal residual noise level with control, the normal estimated secondary path accuracy and the normal threshold $T_d(n)$ are assumed to be T_{r0}, T_{s0} and T_{d0}, respectively. All the powers are estimated recursively similar to Eq. (3.16) with their initial values equal to zero, i.e., $\sigma_p^2(0) = 0$, $\sigma_\varepsilon^2(0) = 0$, $\sigma_x^2(0) = 0$ and $\sigma_l^2(0) = 0$.

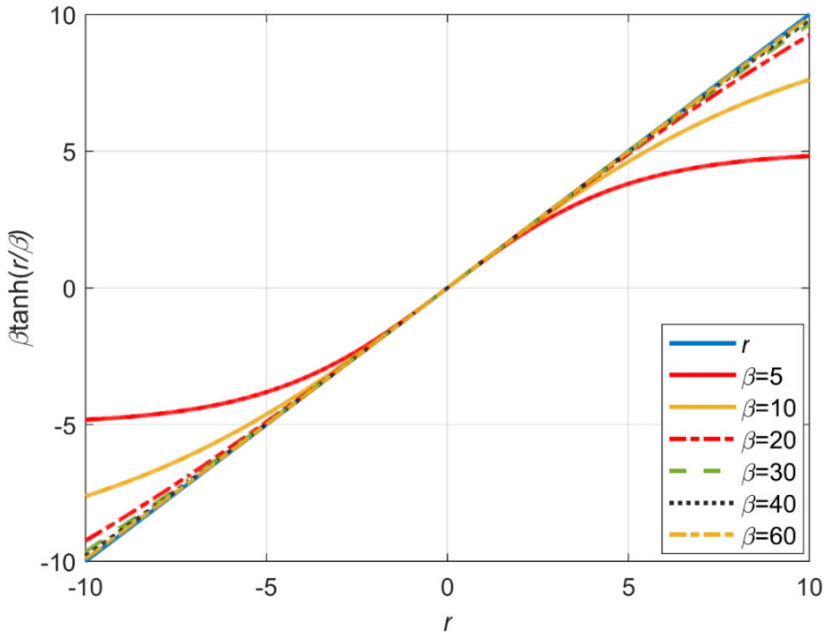

Figure 3.14 Effect of different value of β on mapping of $r(n)$ to the linear range of tanh function.

After initialization, the system enters into the first stage. In the first stage, K_1 is turned on and the other switches are turned off for setting the initial controller. The last coefficient of the control filter is set as a single gain G, and all other coefficients are set as zeros, i.e., $W(z) = z^{-L_w+1}G$, with L_w denoting the length of the control filter. G is tuned in such a way that the amplitude of the residual error signal $e(n)$ is higher than that of the undesired noise $p(n)$ without howling. At this stage, if the power of the residual error signal $e(n)$ becomes 20 dB higher than the power of undesired noise $p(n)$, it is considered as starting of howling.

If a howling happens, record $2L_f$ (L_f denotes the length of $\hat{F}(z)$) controller output signal $y(n)$ and reference microphone signal $m(n)$ and use them directly to calculate a nominal estimate of $F(z)$. The nominal estimate of $F(z)$ can be obtained as

$$\hat{\boldsymbol{f}}_n(n) = \text{IFFT}\left(\frac{M(\omega)}{Y(\omega)}\right), \tag{3.17}$$

where IFFT denotes the inverse Fourier transform, $\hat{\boldsymbol{f}}_{\mathrm{n}}(n)$ is the impulse response vector of the nominal estimate, $M(\omega)$ is the FFT of the microphone signal $m(n)$, and $Y(\omega)$ is the FFT of $y(n)$. Although Eq. (3.17) might not provide an exact estimate of $F(\mathrm{z})$ because the reference signal is contaminated, it can be used to stabilize the system for further feedback path modelling. It should be noted that the magnitude of $y(n)$ should be quite large in the above identification because it makes the power of the residual error signal $e(n)$ about 20 dB higher than the power of $p(n)$ when a howling happens.

If there is no howling, the controller G is increased from a small pre-defined value (for example, G = 1% of the maximal gain can be applied on the system without causing a howling) by 2 times each step until $\sigma_{\mathrm{e}}^2(n) > \sigma_{\mathrm{p}}^2(n)$. That means the system stays in the first stage until $\sigma_{\mathrm{e}}^2(n) > \sigma_{\mathrm{p}}^2(n)$ without causing howling. Once the system is stable and the above condition is satisfied, it is ready to enter the second stage.

In the second stage, K_1 and K_3 are turned on and the other switches are turned off. The feedback path $F(z)$ is estimated as an FIR filter $\hat{F}(z)$ using the control signal as the excitation signal. The initial impulse response vector of $\hat{F}(z)$ can be a vector of zeros if no howling occurs in the first stage or the one obtained with Eq. (3.17) if a howling occurs. Because the control signal $y(n)$ and reference signal $r(n)$ are correlated, the obtained model is biased. Although a delay present in the control filter in the first stage can reduce correlation somehow, normalized least mean square (NLMS) decorrelation filters are used in this stage to whiten the signals used in the feedback path modelling process to increase the convergence speed and reduce the bias of the adaptive filter (Mboup, Bonnet & Bershad 1994; Zhang et al. 2017).

Two identical adaptive decorrelation filters $L(z) = 1 - z^{-1}A(z)$ are employed to address the bias and slow convergence issue of feedback path modelling in the second stage, where $A(z)$ is the z-transform of $\boldsymbol{a}(n) = [a_0(n), a_1(n), \dots, a_{N-1}(n)]^{\mathrm{T}}$ with N denoting

the tap-weight length of $A(z)$. The feedback compensated signal $x(n) = r(n) + f(n) - \hat{f}(n)$ passes through the adaptive decorrelation filter to provide the signal $x'(n) = x(n) - \boldsymbol{a}^{\mathrm{T}}(n)\boldsymbol{x}_1(n)$, where $\boldsymbol{x}_1(n) = [x(n-1),\ x(n–2), \ldots,\ x(n–N)]^{\mathrm{T}}$. Similarly, the control signal $y(n)$ passes through the decorrelation filter to provide $y'(n) = y(n) - \boldsymbol{a}^{\mathrm{T}}(n)\boldsymbol{y}_1(n)$, where $\boldsymbol{y}_1(n) = [y(n-1), y(n–2), \ldots, y(n–N)]^{\mathrm{T}}$. The pre-whitened signals $y'(n)$ and $x'(n)$ are used to update the filter $\hat{F}(z)$.

The adaptive decorrelation filter is updated using the NLMS algorithm as

$$\boldsymbol{a}(n+1) = \boldsymbol{a}(n) + \mu_l \frac{x'(n)\boldsymbol{x}_1(n)}{\boldsymbol{x}_1^{\mathrm{T}}(n)\boldsymbol{x}_1(n) + \delta} \tag{3.18}$$

where μ_l is the step size and δ is used to avoid divide by zero. The tap-weights of $\hat{F}(z)$ are updated as

$$\hat{\boldsymbol{f}}(n+1) = \hat{\boldsymbol{f}}(n) + \mu_{\mathrm{f}} \frac{x'(n)\boldsymbol{y}'(n)}{\boldsymbol{y}'^{\mathrm{T}}(\boldsymbol{n})\boldsymbol{y}'(n) + \varepsilon} \tag{3.19}$$

where μ_{f} is the step size, ε is used to avoid divide by zero, and $\boldsymbol{y}'(n) = [y'(n), y'(n-1), \ldots, y'(n - L_{\mathrm{f}} + 1)]^{\mathrm{T}}$. It is to be noted that the above described method is applicable for broadband control only. In this stage, the feedback path modelling is carried out for a certain time, which depends on the feedback signal to reference signal amplitude ratio. A higher value of the feedback to reference signal ratio can have shorter time, whereas a smaller value requires a longer time. Here, the modelling time duration is chosen by trial and error and can be started with the same time that is used to model the secondary path.

In the third stage, the switches K_1 and K_2 are turned on and the other switches are turned off, the control operation is carried out with the FxLMS algorithm. The control weights are updated as

$$\boldsymbol{w}(n+1) = \boldsymbol{w}(n) - \mu_w e(n)\boldsymbol{x}_s(n), \tag{3.20}$$

where μ_w is the step size with initial control weights $\boldsymbol{w}(0) = \mathbf{0}$, a null vector of length L_w, $\boldsymbol{x}_s(n) = [x_s(n), x_s(n-1), \ldots, x_s(n-L_w+1)]^T$ with L_w denoting the tap-weight length of the control filter, and $x_s(n)$ is the filtered reference signal, which is obtained by filtering $x(n)$ with the secondary path estimate $\hat{\boldsymbol{s}}(n)$. The residual noise is reduced continuously towards normal noise reduction T_{r0}. If the noise reduction level increases suddenly, it triggers the system into the fourth stage.

The fourth stage involves the feedback path changing detection. Assume that the normal residual noise level is $T_{r0} = -10$ dB in the operation. If suddenly it becomes greater than −10 dB, i.e., $T_r(n) > T_{r0}$, there is a path change. It is to be noted that $T_r(n)$ is calculated for each instance of time. At the same time, $\sigma_x^2(n)$, $\sigma_l^2(n)$ and $T_d(n)$ are also estimated in a side branch of the system (Detector in the schematic diagram shown in Figure 3.3). If $T_d(n) < T_{d0}$ ($T_{d0} = -10$ dB for example), the system is stable and the change is caused by the primary path and the control operation is resumed. If $T_d(n) > T_{d0}$, the rise in $T_r(n)$ may be due to the secondary path change or the feedback path change, and the control filter update is ceased by turning off K_2. In practice, the secondary path and the feedback path usually change simultaneously when the secondary source or sound propagation paths change.

To check whether the change is due to the secondary path, K_1, K_4 and K_5 are turned on and the other switches are turned off. At this time, there is controller output but without controller update, $\sigma_\varepsilon^2(n)$ and $T_s(n)$ are estimated. If $T_s(n) > T_{s0}$ ($T_{s0} = -15$ dB for example), the change is in the secondary path. In this case, the secondary path is remodelled and then the control operation is resumed with the new model. Here, $T_{s0} = -15$ dB is chosen based on an adequate secondary path model, which can be obtained with the extended filtering method (Kuo & Morgan 1999; Zhao et al. 2017). Though the proposed method

focuses on the feedback path modelling, the secondary path modelling is highlighted here for the sake of completeness of the whole ANC system.

If $T_s(n) < T_{s0}$ (when K_1, K_4 and K_5 are turned on and the other switches are turned off), the rise in $e(n)$ is due to the feedback path change. The feedback path is modelled by turning on switches K_1 and K_3 and turning off the other switches with the previously obtained $W(z)$. After obtaining a new $\hat{F}(z)$, K_1 and K_2 are turned on, the other switches are turned off, the active control operation is resumed by updating the control coefficients as in Eq. (3.20), and the system runs in the third stage.

3.3.2 Numerical experiments

In this subsection, the simulation results are presented for the method described in subsection 3.3.1. In the literature, little research can be found for feedback path modelling using the control signal. The closest related algorithm is Akhtar's method (Akhtar, Abe & Kawamata 2007), which uses random noise for online feedback path modelling, so it is used as a benchmark for comparison with the proposed method. In the simulations, the primary path $P(z)$, secondary path $S(z)$ and the feedback path $F(z)$ are FIR filters of lengths 48, 16 and 32, respectively, which are collected from the data provided by Kuo and Morgan (1996), Their spectra are shown in Figure 3.15. The adaptive filters $W(z)$, $\hat{S}(z)$ and $\hat{F}(z)$ are selected as FIR filters of lengths L_w = 48, L_s = 16 and L_f = 32, respectively. The adaptive de-correlation filter $A(z)$ is an FIR filter of length N = 5.

The reference signal r(n) is generated from an autoregressive process

$$r(n) = 0.9r(n-1) + v(n) \tag{3.21}$$

where $v(n)$ is a white noise with zero-mean and unit variance. The white noise injected in Akhtar's method is a zero-mean with variance 0.05. The sampling frequency used in the simulation is 2 kHz. All the simulation results are averaged over 10 independent

realizations. The mean square error defined in Eq. (3.10) and the relative modelling error ΔF defined in Eq. (3.22) are used as the metrics for comparison.

$$\Delta F \text{ (dB)} = 10 \log_{10} \left\{ \frac{\left\| \boldsymbol{f}(n) - \hat{\boldsymbol{f}}(n) \right\|^2}{\|\boldsymbol{f}(n)\|^2} \right\}. \tag{3.22}$$

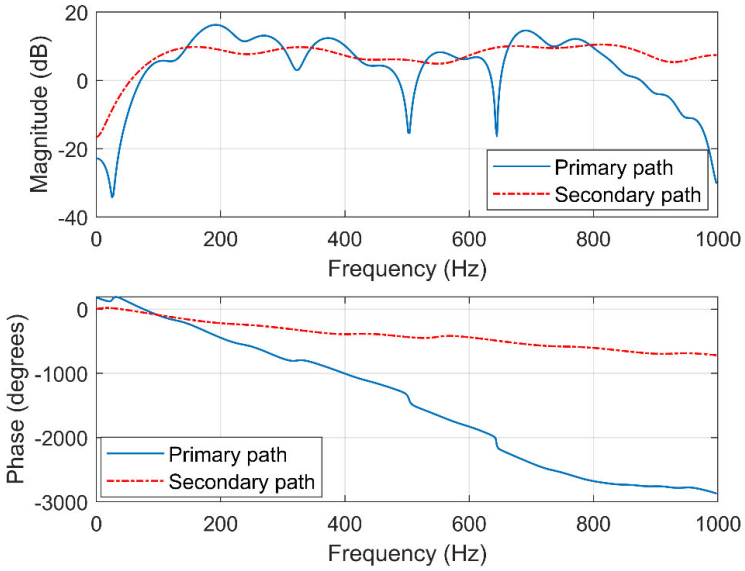

(a)

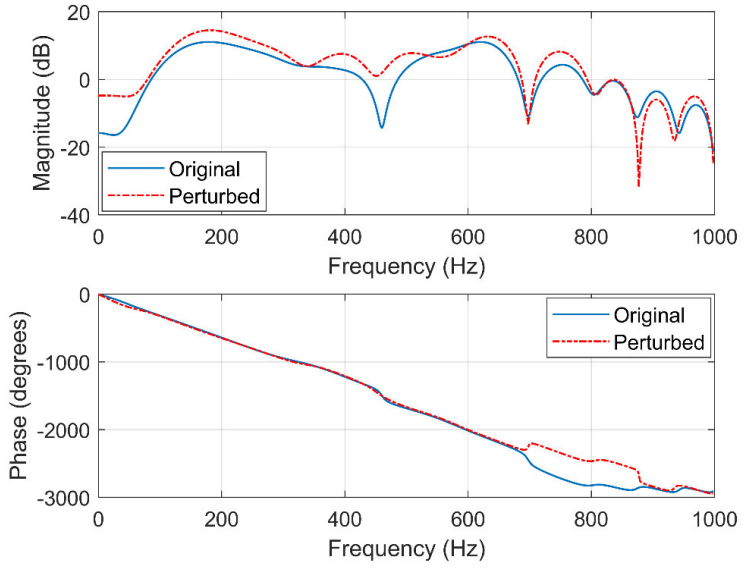

(b)

Figure 3.15 Frequency response of (a) the primary path and the secondary path and (b) feedback path.

In the first stage of the proposed online feedback path modelling method, K_1 is turned on and the other switches are turned off for initializing the controller. The control filter is set as $W(z) = z^{-47}$, representing a delay of $L_w - 1$ samples followed by unit gain. The amplitude of the residual error signal $e(n)$ is higher than that of the undesired noise $p(n)$ in this initialization, a howling occurs. A nominal estimate of the feedback path using Eq. (3.17) is used to maintain the stability of the control system. In the second stage, the feedback path modelling is carried out using the proposed decorrelation filters for 10 seconds, during which K_1 and K_3 are turned on and the other switches are turned off. The benefit of using the decorrelation filters can be noticed from the modelling error shown in Figure 3.16.

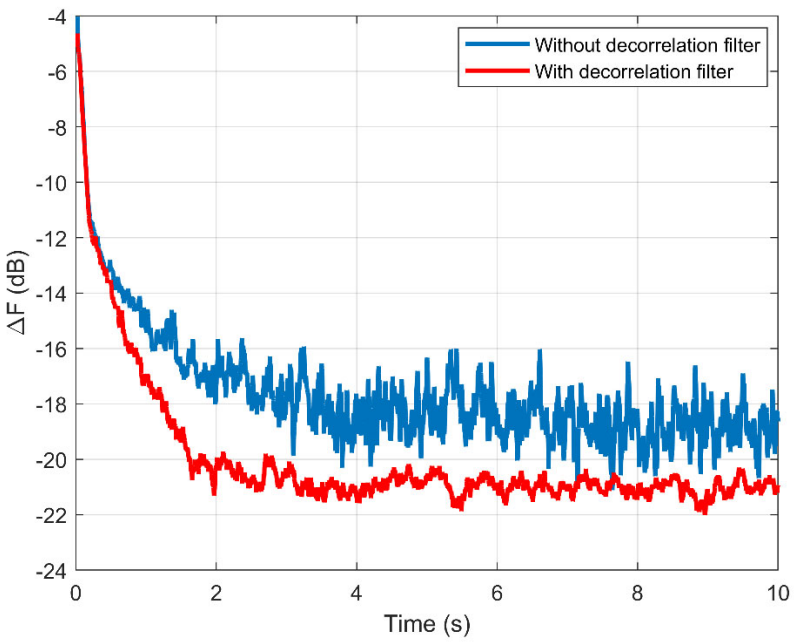

Figure 3.16 Feedback path modelling error in the second stage.

The improved modelling accuracy is due to the reduction of bias, which is achieved by the whitening property of the decorrelation filter. The steady-state modelling error without using the decorrelation filters fluctuate more as compared to the one with the decorrelation filters due to the existence of bias. Furthermore, the decorrelation filters aid

in faster convergence of the adaptive filter, e.g., to achieve −16 dB modelling error, the one with the decorrelation filters takes 0.7 second compared to 1.1 seconds taken by the one without decorrelation filters. The modelling error obtained with and without decorrelation filters at 2.0 second are −20.3 dB and −17.4 dB, respectively.

After the feedback path modelling, K_1 and K_2 are turned on and the other switches are turned off, the simulation for control operation runs for 50 seconds with the original acoustic paths shown in Figure 3.15. Then the feedback path changes suddenly, resulting in a situation $T_r(n) > -10$ dB and $T_d(n) > -10$ dB, the control update is ceased. The switches K_1, K_4 and K_5 are turned on and the other switches are turned off, the threshold $T_s(n)$ is checked confirming a feedback path change. The feedback path remodelling is carried out to estimate the new feedback path. After an adequate modelling, the control operation is resumed. The simulation parameters used for the proposed method are: $\mu_w = 0.0001$, $\mu_f = 0.03$, $\mu_l = 0.01$, $\delta = \varepsilon = 0.00001$, and $\beta = 60$. For Akhtar's method $\mu_w = 0.0001$, $\mu_f = 0.001$, and $\mu_h = 0.0001$. The step sizes are chosen by trial and error to make system stable yet with the fastest convergence speed.

Figure 3.17(a) depicts the modelling error obtained for the whole duration of control operation. One can notice that the proposed method maintains constant modelling error for the first 50 seconds because the feedback path is modelled before the control operation. After the detection of feedback path change at the 50th second, the controller update is ceased, K_1 and K_3 are turned on and the other switches are turned off. The feedback path modelling is carried out from the 50th second to the 70th second, and reasonably accurate feedback path is obtained using the decorrelation filters. The feedback path remodelling in the fourth stage takes longer time compared to the feedback path modelling in the second stage because of the presence of the control filter, whose frequency response is not flat in general.

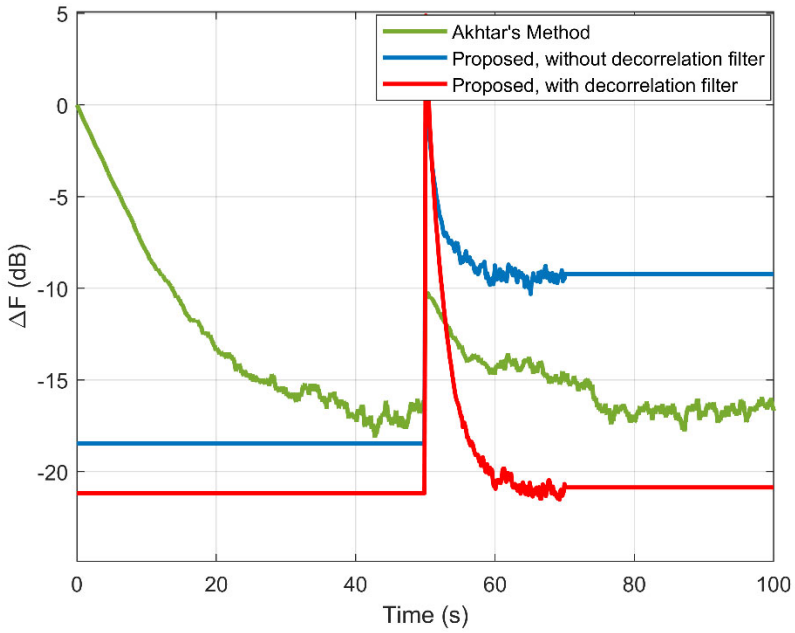

(a)

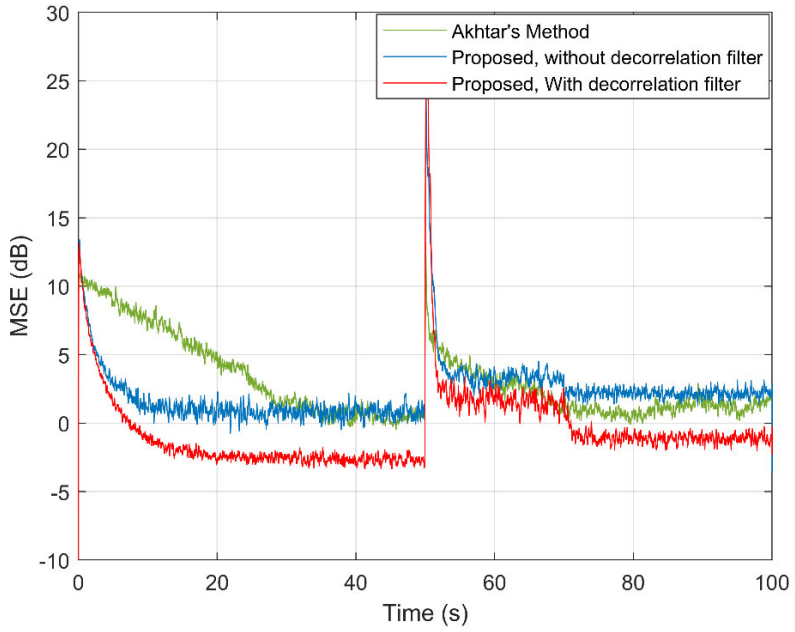

(b)

Figure 3.17 (a) Feedback path modelling error, (b) learning curve for the whole duration of control operation.

The control operation is resumed after the 70th second, K_1 and K_2 are turned on, the other switches are turned off and thus the modelling error is constant. But for Akhtar's

method, both the control operation and feedback path modelling occur simultaneously, resulting in a continuous variation of modelling error. It is important to notice that the proposed method with the decorrelation filters obtained approximately 11 dB less modelling error than the one without using the decorrelation filters and approximately 6 dB less modelling error than Akhtar's method.

The learning curves for the control operation are depicted in Figure 3.17(b), which shows the superiority of the proposed method with the decorrelation filters before and after the feedback path change. For the first 50 seconds, the proposed method achieves faster convergence and lower steady-state residual error. The convergence of Akhtar's method is slow due to the fact that the control operation and feedback path modelling process interfere with each other. An inaccurate feedback path estimation filter leads to increased interferences in control operation, i.e., the presence of feedback component in reference signal affects the active control performance.

After the 50^{th} second, the feedback path is changed, and therefore the residual error increases sharply. From the 50^{th} second to the 70^{th} second, feedback path modelling is carried out neutralizing the feedback component, and hence the magnitude of the feedback compensated input signal to the control filter is reduced, consequently the error level reduces due to the existence of the fixed control filter. After the 70^{th} second, the control operation is resumed and the noise is further reduced. The improvement in control performance in the proposed method is attributed to the inclusion of the decorrelation filters to address the issue of biased estimation and the decoupling between the control operation and feedback path modelling.

3.3.3 Computational complexity

Using decorrelation filters in the proposed method increases the computational load, which include two identical decorrelation filtering, the coefficient update of the decorrelation filter and obtaining the prewhitening signal, but it has less computational burden compared to Akhtar's method using auxiliary noise, which uses an adaptive noise cancellation filter (ADNC) of length L_{h} and two separate filters for FBPM and FBPN. Furthermore, it is to be noted that the feedback path modelling and the control operation are not carried out simultaneously, leading to a reduced computational load.

The computational complexity is calculated in terms of number of multiplications (per samples) and number of additions (per sample). All the methods require L_{w} multiplications and $L_{\mathrm{w}}-1$ additions to obtain the controller output; L_{s} multiplications and $L_{\mathrm{s}}-1$ additions to obtain the filtered reference signal; L_{f} multiplications and $L_{\mathrm{f}}-1$ additions to obtain the estimated feedback signal; $L_{\mathrm{w}}+1$ multiplications and L_{w} additions to update the control filter. Unlike Akhtar's method a single filter is used for feedback path modelling and neutralization. The proposed method requires $2N$ multiplications and $2(N-1)$ additions to obtain the decorrelation filter outputs; $2L_{\mathrm{f}}+1$ multiplications and $2L_{\mathrm{f}}-1$ additions for updating the feedback path modelling and neutralization filter; $2N+1$ multiplications and $2N-1$ additions for updating the decorrelation filter. Akhtar's method requires L_{h} multiplications and $L_{\mathrm{h}}-1$ additions for obtaining the ADNC filter output; $2L_{\mathrm{h}}+1$ multiplications and $2L_{\mathrm{h}}-1$ additions for updating the ADNC filter using NLMS algorithm. The basic computational load (filtering and filter update) for the related methods are summarized in Table 3.4, in which $(\times)$ denotes the number of multiplications per sample and $(+)$ denotes the number of additions per sample associated with different operations. For a particular case considered

in the simulations, the total number of multiplications per sample and additions per sample are also included in the last row of Table 3.4.

Table 3.4 Computational load for different methods

Operation	Proposed (with the decorrelation filters)		Proposed (without the decorrelation filters)		Akhtar's Method	
	×	+	×	+	×	+
Controller output	L_{w}	$L_{\mathrm{w}}-1$	L_{w}	$L_{\mathrm{w}}-1$	L_{w}	$L_{\mathrm{w}}-1$
Filtered signal	L_{s}	$L_{\mathrm{s}}-1$	L_{s}	$L_{\mathrm{s}}-1$	L_{s}	$L_{\mathrm{s}}-1$
Controller update	$L_{\mathrm{w}}+1$	L_{w}	$L_{\mathrm{w}}+1$	L_{w}	$L_{\mathrm{w}}+1$	L_{w}
Neutralization filter output	L_{f}	$L_{\mathrm{f}}-1$	L_{f}	$L_{\mathrm{f}}-1$	L_{f}	$L_{\mathrm{f}}-1$
Neutralization filter update	$2L_{\mathrm{f}}+1$	$2L_{\mathrm{f}}-1$	$2L_{\mathrm{f}}+1$	$2L_{\mathrm{f}}-1$	None	None
Decorrelation filter output	$2N$	$2(N-1)$	None	None	None	None
Decorrelation filter update	$2N+1$	$2N-1$	None	None	None	None
ADNC filter output	None	None	None	None	L_{h}	$L_{\mathrm{h}}-1$
ADNC filter update	None	None	None	None	$2L_{\mathrm{h}}+1$	$2L_{\mathrm{h}}-1$
FBPM filter output	None	None	None	None	L_{f}	$L_{\mathrm{f}}-1$
FBPM filter update	None	None	None	None	$2L_{\mathrm{f}}$+1	$2L_{\mathrm{f}}-1$
Total	$2L_{\mathrm{w}}+L_{\mathrm{s}}+3L_{\mathrm{f}}+4N+3$	$2L_{\mathrm{w}}+L_{\mathrm{s}}+3L_{\mathrm{f}}+4N-7$	$2L_{\mathrm{w}}+L_{\mathrm{s}}+3L_{\mathrm{f}}+2$	$2L_{\mathrm{w}}+L_{\mathrm{s}}+3L_{\mathrm{f}}-4$	$2L_{\mathrm{w}}+L_{\mathrm{s}}+4L_{\mathrm{f}}+3L_{\mathrm{h}}+3$	$2L_{\mathrm{w}}+L_{\mathrm{s}}+4L_{\mathrm{f}}+3L_{\mathrm{h}}-7$
L_{w} = 48, L_{f} = 32, L_{s} = 16, L_{h} =16, N = 5	231	221	210	204	291	281

3.4 Summary

In summary, the proposed five-stage method and the decorrelation filter maintain the control operation when both the primary and the secondary path change. Unlike the existing algorithms, the proposed method detects the change of acoustic paths by monitoring the pre-set thresholds, and then uses three switches for choosing the active control operation, remodelling the primary path and remodelling the secondary path. It removes the primary disturbance during secondary path modelling, reduces the convergence time of the control filter by reducing the remodelling time of the secondary

path modelling filter with the decorrelation filter. The proposed method possesses larger computational complexity than the EF-1, the EF-2 algorithms and Yang's method due to the threshold detections, the presence of two identical decorrelation filters, the coefficient update of the decorrelation filters and obtaining the pre-whitened signals. Furthermore, the remodelling of the acoustic paths requires few seconds. The proposed method is affected by measurement noise of SNR values less than 10 dB. However, the measurement noise of SNR values greater than 20 dB has little effect on the control performance. Although the proposed method can be useful for narrowband and broadband signals for handling both the primary and the secondary path change, it may not provide significant improvement in performance in situations where the excitation signal is tonal or white and the changes in the acoustic paths occur more frequently before one remodelling is completed.

The proposed four-stage method and the decorrelation filters maintain the control operation with improved performance and system stability when the feedback path changes. In contrast to the existing algorithm, the proposed method detects the change of acoustic paths by monitoring the preset thresholds, and uses five switches to decouple the feedback path modelling from control operation. Therefore, the implementation of the proposed algorithm is quite simple. Although, the proposed method can be useful for broadband signals for feedback path modelling, it is not effective for tonal signals because it is not possible to compensate all the feedback component when the feedback path modelling is carried out using tonal control signal. The auxiliary noise injection method still holds good for tonal active control system.

4 Affine combination of adaptive filters for active control

4.1 Introduction

The filtered-x least mean square algorithm is extensively employed for active control, which exhibits a trade-off between convergence speed and the steady-state control performance. In this chapter, an affine combination strategy of the filtered-x least mean square and fourth algorithms is proposed, which can be regarded as a generalized convex combination[1]. Unlike the convex combination, the combining parameter in this linear combination is not constrained to lie in a specific interval and plays a vital role in deciding the overall system performance. An adaptation rule is developed for updating the combining parameter. The proposed affine combination strategy is used to control white noise and multi-tone noise. The simulation results demonstrate that the proposed algorithm provides faster convergence and improved steady-state control performance. Furthermore, the proposed affine combination is also robust with an imperfect secondary path model.

[1] This chapter has been published as: Pradhan, S., Qiu, X. & Ji, J. 2021, 'Affine combination of the filtered-x LMS/F algorithms for active control', Vibration Engineering for a Sustainable Future, Springer, pp. 313-9.

5 A time-frequency domain flexible structure for active control

5.1 Introduction

Frequency domain filtered-x least mean square algorithms can reduce the computational complexity of the time domain counterpart with long filters; however, suffer from large block delay, additional quantization error due to large size transformations and implementation difficulties in existing DSP hardware. In this work, a time-frequency domain flexible structure is proposed using the partitioned block frequency domain adaptive filtering technique, which has no signal path delay and is well suited for low-cost DSP implementation[1]. The proposed structure divides the long filters into many equal partitions and carry out the control filter update in frequency domain while generating the control signal in both time and frequency domains. The simulation results using the measured acoustic paths demonstrate that the proposed structure maintains similar performance as that of the time domain algorithm but with much less computational complexity.

5.2 The proposed structure

Figure 5.1 shows the schematic block diagram of the proposed structure for a single channel feedforward ANC system, where, $P(z)$, $S(z)$ and $\hat{S}(z)$ represent the transfer function of the primary path, the secondary path and the secondary path model, respectively. The L_w long control filter is $\boldsymbol{w}(n) = [w_0(n), w_1(n), \dots, w_{L_w-1}(n)]^T$ and the L_s long secondary path model is $\hat{\boldsymbol{s}}(n) = [\hat{s}_0(n), \hat{s}_1(n), \dots, \hat{s}_{L_s-1}(n)]^T$. $x(n)$ is the

[1] A portion of this chapter has been submitted as: Pradhan, S., Qiu, X. & Ji, J. 2020, 'A time-frequency domain flexible structure of delayless partitioned block adaptive filters for active control', submitted to *Applied Acoustics* [under revision].

reference signal, $p(n)$ is the primary disturbance signal at the error microphone, $y(n)$ is the control signal, $s(n)$ is the cancelling signal, and $e(n)$ is the residual error signal. In the figure, S/P, P/S and z^{-D} denotes the serial-to-parallel converter, parallel-to-serial converter, and a block size delay of D, respectively.

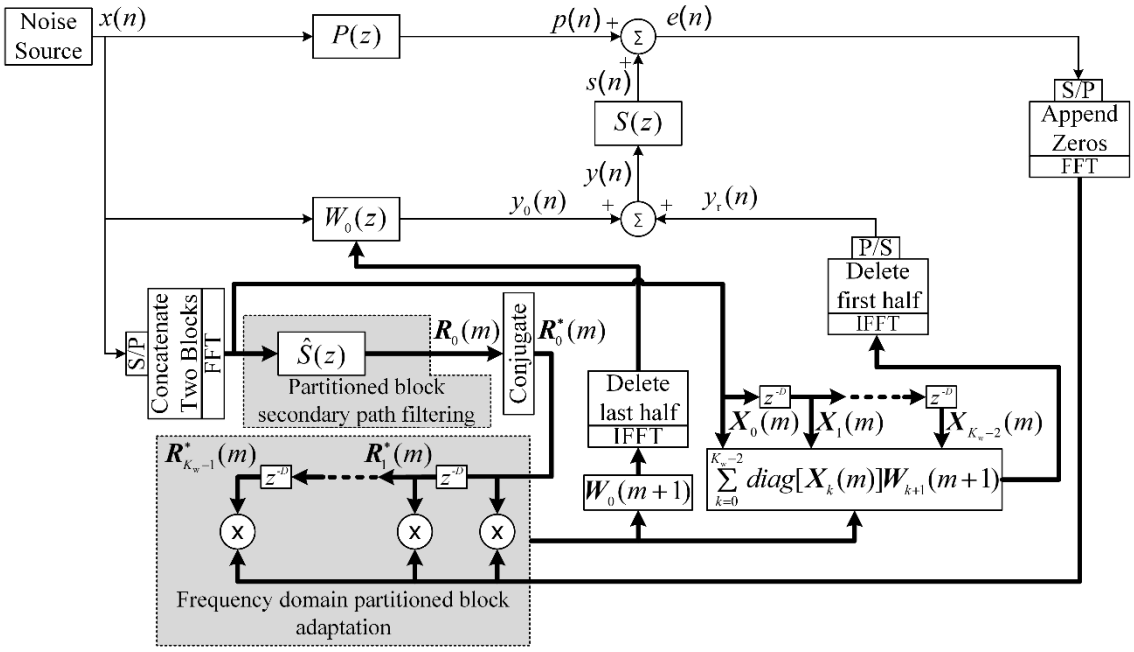

Figure 5.1 Block diagram of the proposed structure for a single channel feedforward ANC system.

The control filter is partitioned into K_w segments, and $N = L_w/K_w$ is the length of each segment which can be expressed as

$$\boldsymbol{w}_{kN}(n) = [w_{kN}(n), w_{kN+1}(n), \dots, w_{kN+N-1}(n)]^{\mathrm{T}}, \tag{5.1}$$

where $k = 0, 1, \dots, K_w-1$. Using the overlap-save method, N point zeros are appended at the end of the kth control sub-filter so that a $2N$ point FFT is applied to have $\boldsymbol{W}_k(m) = FFT[w_{kN}(n), w_{kN+1}(n), \dots, w_{kN+N-1}(n), 0,0, \dots, 0]^{\mathrm{T}}$, where $m = n/N$ is the block index. The control signal $y(n)$ can be written as

$$y(n) = \sum_{k=0}^{K_w-1} y_k(n) = \sum_{k=0}^{K_w-1} \boldsymbol{w}_{kN}^{\mathrm{T}}(n)\boldsymbol{u}_{kN}(n), \tag{5.2}$$

where $y_k(n)$ is the output of the kth partition and $\boldsymbol{u}_{kN}(n) = [x(n-kN), x(n-kN-1), \ldots, x(n-(k+1)N+1)]^{\mathrm{T}}$. $y(n)$ can otherwise be written as $y(n) = y_0(n) + y_r(n)$, where $y_0(n)$ is the output of the first partition which is obtained in time domain in the proposed structure. The remaining part of the output is

$$y_{\mathrm{r}}(n) = \sum_{k=1}^{K_{\mathrm{w}}-1} y_k(n), \tag{5.3}$$

which is obtained in frequency domain. For a block of reference signal $\boldsymbol{x}_N(m) = [x(n), x(n+1), \ldots, x(n+N-1)]^{\mathrm{T}}$, the block of control signal $\boldsymbol{y}_N(m) = [y(n), y(n+1), \ldots, y(n+N-1)]^{\mathrm{T}}$ can be obtained by

$$\boldsymbol{y}_N(m) = [\boldsymbol{0}_N \; \boldsymbol{I}_N] \sum_{k=0}^{K_{\mathrm{w}}-1} IFFT\{diag[\boldsymbol{X}_k(m)]\boldsymbol{W}_k(m)\}, \tag{5.4}$$

where $[\boldsymbol{0}_N \; \boldsymbol{I}_N]$ is an $N\times 2N$ matrix, $\boldsymbol{X}_k(m) = FFT\{[\boldsymbol{x}_N^{\mathrm{T}}(m-1) \; \boldsymbol{x}_N^{\mathrm{T}}(m)]^{\mathrm{T}}\}$. Defining $\boldsymbol{y}_{\mathrm{r}}(m) = [y_{\mathrm{r}}(n), y_{\mathrm{r}}(n+1), y_{\mathrm{r}}(n+N-1)]^{\mathrm{T}}$ and using Eqs. (5.3) and (5.4), it has

$$\boldsymbol{y}_{\mathrm{r}}(m+1) = [\boldsymbol{0}_N \; \boldsymbol{I}_N] \sum_{k=1}^{K_{\mathrm{w}}-1} IFFT\{diag[\boldsymbol{X}_k(m+1)]\boldsymbol{W}_k(m+1)\} \tag{5.5}$$

In Eq. (5.5), $\boldsymbol{X}_k(m+1)$ is obtained by shifting operation $\boldsymbol{X}_k(m+1) = \boldsymbol{X}_{k-1}(m)$, and it has

$$\boldsymbol{y}_{\mathrm{r}}(m+1) = [\boldsymbol{0}_N \; \boldsymbol{I}_N] \sum_{k=0}^{K_{\mathrm{w}}-2} IFFT\{diag[\boldsymbol{X}_k(m)]\boldsymbol{W}_{k+1}(m+1)\}. \tag{5.6}$$

The $(m+1)$th block contains samples with $n = (m+1)N, \ldots, (m+2)N-1$. Considering the pth element of $\boldsymbol{y}_{\mathrm{r}}(m+1)$ as $\boldsymbol{y}_{\mathrm{r_p}}(m+1)$, $0 \le p \le N-1$, it has $y_{\mathrm{r}}(n) = \boldsymbol{y}_{\mathrm{r}_{n-(m+1)N}}(m+1)$. Therefore, the output $y(n)$ in block $(m+1)$ can be obtained as

$$y(n) = y_0(n) + y_{\mathrm{r}}(n) = \boldsymbol{w}_0^{\mathrm{T}}(n)\boldsymbol{u}_0(n) + \boldsymbol{y}_{\mathrm{r}_{n-(m+1)N}} \tag{5.7}$$

It can be observed from Eqs. (5.6) and (5.7) that $y_{\mathrm{r}}(n)$ in block (m+1) can be efficiently pre-obtained without waiting for the accumulation of the new block of samples, and $y_0(n)$ can be obtained in real time by using linear convolution in the first partition. Hence, there is no signal path delay in obtaining the control signal $y(n)$.

The time domain filter coefficients of the first partition are obtained from the frequency domain updated weights as

$$\boldsymbol{w}_0(n) = [\boldsymbol{I}_N \ \boldsymbol{0}_N] IFFT[\boldsymbol{W}_0(m+1)]. \tag{5.8}$$

Therefore, $\boldsymbol{W}_k(m+1), 0 \le k \le K_{\mathrm{w}} - 1$ can be adapted using the conventional FPBFxLMS algorithm and $\boldsymbol{w}_0(n)$ is obtained once every N samples by Eq. (5.8). The frequency domain residual error signal vector is obtained by taking 2N point FFT of the error vector $\boldsymbol{e}_N(m) = [e(n), e(n+1), \ldots, e(n+N-1)\ ]^{\mathrm{T}}$ with N zeros appended at the beginning, and can be written as

$$\boldsymbol{E}(m) = FFT[0,0 \ldots,0, e(n), e(n+1), \ldots, e(n+N-1)\ ]^{\mathrm{T}} \tag{5.9}$$

The estimated secondary path filter is partitioned into K_{s} segments, each with a length of $N = L_{\mathrm{s}}/K_{\mathrm{s}}$, and the 2$N$ point FFT is calculated for each partition with N zeros appended at the end as

$$\boldsymbol{S}_k(m) = FFT[\hat{s}_{kN}(n), \hat{s}_{kN+1}(n), \ldots, \hat{s}_{kN+N-1}(n), 0,0, \ldots,0]^{\mathrm{T}}, \tag{5.10}$$

where k = 0, 1, …, K_{s}–1. The filtered reference signal vector can be obtained as

$$\boldsymbol{r}_N(m) = [\boldsymbol{0}_N \ \boldsymbol{I}_N] \sum_{k=0}^{K_{\mathrm{s}}-1} IFFT\{diag[\boldsymbol{X}_k(m)]\boldsymbol{S}_k(m)\}. \tag{5.11}$$

These filtered reference signal samples of length N are appended with the past N samples. The frequency domain filtered reference signal vector so formed can be expressed as

$$\boldsymbol{R}_k(m) = FFT\{[\boldsymbol{r}_N^{\mathrm{T}}(m-1) \ \boldsymbol{r}_N^{\mathrm{T}}(m)]^{\mathrm{T}}\}. \tag{5.12}$$

The control filter weight update equation for partition index k = 0, 1, …, K_{w}–1 are

$$\boldsymbol{W}_k(m+1) = \boldsymbol{W}_k(m) - \mu FFT\left\{\begin{bmatrix}\boldsymbol{I}_N & \boldsymbol{0}_N \\ \boldsymbol{0}_N & \boldsymbol{0}_N\end{bmatrix} IFFT\{diag[\boldsymbol{R}_k^*(m)]\boldsymbol{E}(m)\}\right\}. \quad (5.13)$$

The above described structure is hereafter termed as the Time-Frequency domain delayless Partitioned Block FxLMS algorithm (TFPBFxLMS). It is worth noting that the proposed time-frequency domain flexible structure can incorporate the time domain filtering for control signal generation in more than one partition depending on the delay between the noise source and error sensors while the whole control filter is still updated in frequency domain.

5.3 Numerical experiments

In this subsection results are presented for the delayless partitioned block frequency domain adaptive filtering described in Section 5.2, and its flexible structure for active control is also presented. The performance of the proposed algorithm is demonstrated by comparing it with that of the conventional time domain FxLMS, the FBFxLMS and the FPBFxLMS algorithms. The normalized MSE is used as the metric to assess the performance, and it is defined as

$$\text{Normalized MSE (dB)} = 10\log_{10}\left[\frac{E[e^2(n)]}{\sigma_{\text{p}}^2}\right], \quad (5.14)$$

where σ_{p}^2 is the variance of the primary noise at the error microphone phone.

5.3.1 Case 1: White noise

The simulations were carried out with the acoustic paths measured in an acrylic glass rectangular duct of size 150 cm × 32 cm × 25 cm. One end of the duct was rigidly terminated and the other end was open from one of its side wall. The measurement was

conducted in the listening room of the Centre for Audio, Acoustics and Vibration, University of Technology Sydney with a sampling rate of 16 kHz, and the arrangement is depicted in Figure 5.2(a).

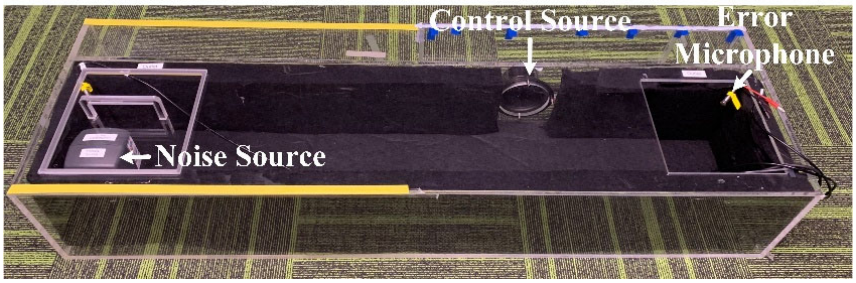

(a)

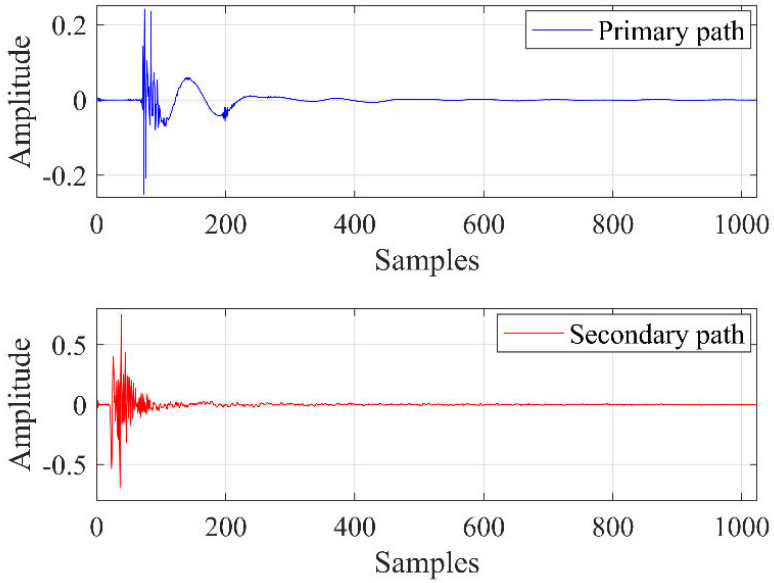

(b)

Figure 5.2 (a) Acoustic path measurement setup in a duct, (b) impulse responses of the primary and secondary paths.

The primary sound source is placed at the corner of the rigid end and the center of the control source is 100 cm away from the rigid terminal while the error microphone is placed 38 cm downstream from the center of control source. The primary path considered

here is the acoustic path from the primary sound source to the error microphone. The primary and secondary paths are measured as FIR filters of length 1024 each with white noise excitation, and their impulse responses are shown in Figure 5.2(b). The control filter is also an FIR filter with a length of $L_w = 1024$, and the partition size of the control filter and the estimated secondary path filter are $N = 64$ with $K_w = K_s = 16$ partitions. All the simulations are averaged over 50 independent realizations and smoothed by moving-average method using a window of 1000 samples.

The input signal considered is a white noise, and the sound pressure level at the error sensor without control is 70 dB. The primary path and the secondary path has delay around 70 samples and 20 samples, respectively, and hence the causality constraint is maintained for the FxLMS algorithm and the TFPBFxLMS algorithm. However, the delay due to the block size of 1024 samples in the FBFxLMS algorithm does not meet the causality requirement, and results in little noise reduction. The delay of 64 samples in the FPBFxLMS algorithm results in negligible noise reduction.

The variation of normalized mean square error with respect to time for all the algorithms are depicted in Figure 5.3(a), from which one can observe that the FxLMS algorithm and the TFPBFxLMS algorithm achieves similar noise reduction. The steady-state normalized MSE values for the FXLMS, TFBFxLMS algorithms are similar, i.e., –17.4 dB, where the last 10 sec samples are considered to obtain the steady state values. The FBFxLMS algorithm fails to achieve any noise reduction because of the violation of the causality constraint. The FPBFxLMS algorithm achieves around 2 dB of noise reduction. The step size used for all the algorithm is $\mu = 4.5 \times 10^{-5}$ and it has been observed that a higher value of step size results in algorithmic divergence. The convergence time of the algorithms is longer due to the large control filter length of 1024.

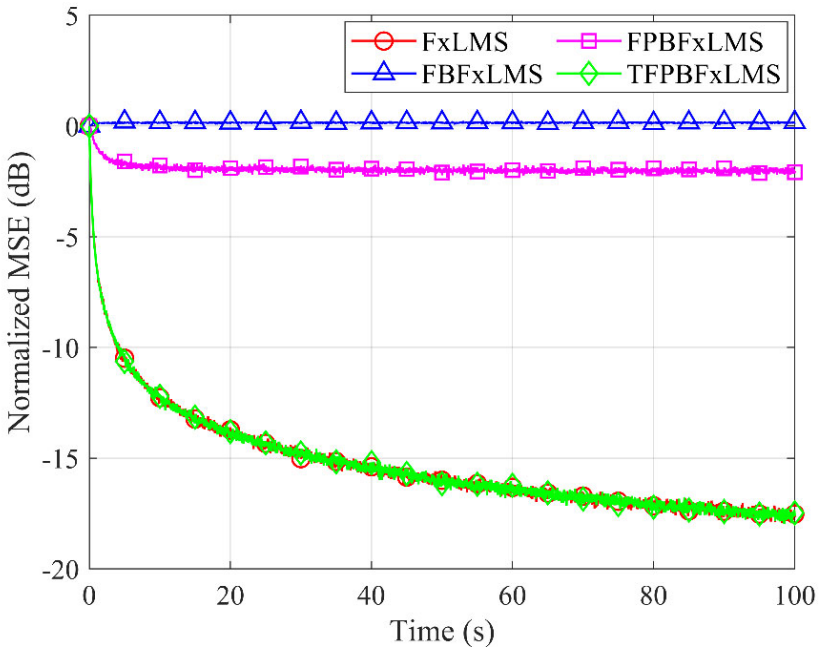

(a)

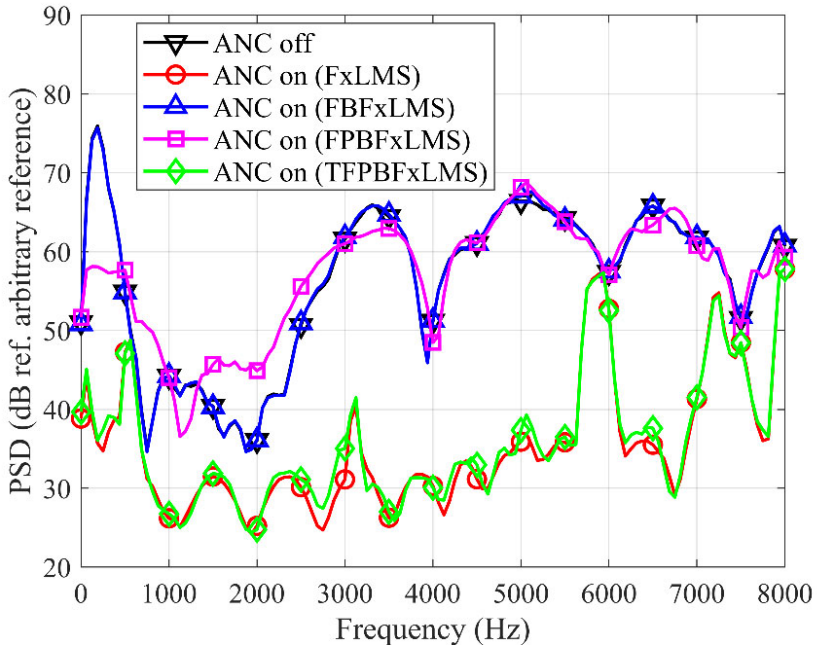

(b)

Figure 5.3 (a) Normalized MSE curves for white noise using different algorithms and (b) the power spectral density with and without noise control.

The power spectral density (PSD) of the error signal with and without control for all the algorithms are illustrated in Figure 5.3(b). One can observe that the FBFxLMS algorithm does not achieve any noise reduction and the FPBFxLMS algorithm achieves noise reduction only for the frequencies below 500 Hz, while the FxLMS algorithm and the proposed TFPBFxLMS algorithm achieve similar noise reduction. There is little noise reduction around some frequencies such as 600 Hz, 5900 Hz and 7500 Hz due to the location of the secondary source where the loudspeaker cannot generate enough sound at these frequencies at the error microphone location. It should be emphasized that the main contribution of the proposed algorithm is to find a balance between reducing computational complexity and maintaining the causality requirement.

5.3.2 Case 2: Traffic noise

To further demonstrate the flexibility of the proposed algorithm, active control of traffic noise in free space is considered. The traffic noise was recorded from a highway. The primary and secondary paths are FIR filters of length 1024 each, which were measured in a normal room in the Lab with a sampling rate of 16 kHz as depicted in Figure 5.4(a). The primary noise source was placed at 150 cm away from the secondary source and the distance from the center of the secondary source to the error microphone was set as 15 cm. The impulse responses of the acoustic paths are depicted in Figure 5.4(b). The primary path and the secondary path has delay around 70 samples and 7 samples, respectively, and the causality constraint is maintained for the FxLMS algorithm and the proposed algorithm. However, the delay due to the block size of 1024 samples in the FBFxLMS algorithm does not meet the causality requirement. The delay of 64 samples in the FPBFxLMS algorithm affects the control performance. The impulse response of

the primary path contains around 500 significant coefficients, so the time domain control filtering is adopted in the first and second partitions of the proposed structure.

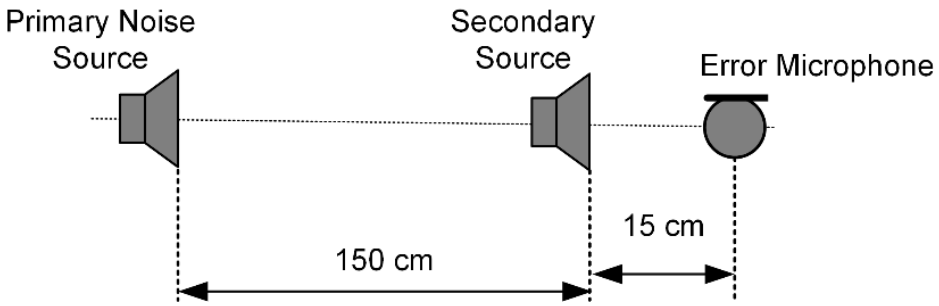

(a)

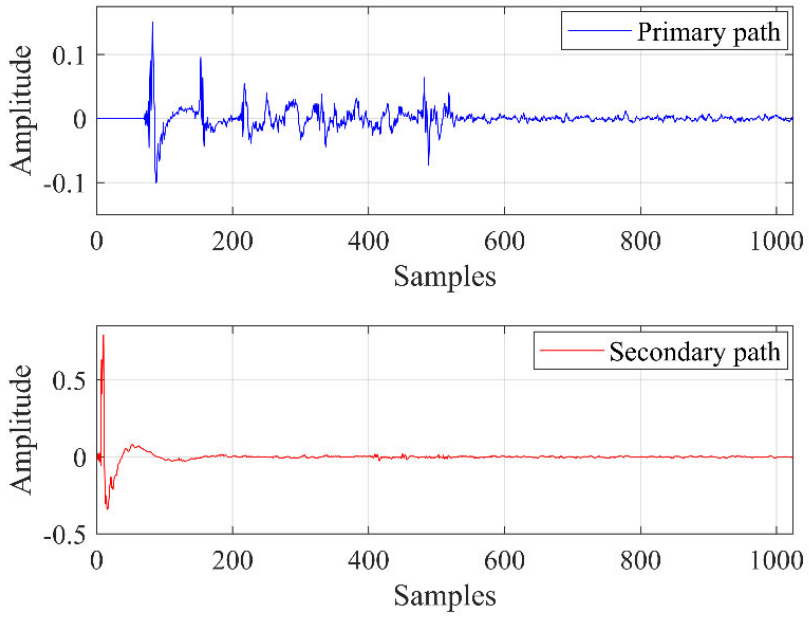

(b)

Figure 5.4 (a) Position of source and sensor in the measurement and (b) Impulse responses of the primary and secondary paths measured in a normal room.

The variation of normalized MSE with respect to time for all the algorithms are depicted in Figure 5.5(a), where TFPFxLMS-I stands for the TFPFxLMS algorithm with time domain filtering in the first partition and TFPFxLMS-II stands for the algorithm with

time domain filtering in the first and second partitions. The proposed TFPFxLMS algorithm with two time domain partitions achieves similar normalized MSE as that of the FxLMS algorithm while the TFPFxLMS algorithm with only one time domain partitions gain less noise reduction due to the fact that the causality requirement is not met for some part of the primary disturbance. The FBFxLMS algorithm achieve no noise reduction because of the violation of the causality constraint and the PFBFxLMS algorithm achieves noise reduction around 5 dB due to large signal path delay. The step size used for all the algorithm is $\mu = 5 \times 10^{-6}$ and a higher value of step size results in algorithmic divergence. The PSD of the residual error signal with and without control for all the algorithm are depicted in Figure 5.5(b). It can be observed that the noise reduction of the TFPBFxLMS-I algorithm is less compared to that of the TFPBFxLMS-II algorithm. The noise reduction performance of the TFPBFxLMS-II is similar to that of the FxLMS algorithm in most of the frequency band while there is some difference in PSD at certain frequencies.

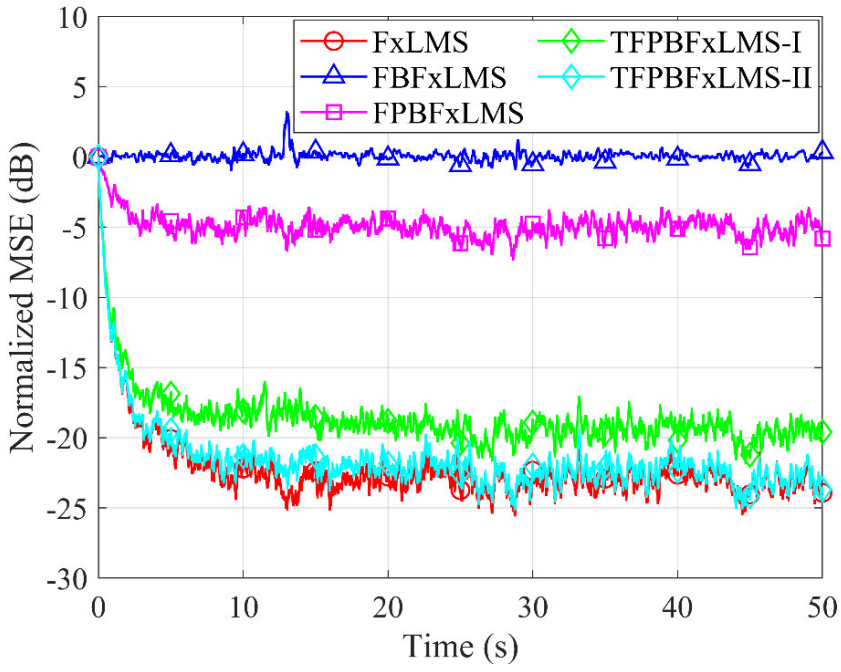

(a)

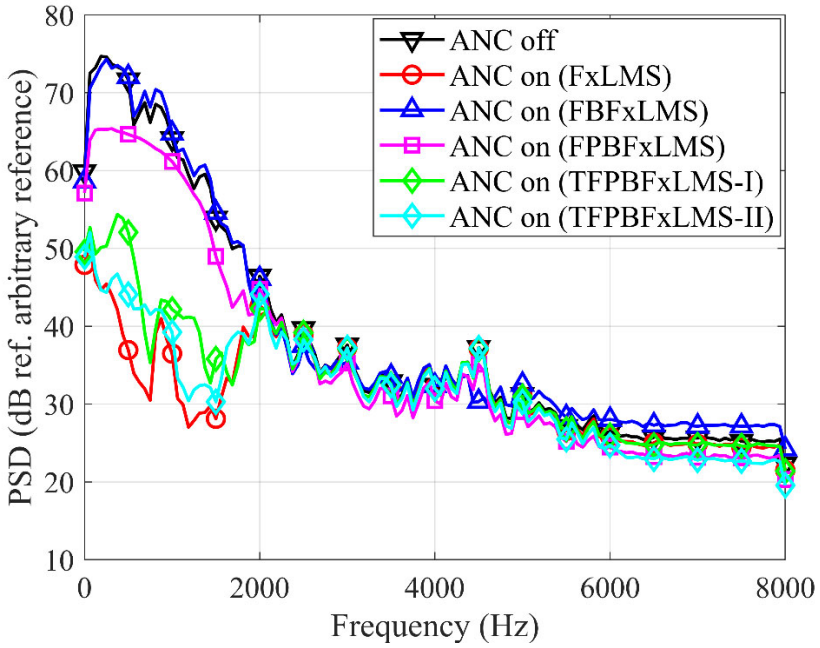

(b)

Figure 5.5 (a) Normalized MSE curves for traffic noise using different algorithms and (b) the power spectral density with and without noise control.

5.4 Computational complexity

The computational complexity of the proposed structure is evaluated in terms of average number of real multiplications per input samples with the assumption that the FFT and IFFT operations involves same number of computations, and the length of the control filter is same as that of the estimated secondary path filter. For generating the control signal, $N+8(K_w-1)$ real multiplications are required, $8K_w$ real multiplications are needed for obtaining the filtered reference signal, $8K_w$ real multiplications are needed for updating the control filter weights and $16\log_2(2N)$ real multiplications are needed for FFT/IFFT operations. Hence, a total of $24K_w+16\log_2(2N)+N-8$ real multiplications are required in the proposed TFPBFxLMS algorithm. The FPBFxLMS algorithm, the FBFxLMS algorithm and the FxLMS algorithm require a total of $24K_w+14\log_2(2N)$ real

multiplications, $24+14\log_2(2L_w)$ real multiplications and $3L_w$ real multiplications, respectively.

The computational complexity is summarized in Table 5.1, and for a straight forward comparison, one example is provided with $L_w = 1024$, $N = 64$ and $K_w = 16$. One can observe that the computational complexities of the proposed TFPBFXLMS algorithm is much lower than that of the time domain one while it is a bit higher than that of the FPBFxLMS algorithm which has a signal path delay of 64 samples. The FBFxLMS algorithm has the least computational complexity. However, it has a delay of 1024 samples.

Table 5.1 The average number of real multiplications required for different algorithms

Algorithms	Total real multiplications	Example	
		Multiplication	Delay
FxLMS	$3L_w$	3072	0
FBFxLMS	$24 + 14\log_2(2L_w)$	178	1024
FPBFxLMS	$24K_w + 14\log_2(2N)$	482	64
TFPBFxLMS	$24K_w + 16\log_2(2N) + N - 8$	552	0

In some ANC applications, significant portions of the primary disturbance might take very short time to reach the error sensor. In such a scenario, more than one partitions have to adopt time domain filtering for control signal generation in order to maintain causality, which in turn increases the computational burden of the proposed structure. Table 5.2 lists the computational complexity and the length of the control filter part that uses time domain filtering with respect to the number of partitions ($i = 0, 1, \ldots, K_w$) used for control signal generation in time domain, where $N = 64$ and $K_w = 16$, and the total computational complexity in a generalized form is $24K_w+(14+2i)\log_2(2N)+(N-8)i$. One can observe that the computational complexity is same as that of the FPBFxLMS algorithm for $i = 0$ and

increases as the number of partitions for control signal generation increases.

Table 5.2 The average number of real multiplications required with respect to the number of partitions used for control signal generation.

i	Total real multiplications	Filter length with time domain filtering (samples)
0	482	0
1	552	64
2	622	128
3	692	192
i	$24K_w+(14+2i)\log_2(2N)+(N-8)i$	iN

5.5 Summary

In summary, a time-frequency domain delayless portioned block adaptive filter is proposed for active control operation at high sampling frequency, which has no signal path delay and it achieves computational saving. In the proposed structure of the filtering technique, the long filters are divided into many equal partitions and the control filter update is performed in frequency domain, and the control signal is generated in both time and frequency domains. The simulation results using the measured acoustic paths demonstrate the effectiveness of the proposed structure. The proposed structure is capable of maintaining the causality requirement for broadband noise.

6 Decentralized algorithm for broadband active control

6.1 Introduction

Due to their low computational complexity, reduced wiring cost, and flexibility of scaling up, decentralized multiple channel active control systems are attractive in many applications. In a decentralized multiple channel active control system, a number of small subsystems are constructed, which are updated independently with only the associated error signals. In this work, a novel two channel decentralized ANC (DANC) framework in time domain is proposed for controlling broadband noise[1]. The DANC solution in the frequency domain is obtained first and then the optimized time domain algorithm is developed. The novelties of this work are two-fold. First, the genetic algorithm (GA) is employed to compute the DANC solution in the frequency domain, where different frequency bins can have different convergence behaviours with the steepest descent algorithm (Zhang, Tao & Qiu 2019). The solution obtained from the GA undergoes a scaling process so that different frequencies have roughly the similar convergence behaviors, which is crucial for broadband control. Second, a new and simple FIR filter design method is adopted for designing the auxiliary filters.

[1] This chapter has been published as: Pradhan, S., Zhang, G. & Qiu, X. 2020, 'A time domain decentralized algorithm for two channel active noise control', *The Journal of the Acoustical Society of America*, vol. 147, no. 6, pp. 3808–13. https://doi.org/10.1121/10.0001401

7 Conclusions and future work

In this chapter, the general conclusions drawn from this PhD thesis are presented, and also the future research directions arising from this work are outlined.

7.1 Conclusions

The objectives of this PhD research were to develop low-complexity algorithms for online modelling of acoustic paths without affecting noise reduction performance, achieving improved control performance at transient and steady state, high sampling frequency operation and broadband noise control and multiple channel decentralized active control systems for broadband noise control. In order to achieve these objectives, an extensive literature review was presented, which was the foundation for the proposed work. Numerical experiments were carried out to validate the proposed work.

A five-stage systematic method is proposed for practical active control operation which can maintain control when both the primary and the secondary path change. To improve the convergence speed of the secondary path modelling with the control signal, adaptive decorrelation filters are incorporated in the online secondary path modelling by pre-whitening the modelling signals used in the modelling. The proposed method has been shown to outperform the existing competent methods in terms of convergence rate, stability, and noise reduction. However, the proposed five-stage method is ill-suited for the situation where the changes in the acoustic paths occur more frequently before one remodelling is completed. The convergence time of the acoustic path remodelling might be reduced at the expense of modelling accuracy, which in turn would affect the control performance. Although the use of decorrelation filter reduces the modelling time of the secondary path modelling for broadband and narrowband signals, it is not effective for tonal and white excitation signals.

A systematic four-stage method is proposed for feedforward active control systems to perform online feedback path modelling with the control signal. The proposed method avoids the interference between the control operation and feedback path modelling by appropriate toggling of the switches used for managing the control flow. Furthermore, adaptive decorrelation filters are employed to improve the feedback path modelling performance, which in turn improves the active control performance. The proposed method has been shown to outperform the state-of-the-art method in terms of faster convergence and lower residual noise. However, the proposed method is effective for broadband control only due to the fact that the feedback path modelling performance is highly reliant on the frequency content of the control signal.

An affine combination of the FxLMS/F algorithms is proposed to achieve faster convergence in the transient-state and lower residual error in the steady-state. The combining parameter is updated using a gradient based update rule. The proposed affine combination algorithm is effective for controlling different types of noise, and it is also effective when a perfect model of the secondary path is not available.

A time-frequency domain flexible structure is proposed, which divides the long filters into many equal partitions and carries out the control filter update in frequency domain while generating the control signal in both time and frequency domains. The simulation results using the measured acoustic paths demonstrate the feasibility and flexibility of the proposed structure. In the application scenarios where the associated signal path delay violates the causality requirement, the frequency domain block FxLMS and the frequency domain partitioned block FxLMS fail to have effective control; however, the proposed algorithm achieves similar noise reduction as that of the time domain FxLMS algorithm, but with much less computational load.

A time domain decentralized adaptive control algorithm is proposed for the multiple channel ANC system. The frequency responses of the auxiliary filters are optimized using the GA followed by a scaling process. Unlike the existing methods, a simplified filter design method is developed. The simulation results with the measured acoustic paths demonstrate that the proposed algorithm is able to achieve similar noise reduction performance as the centralized algorithm. The convergence behaviour and noise reduction performance of the proposed algorithm is better than that of the conventional decentralized algorithms.

7.2 Future works

This section discusses some future research directions, which can enhance the scope of application of low-complexity adaptive algorithms for active control systems.

- Applying variable-tap-length algorithms to find the optimum number of decorrelation filter coefficients necessary to pre-whiten complicated coloured signals in the online modelling process of acoustic paths. This will aid in reducing the computational complexity imposed by the use of the decorrelation filters.
- Investigating a proper howling detection technique in the online feedback path modelling that can provide high sensitivity for stability detection and a less distorted reference signal for effective control operation.
- Extending the proposed decentralized algorithm to multichannel ANC systems with large channel number (>2) for broadband noise control.
- Studying the affine combination of the proposed time-frequency domain flexible structure for active control. This will help to achieve improved performance in transient and steady state, and maintain causality requirement for broadband control.

- Implementing the proposed algorithms with graphical user interface that can facilitate the execution of digital instructions to mitigate unwanted noise.

References

Ahmed, S. & Akhtar, M.T. 2016, 'Gain scheduling of auxiliary noise and variable step-size for online acoustic feedback cancellation in narrow-band active noise control systems', *IEEE/ACM Transactions on Audio, Speech, and Language Processing*, vol. 25, no. 2, pp. 333-43.

Ahmed, S., Akhtar, M.T. & Zhang, X. 2013, 'Online acoustic feedback mitigation with improved noise-reduction performance in active noise control systems', *IET Signal Processing*, vol. 7, no. 6, pp. 505-14.

Akhtar, M.T. 2020, 'On Active Impulsive Noise Control (AINC) Systems', *Circuits, Systems, and Signal Processing*, pp. 1-24.

Akhtar, M.T., Abe, M. & Kawamata, M. 2005, 'A new structure for feedforward active noise control systems with improved online secondary path modeling', *IEEE Transactions on Speech and Audio Processing*, vol. 13, no. 5, pp. 1082-8.

Akhtar, M.T., Abe, M. & Kawamata, M. 2006, 'A new variable step size LMS algorithm-based method for improved online secondary path modeling in active noise control systems', *IEEE Transactions on Audio, Speech, and Language Processing*, vol. 14, no. 2, pp. 720-6.

Akhtar, M.T., Abe, M. & Kawamata, M. 2007, 'On active noise control systems with online acoustic feedback path modeling', *IEEE Transactions on Audio, Speech, and Language Processing*, vol. 15, no. 2, pp. 593-600.

Akhtar, M.T., Abe, M., Kawamata, M. & Mitsuhashi, W. 2009, 'A simplified method for online acoustic feedback path modeling and neutralization in multichannel active noise control systems', *Signal Processing*, vol. 89, no. 6, pp. 1090-9.

Akhtar, M.T. & Mitsuhashi, W. 2011, 'Variable step-size based method for acoustic feedback modeling and neutralization in active noise control systems', *Applied Acoustics*, vol. 72, no. 5, pp. 297-304.

Al Omour, A.M., Zidouri, A., Iqbal, N. & Zerguine, A. 2016, 'Filtered-x least mean fourth (FXLMF) and leaky FXLMF adaptive algorithms', *EURASIP Journal on Advances in Signal Processing*, vol. 2016, no. 1, pp. 1-20.

An, F., Cao, Y. & Liu, B. 2018, 'Optimized decentralized adaptive control of noise and vibration for periodic disturbances', *The Journal of the Acoustical Society of America*, vol. 144, no. 4, pp. EL275-EL80.

An, F., Cao, Y., Wu, M., Sun, H., Liu, B. & Yang, J. 2019, 'Robust Wiener controller design with acoustic feedback for active noise control systems', *The Journal of the Acoustical Society of America*, vol. 145, no. 4, pp. EL291-EL6.

An, F., Cao, Y. & Liu, B. 2021, 'Optimized decentralized filtered-x least mean square algorithm for over-determined systems with periodic disturbances', *Journal of Sound and Vibration*, vol. 491, p. 115763.

Ardekani, I.T. & Abdulla, W.H. 2010, 'Theoretical convergence analysis of FxLMS algorithm', *Signal Processing*, vol. 90, no. 12, pp. 3046-55.

Arenas-Garcia, J., Azpicueta-Ruiz, L.A., Silva, M.T., Nascimento, V.H. & Sayed, A.H. 2015, 'Combinations of adaptive filters: performance and convergence properties', *IEEE Signal Processing Magazine*, vol. 33, no. 1, pp. 120-40.

Arenas-Garcia, J., Figueiras-Vidal, A.R. & Sayed, A.H. 2006, 'Mean-square performance of a convex combination of two adaptive filters', *IEEE Transactions on Signal Processing*, vol. 54, no. 3, pp. 1078-90.

Aslam, M.S., Shi, P. & Lim, C.-C. 2021, 'Self-adapting variable step size strategies for active noise control systems with acoustic feedback', *Automatica*, vol. 123, p. 109354.

Bendel, Y., Burshtein, D., Shalvi, O. & Weinstein, E. 2001, 'Delayless frequency domain acoustic echo cancellation', *IEEE Transactions on Speech and Audio Processing*, vol. 9, no. 5, pp. 589-97.

Benesty, J., Rey, H., Vega, L.R. & Tressens, S. 2006, 'A nonparametric vss nlms algorithm', *IEEE Signal Processing Letters*, vol. 13, no. 10, pp. 581-4.

Bershad, N.J., Bermudez, J.C.M. & Tourneret, J.-Y. 2008, 'An affine combination of two LMS adaptive filters—transient mean-square analysis', *IEEE Transactions on Signal Processing*, vol. 56, no. 5, pp. 1853-64.

Bjarnason, E. 1995, 'Analysis of the filtered-X LMS algorithm', *IEEE Transactions on Speech and Audio Processing*, vol. 3, no. 6, pp. 504-14.

Borrallo, J.P. & Otero, M.G. 1992, 'On the implementation of a partitioned block frequency domain adaptive filter (PBFDAF) for long acoustic echo cancellation', *Signal Processing*, vol. 27, no. 3, pp. 301-15.

Bouchard, M. 2003, 'Multichannel affine and fast affine projection algorithms for active noise control and acoustic equalization systems', *IEEE Transactions on Speech and Audio Processing*, vol. 11, no. 1, pp. 54-60.

Buck, J., Jukkert, S. & Sachau, D. 2018, 'Performance evaluation of an active headrest considering non-stationary broadband disturbances and head movement', *The Journal of the Acoustical Society of America*, vol. 143, no. 5, pp. 2571-9.

Candido, R., Silva, M.T. & Nascimento, V.H. 2010, 'Transient and steady-state analysis of the affine combination of two adaptive filters', *IEEE Transactions on Signal Processing*, vol. 58, no. 8, pp. 4064-78.

Canevet, G. 1978, 'Active sound absorption in an air conditioning duct', *Journal of Sound and Vibration*, vol. 58, no. 3, pp. 333-45.

Carini, A. & Malatini, S. 2008, 'Optimal variable step-size NLMS algorithms with auxiliary noise power scheduling for feedforward active noise control', *IEEE Transactions on Audio, Speech, and Language Processing*, vol. 16, no. 8, pp. 1383-95.

Carini, A. & Sicuranza, G.L. 2007, 'Optimal regularization parameter of the multichannel filtered- x affine projection algorithm', *IEEE Transactions on Signal Processing*, vol. 55, no. 10, pp. 4882-95.

Chan, K.S. & Farhang-Boroujeny, B. 2001, 'Analysis of the partitioned frequency-domain block LMS (PFBLMS) algorithm', *IEEE Transactions on Signal Processing*, vol. 49, no. 9, pp. 1860-74.

Chang, D. C. & Chu, F. T. 2013, 'A new variable tap-length and step-size FxLMS algorithm', *IEEE Signal Processing Letters*, vol. 20, no. 11, pp. 1122-5.

Chaplin, G. & Smith, R. 1983, 'Waveform synthesis--The Essex solution to repetitive noise and vibration,' *Proceedings of Inter-Noise*, pp. 399-402.

Crawford, D.H. & Stewart, R.W. 1997, 'Adaptive IIR filtered-v algorithms for active noise control', *The Journal of the Acoustical Society of America*, vol. 101, no. 4, pp. 2097-103.

Das, D., Panda, G. & Kuo, S. 2007, 'New block filtered-X LMS algorithms for active noise control systems', *IET Signal Processing*, vol. 1, no. 2, pp. 73-81.

Das, D.P., Moreau, D.J. & Cazzolato, B.S. 2013, 'A computationally efficient frequency-domain filtered-X LMS algorithm for virtual microphone', *Mechanical Systems and Signal Processing*, vol. 37, no. 1-2, pp. 440-54.

Das, K.K. & Satapathy, J.K. 2008, 'Frequency-domain block filtered-x NLMS algorithm for multichannel ANC', *2008 First International Conference on Emerging Trends in Engineering and Technology*, IEEE, pp. 1293-7.

Eghtesadi, K. & Leventhall, H. 1981, 'Active attenuation of noise: the Chelsea dipole', *Journal of Sound and Vibration*, vol. 75, no. 1, pp. 127-34.

Elliott, S. 2000, *Signal processing for active control*, Elsevier.

Elliott, S., Stothers, I. & Nelson, P. 1987, 'A multiple error LMS algorithm and its application to the active control of sound and vibration', *IEEE Transactions on Acoustics, Speech, and Signal Processing*, vol. 35, no. 10, pp. 1423-34.

Elliott, S.J. & Boucher, C.C. 1994, 'Interaction between multiple feedforward active control systems', *IEEE Transactions on Speech and Audio Processing*, vol. 2, no. 4, pp. 521-30.

Eriksson, L. 1991, 'Development of the filtered-U algorithm for active noise control', *The Journal of the Acoustical Society of America*, vol. 89, no. 1, pp. 257-65.

Eriksson, L.J. & Allie, M.C. 1989, 'Use of random noise for on-line transducer modeling in an adaptive active attenuation system', *The Journal of the Acoustical Society of America*, vol. 85, no. 2, pp. 797-802.

Farhang-Boroujeny, B. & Chan, K.S. 2000, 'Analysis of the frequency-domain block LMS algorithm', *IEEE Transactions on Signal Processing*, vol. 48, no. 8, pp. 2332-42.

Ferrara, E. 1980, 'Fast implementations of LMS adaptive filters', *IEEE Transactions on Acoustics, Speech, and Signal Processing*, vol. 28, no. 4, pp. 474-5.

Ferrer, M., de Diego, M., Piñero, G. & Gonzalez, A. 2015, 'Active noise control over adaptive distributed networks', *Signal Processing*, vol. 107, pp. 82-95.

Ferrer, M., de Diego, M., Piñero, G. & Gonzalez, A. 2020, 'Affine Projection Algorithm Over Acoustic Sensor Networks for Active Noise Control', *IEEE/ACM Transactions on Audio, Speech, and Language Processing*, vol. 29, pp. 448-61.

Ferrer, M., Gonzalez, A., de Diego, M. & Pinero, G. 2008, 'Fast affine projection algorithms for filtered-x multichannel active noise control', *IEEE Transactions on Audio, Speech, and Language Processing*, vol. 16, no. 8, pp. 1396-408.

Ferrer, M., Gonzalez, A., de Diego, M. & Pinero, G. 2012, 'Convex combination filtered-x algorithms for active noise control systems', *IEEE Transactions on Audio, Speech, and Language Processing*, vol. 21, no. 1, pp. 156-67.

Gaiotto, S., Laudani, A., Lozito, G.M. & Riganti Fulginei, F. 2020, 'A Computationally Efficient Algorithm for Feedforward Active Noise Control Systems', *Electronics*, vol. 9, no. 9, p. 1504.

Gao, M., Lu, J. & Qiu, X. 2016, 'A simplified subband ANC algorithm without secondary path modeling', *IEEE/ACM Transactions on Audio, Speech, and Language Processing*, vol. 24, no. 7, pp. 1164-74.

George, N.V. & Panda, G. 2012, 'A particle-swarm-optimization-based decentralized nonlinear active noise control system', *IEEE Transactions on Instrumentation and Measurement*, vol. 61, no. 12, pp. 3378-86.

Ghanati, G. & Azadi, S. 2020, 'Decentralized robust control of a vehicle's interior sound field', *Journal of Vibration and Control*, vol. 26, no. 19-20, pp. 1815-23.

Goldberg, D.E. 2006, *Genetic algorithms*, Pearson Education India.

Gonzalez, A., Ferrer, M., De Diego, M., Pinero, G. & Garcia-Bonito, J. 2003, 'Sound quality of low-frequency and car engine noises after active noise control', *Journal of Sound and Vibration*, vol. 265, no. 3, pp. 663-79.

Hansen, C., Snyder, S., Qiu, X., Brooks, L. & Moreau, D. 2012, *Active control of noise and vibration*, CRC press.

Haseeb, A., Tufail, M., Ahmed, S. & Ahmed, W. 2018, 'A robust approach for online feedback path modeling in single-channel narrow-band active noise control systems using two distinct variable step size methods', *Applied Acoustics*, vol. 133, pp. 133-43.

Haykin, S.S. 2005, *Adaptive filter theory*, Pearson Education India.

Hu, M., Wang, J., Xue, J. & Lu, J. 2019, 'Inspection of the secondary path modeling in active noise control from the viewpoint of channel identification in stereo acoustic echo cancellation', *The Journal of the Acoustical Society of America*, vol. 145, no. 5, pp. 3024-30.

Hu, M., Xue, J. & Lu, J. 2019, 'Online multi-channel secondary path modeling in active noise control without auxiliary noise', *The Journal of the Acoustical Society of America*, vol. 146, no. 4, pp. 2590-5.

Huang, B., Xiao, Y., Sun, J. & Wei, G. 2012, 'A variable step-size FXLMS algorithm for narrowband active noise control', *IEEE Transactions on Audio, Speech, and Language Processing*, vol. 21, no. 2, pp. 301-12.

Jung, W., Elliott, S.J. & Cheer, J. 2019, 'Local active control of road noise inside a vehicle', *Mechanical Systems and Signal Processing*, vol. 121, pp. 144-57.

Kajikawa, Y., Gan, W.-S. & Kuo, S.M. 2012, 'Recent advances on active noise control: open issues and innovative applications', *APSIPA Transactions on Signal and Information Processing*, vol. 1.

Kim, D.W., Hur, J. & Park, P. 2020, 'Two-stage active noise control with online secondary-path filter based on an adapted scheduled-stepsize NLMS algorithm', *Applied Acoustics*, vol. 158, p. 107031.

Kim, H. S. & Park, Y. 1998, 'Delayed-X LMS algorithm: An efficient ANC algorithm utilizing robustness of cancellation path model', *Journal of sound and vibration*, vol. 212, no. 5, pp. 875-87.

Kong, X. & Kuo, S.M. 1999, 'Study of causality constraint on feedforward active noise control systems', *IEEE Transactions on Circuits and Systems II: Analog and Digital Signal Processing*, vol. 46, no. 2, pp. 183-6.

Kujawa, S.G. & Liberman, M.C. 2009, 'Adding insult to injury: cochlear nerve degeneration after "temporary" noise-induced hearing loss', *Journal of Neuroscience*, vol. 29, no. 45, pp. 14077-85.

Kukde, R., Manikandan, M.S. & Panda, G. 2019, 'Reduced complexity diffusion filtered x least mean square algorithm for distributed active noise cancellation', *Signal, Image and Video Processing*, vol. 13, no. 3, pp. 447-55.

Kuo, S.M. 1999, 'Active noise control system and method for on-line feedback path modeling and on-line secondary path modeling', Google Patents.

Kuo, S.M. 2002, 'Active noise control system and method for on-line feedback path modeling', Google Patents.

Kuo, S.M., Chen, Y. R., Chang, C. Y. & Lai, C. W. 2018, 'Development and evaluation of light-weight active noise cancellation earphones', *Applied Sciences*, vol. 8, no. 7, p. 1178.

Kuo, S.M., Mitra, S. & Gan, W. S. 2006, 'Active noise control system for headphone applications', *IEEE Transactions on Control Systems Technology*, vol. 14, no. 2, pp. 331-5.

Kuo, S.M. & Morgan, D.R. 1996, *Active noise control systems*, vol. 4, Wiley, New York.

Kuo, S.M. & Morgan, D.R. 1999, 'Active noise control: a tutorial review', *Proceedings of the IEEE*, vol. 87, no. 6, pp. 943-73.

Kuo, S.M. & Vijayan, D. 1997, 'A secondary path modeling technique for active noise control systems', *IEEE Transactions on Speech and Audio Processing*, vol. 5, no. 4, pp. 374-7.

Leboucher, E., Micheau, P., Berry, A. & L'Espérance, A. 2002, 'A stability analysis of a decentralized adaptive feedback active control system of sinusoidal sound in free space', *The Journal of the Acoustical Society of America*, vol. 111, no. 1, pp. 189-99.

Lee, S. K., Lee, S., Back, J. & Shin, T. 2018, 'A new method for active cancellation of engine order noise in a passenger car', *Applied Sciences*, vol. 8, no. 8, p. 1394.

Li, Y., Wang, Y. & Jiang, T. 2016, 'Norm-adaption penalized least mean square/fourth algorithm for sparse channel estimation', *Signal processing*, vol. 128, pp. 243-51.

Lopes, P.A. & Gerald, J.A. 2015, 'Auxiliary noise power scheduling algorithm for active noise control with online secondary path modeling and sudden changes', *IEEE Signal Processing Letters*, vol. 22, no. 10, pp. 1590-4.

Lorente, J., Ferrer, M., De Diego, M. & González, A. 2014, 'GPU implementation of multichannel adaptive algorithms for local active noise control', *IEEE/ACM Transactions on Audio, Speech, and Language Processing*, vol. 22, no. 11, pp. 1624-35.

Lu, J., Qiu, X. & Zou, H. 2014, 'A modified frequency-domain block LMS algorithm with guaranteed optimal steady-state performance', *Signal Processing*, vol. 104, pp. 27-32.

Lu, J., Shen, C., Qiu, X. & Xu, B. 2003, 'Lattice form adaptive infinite impulse response filtering algorithm for active noise control', *The Journal of the Acoustical Society of America*, vol. 113, no. 1, pp. 327-35.

Mboup, M., Bonnet, M. & Bershad, N. 1994, 'LMS coupled adaptive prediction and system identification: A statistical model and transient mean analysis', *IEEE Transactions on Signal Processing*, vol. 42, no. 10, pp. 2607-15.

Morgan, D. 1980, 'An analysis of multiple correlation cancellation loops with a filter in the auxiliary path', *IEEE Transactions on Acoustics, Speech, and Signal Processing*, vol. 28, no. 4, pp. 454-67.

Moulines, E., Amrane, O.A. & Grenier, Y. 1995, 'The generalized multidelay adaptive filter: Structure and convergence analysis', *IEEE Transactions on Signal processing*, vol. 43, no. 1, pp. 14-28.

Münzel, T., Gori, T., Babisch, W. & Basner, M. 2014, 'Cardiovascular effects of environmental noise exposure', *European heart journal*, vol. 35, no. 13, pp. 829-36.

Murao, T., Shi, C., Gan, W. S. & Nishimura, M. 2017, 'Mixed-error approach for multi-channel active noise control of open windows', *Applied Acoustics*, vol. 127, pp. 305-15.

Nelson, P.A. & Elliott, S.J. 1991, *Active control of sound*, Academic press.

W.H. O. 2018, 'Environmental noise guidelines for the European region'.

Park, S.J., Yun, J.H., Park, Y.C. & Youn, D.H. 2001, 'A delayless subband active noise control system for wideband noise control', *IEEE Transactions on Speech and Audio Processing*, vol. 9, no. 8, pp. 892-9.

Pawelczyk, M. 2004, 'Adaptive noise control algorithms for active headrest system', *Control Engineering Practice*, vol. 12, no. 9, pp. 1101-12.

Prince, M.M., Stayner, L.T., Smith, R.J. & Gilbert, S.J. 1997, 'A re-examination of risk estimates from the NIOSH Occupational Noise and Hearing Survey (ONHS)', *The Journal of the Acoustical society of America*, vol. 101, no. 2, pp. 950-63.

Qiu, X., Li, N., Chen, G. & Hansen, C.H. 2006, 'The implementation of delayless subband active noise control algorithms', *Proceedings of the 2006 International Symposium on Active control of Sound and Vibration*.

Quintana, R. & Patino, D. 2018, 'A game-theoretical perspective for decentralized active noise control', *Journal of Vibration and Control*, vol. 24, no. 21, pp. 5062-71.

Reddy, R.M., Panahi, I.M. & Briggs, R. 2010, 'Hybrid FxRLS-FxNLMS adaptive algorithm for active noise control in fMRI application', *IEEE Transactions on Control Systems Technology*, vol. 19, no. 2, pp. 474-80.

Rotaru, M., Albu, F. & Coanda, H. 2012, 'A variable step size modified decorrelated NLMS algorithm for adaptive feedback cancellation in hearing aids', *2012 10th International Symposium on Electronics and Telecommunications*, IEEE, pp. 263-6.

Rout, N.K., Das, D.P. & Panda, G. 2015, 'Computationally efficient algorithm for high sampling-frequency operation of active noise control', *Mechanical Systems and Signal Processing*, vol. 56, pp. 302-19.

Saito, N. & Sone, T. 1996, 'Influence of modeling error on noise reduction performance of active noise control systems using filtered-x LMS algorithm', *Journal of the Acoustical Society of Japan (E)*, vol. 17, no. 4, pp. 195-202.

Shen, Q. & Spanias, A. 1992, 'Time and frequency domain X block LMS algorithms for single channel active noise control', *Proc. 2nd Int. Congr. Recent Developments in Air-and Structure-Borne Sound Vibration*, pp. 353-60.

Shen, Q. & Spanias, A. 1996, 'Time-and frequency-domain X-block least-mean-square algorithms for active noise control', *Noise Control Engineering Journal*, vol. 44, no. 6, pp. 281-93.

Shi, D., Gan, W. S., He, J. & Lam, B. 2019, 'Practical implementation of multichannel filtered-x least mean square algorithm based on the multiple-parallel-branch with folding architecture for large-scale active noise control', *IEEE Transactions on Very Large Scale Integration (VLSI) Systems*, vol. 28, no. 4, pp. 940-53.

Shynk, J.J. 1992, 'Frequency-domain and multirate adaptive filtering', *IEEE Signal Processing Magazine*, vol. 9, no. 1, pp. 14-37.

Song, J. M. & Park, P. 2015, 'An optimal variable step-size affine projection algorithm for the modified filtered-x active noise control', *Signal Processing*, vol. 114, pp. 100-11.

Song, P. & Zhao, H. 2018, 'Filtered-x generalized mixed norm (FXGMN) algorithm for active noise control', *Mechanical Systems and Signal Processing*, vol. 107, pp. 93-104.

Song, P. & Zhao, H. 2019, 'Filtered-x least mean square/fourth (FXLMS/F) algorithm for active noise control', *Mechanical Systems and Signal Processing*, vol. 120, pp. 69-82.

Soo, J. S. & Pang, K.K. 1990, 'Multidelay block frequency domain adaptive filter', *IEEE Transactions on Acoustics, Speech, and Signal Processing*, vol. 38, no. 2, pp. 373-6.

Tao, J., Wang, S., Qiu, X. & Pan, J. 2016, 'Performance of an independent planar virtual sound barrier at the opening of a rectangular enclosure', *Applied Acoustics*, vol. 105, pp. 215-23.

Thi, J. & Morgan, D.R. 1993, 'Delayless subband active noise control', *1993 IEEE International Conference on Acoustics, Speech, and Signal Processing*, vol. 1, IEEE, pp. 181-4.

Tobias, O.J. & Seara, R. 2005, 'Leaky-FXLMS algorithm: stochastic analysis for Gaussian data and secondary path modeling error', *IEEE Transactions on Speech and Audio Processing*, vol. 13, no. 6, pp. 1217-30.

Tufail, M., Ahmed, S., Rehan, M. & Akhtar, M.T. 2019, 'A two adaptive filters-based method for reducing effects of acoustic feedback in single-channel feedforward ANC systems', *Digital Signal Processing*, vol. 90, pp. 18-27.

Wang, J., Xue, J., Lu, J. & Qiu, X. 2019, 'A switching strategy of the frequency-domain adaptive algorithm for active noise control', *The Journal of the Acoustical Society of America*, vol. 146, no. 2, pp. 1045-50.

Warnaka, G.E., Poole, L.A. & Tichy, J. 1984, 'Active acoustic attenuator', Google Patents.

Wu, L., Qiu, X. & Guo, Y. 2018, 'A generalized leaky FxLMS algorithm for tuning the waterbed effect of feedback active noise control systems', *Mechanical Systems and Signal Processing*, vol. 106, pp. 13-23.

Wu, M., Chen, G. & Qiu, X. 2008, 'An improved active noise control algorithm without secondary path identification based on the frequency-domain subband architecture', *IEEE Transactions on Audio, Speech, and Language Processing*, vol. 16, no. 8, pp. 1409-19.

Yang, F., Enzner, G. & Yang, J. 2019, 'Transient Analysis of Partitioned-Block Frequency-Domain Adaptive Filters', *2019 27th European Signal Processing Conference (EUSIPCO)*, IEEE, pp. 1-5.

Yang, F., Wu, M. & Yang, J. 2013, 'A computationally efficient delayless frequency-domain adaptive filter algorithm', *IEEE Transactions on Circuits and Systems II: Express Briefs*, vol. 60, no. 4, pp. 222-6.

Yang, T., Zhu, L., Li, X. & Pang, L. 2018, 'An online secondary path modeling method with regularized step size and self-tuning power scheduling', *The Journal of the Acoustical Society of America*, vol. 143, no. 2, pp. 1076-84.

Zhang, G., Tao, J. & Qiu, X. 2019, 'Empirical study of decentralized multi-channel active noise control based on the genetic algorithm', *Proceedings of the 23rd International Congress on Acoustics*, pp. 6913-20.

Zhang, G., Tao, J., Qiu, X. & Burnett, I. 2018, 'Decentralized two-channel active noise control for single frequency by shaping matrix eigenvalues', *IEEE/ACM Transactions on Audio, Speech, and Language Processing*, vol. 27, no. 1, pp. 44-52.

Zhang, L. & Qiu, X. 2014, 'Causality study on a feedforward active noise control headset with different noise coming directions in free field', *Applied Acoustics*, vol. 80, pp. 36-44.

Zhang, S., So, H.C., Mi, W. & Han, H. 2017, 'A family of adaptive decorrelation NLMS algorithms and its diffusion version over adaptive networks', *IEEE Transactions on Circuits and Systems I: Regular Papers*, vol. 65, no. 2, pp. 638-49.

Zhang, S., Zhang, J. & Han, H. 2016, 'Robust variable step-size decorrelation normalized least-mean-square algorithm and its application to acoustic echo cancellation', *IEEE/ACM Transactions on Audio, Speech, and Language Processing*, vol. 24, no. 12, pp. 2368-76.

Zhang, Y. & Chambers, J.A. 2006, 'Convex combination of adaptive filters for a variable tap-length LMS algorithm', *IEEE Signal Processing Letters*, vol. 13, no. 10, pp. 628-31.

Zhao, T., Liang, J., Zou, L. & Zhang, L. 2017, 'A new FXLMS algorithm with offline and online secondary-path modeling scheme for active noise control of power

transformers', *IEEE Transactions on Industrial Electronics*, vol. 64, no. 8, pp. 6432-42.

Zhou, D. & DeBrunner, V. 2007, 'A new active noise control algorithm that requires no secondary path identification based on the SPR property', *IEEE Transactions on Signal Processing*, vol. 55, no. 5, pp. 1719-29.

Zhou, Y., Chen, J. & Li, X. 2007, 'A time/frequency-domain unified delayless partitioned block frequency-domain adaptive filter', *IEEE Signal Processing Letters*, vol. 14, no. 12, pp. 976-9.

Ziegler Jr, E. 1989, 'Selective active cancellation system for repetitive phenomena', Google Patents.